



**PHOTOCATALYTIC DEGRADATION OF GLYPHOSATE  
PESTICIDE IN THE PRESENCE OF  $\text{TiO}_2$  PELLET  
FOR SUSTAINABLE AGRICULTURE**

**BY**

**MS. KANOKWAN YAMSOMPHONG**

**A THESIS SUBMITTED IN PARTIAL FULFILLMENT OF THE  
REQUIREMENTS FOR THE DEGREE OF MASTER OF ENGINEERING  
(ENGINEERING TECHNOLOGY)**

**SIRINDHORN INTERNATIONAL INSTITUTE OF TECHNOLOGY**

**THAMMASAT UNIVERSITY**

**ACADEMIC YEAR 2019**

**COPYRIGHT OF THAMMASAT UNIVERSITY**

**PHOTOCATALYTIC DEGRADATION OF GLYPHOSATE  
PESTICIDE IN THE PRESENCE OF TIO<sub>2</sub> PELLET  
FOR SUSTAINABLE AGRICULTURE**

**BY**

**MS. KANOKWAN YAMSOMPHONG**

**A THESIS SUBMITTED IN PARTIAL FULFILLMENT OF THE  
REQUIREMENTS FOR THE DEGREE OF MASTER  
OF ENGINEERING (ENGINEERING TECHNOLOGY)  
SIRINDHORN INTERNATIONAL INSTITUTE OF TECHNOLOGY  
THAMMASAT UNIVERSITY  
ACADEMIC YEAR 2019  
COPYRIGHT OF THAMMASAT UNIVERSITY**

THAMMASAT UNIVERSITY  
SIRINDHORN INTERNATIONAL INSTITUTE OF TECHNOLOGY

THESIS

BY

MS. KANOKWAN YAMSOMPHONG

ENTITLED

PHOTOCATALYTIC DEGRADATION OF GLYPHOSATE PESTICIDE  
IN THE PRESENCE OF  $\text{TiO}_2$  PELLET FOR SUSTAINABLE AGRICULTURE

was approved as partial fulfillment of the requirements for  
the degree of Master of Engineering (Engineering Technology)

on August 9, 2019

Chairman



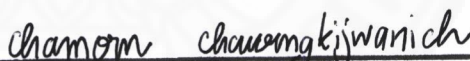
(Associate Professor Pakorn Opaprakasit, Ph.D.)

Member and Advisor



(Assistant Professor Paiboon Sreearunothai, Ph.D.)

Member and Co-advisor



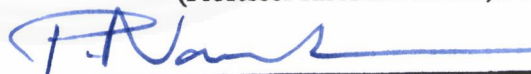
(Chamorn Chawengkijwanich, Ph.D.)

Member



(Professor Hirofumi Hinode, D.Eng.)

Director



(Professor Pruettha Nanakorn, D.Eng.)

Thesis Title	PHOTOCATALYTIC DEGRADATION OF GLYPHOSATE PESTICIDE IN THE PRESENCE OF $\text{TiO}_2$ PELLET FOR SUSTAINABLE AGRICULTURE
Author	MS. Kanokwan Yamsomphong
Degree	Master of Engineering (Engineering and Technology)
Faculty/University	Sirindhorn International Institute of Technology/ Thammasat University
Thesis Advisor	Assistant Professor Paiboon Sreearunothai, Ph.D.
Thesis Co-Advisor	Chamorn Chawengkijwanich, Ph.D.
Academic Years	2019

## ABSTRACT

In Thailand, glyphosate herbicide has been used intensively to prevent food crops from weeds and grass in agriculture, contributing to the contamination in the environment especially in natural water resources. To decontaminate glyphosate in water,  $\text{TiO}_2$  photocatalysis has been an effective process to remove glyphosate in water. Therefore, the present study aims to examine the photocatalytic degradation of glyphosate herbicide by using  $\text{TiO}_2$  pellet. Firstly, the effect of UV types on photocatalytic degradation of glyphosate was studied by using  $\text{TiO}_2$  powder. The removal efficiency of glyphosate by using UVA and UVC irradiation showed a similar result in the range of 92.67% to 99.03 %. Considering the User's Safety, UVA irradiation was applied in this experiment. In order to solve the separation problem of  $\text{TiO}_2$  powder (Degussa -P25) from treated water, clay  $\text{TiO}_2$  pellets were prepared through the calcination temperature at 600 °C for 2 h with range of 0, 5, 10, 20, 30, 40 and 50wt% of  $\text{TiO}_2$  (CT0, CT5, CT10, CT20, CT30, CT40 and CT50 pellets). As shown in this work, the  $\text{TiO}_2$ /clay ratio can affect to the stability of the pellet in water. The stability of the clay  $\text{TiO}_2$  pellets in water decreases with the increasing clay content.

CT0, CT5, CT10, CT20 pellets were unstable in water, whereas CT30, CT40 and CT50 pellets can be immersed in water. Then, these pellets were characterized by X-ray diffraction (XRD), Brunauer-Emmett-Teller (BET) and Scanning electron microscopy with energy dispersive X-ray spectroscopy (SEM/EDX) and Atomic force microscope (AFM). Next, CT30, CT40 and CT50 pellets were preliminarily applied for the photocatalytic degradation by using methylene blue (MB) as a model organic pollutant. As a result, CT30, CT40 and CT50 pellets can remove MB ( $10 \text{ mgL}^{-1}$ ) in water under UVA light ( $1700 \text{ }\mu\text{W/cm}^2$ ) within 120 mins. CT30 pellets showed the highest photocatalytic activity for MB, with approximately 79.01%. This is due to the roughest surface of CT30 pellets as shown in SEM and AFM images. A rough surface might provide more contact area between reactive oxygen species (ROS) and adsorbed MB on the surface of clay  $\text{TiO}_2$  pellets. Additionally, the decrease of MB under the dark condition was mainly adsorbed by clay. The enhanced adsorption provided by the clay in CT30 pellets could be direct more contaminants to the surface of clay  $\text{TiO}_2$  pellet for photocatalysis. In order to decontaminate glyphosate in water, the photocatalytic degradation of glyphosate by using CT30, CT40 and CT50 pellets also was studied. CT30, CT40 and CT50 pellets can effectively remove glyphosate ( $1 \text{ mgL}^{-1}$ ) under UVA light ( $2497 \text{ }\mu\text{W/cm}^2$ ) within 240 mins, with approximately 98% of removal efficiency. Also, the photocatalytic degradation rate constant of CT30, CT40 and CT50 pellets were quite similar. Therefore, considering the high-performance removal in both MB (cationic molecule) and glyphosate (anionic molecule), CT30 pellets showed optimum weight percentage of  $\text{TiO}_2$  and clay in this experiment. Then, the removal efficiency of glyphosate by using CT30 pellets were continued compared with commercial PE- $\text{TiO}_2$  pellets within 240 mins under UVA light. Results showed that removal efficiency of glyphosate was reached 99.15% by using CT30 pellets, while the removal efficiency of glyphosate by using PE- $\text{TiO}_2$  pellets was lower, with 74.36%. This is probably due to mixture of anatase-rutile in CT30 pellets, leading to improve electron-hole separation. For PE- $\text{TiO}_2$  pellets, only anatase phase was observed. Also, CT30 pellets showed a larger surface area than PE- $\text{TiO}_2$  pellets. Lastly, photocatalytic degradation of glyphosate by using  $\text{TiO}_2$  powder found only  $\text{PO}_4^{3-}$ , while photocatalytic degradation of the glyphosate by using CT30 pellets found both AMPA and  $\text{PO}_4^{3-}$ . This difference might be due to the lower photocatalytic activity of CT30 pellets than  $\text{TiO}_2$  powder,

resulting in AMPA is not rapidly decomposed. Due to AMPA are more toxic and longer half-life than glyphosate, complete degradation of AMPA is essential. With increasing reaction time into 300 mins, thereby, AMPA can be completely disappeared during the photocatalytic reaction by using CT30 pellets. Consequently, CT30 pellets were simply prepared and easily removed from water. Also, glyphosate was easily degraded by using CT30 pellets under UVA light.

**Keywords:** Glyphosate,  $\text{TiO}_2$ , Photocatalysis, Contamination



## ACKNOWLEDGEMENTS

I would first like to thank my thesis advisor Dr. Chamorn Chawengkijwanich (National Science and Technology Development Agency) as well as Assist. Prof. Paiboon Sreearunothai whenever I ran into a trouble spot or had a question about my research or writing. They consistently suggested me in the right the direction whenever they thought I needed it. I am also immensely grateful to Miss Chonlada Pokhum and Miss Duangkamon Viboonratanasri (senior assistant research) for technical help in instrument.

I would also like to acknowledge Prof. Pakorn Opaprakasit. (Sirindhorn International Institute of Technology), Prof. Hirofumi Hinode, Dr. Eden G Mariquit and Assist. Prof. Winarto Kurniawan (Tokyo Institute of Technology). I am gratefully indebted to their very valuable comments on this thesis.

The author is grateful to National Nanotechnology Center (NANOTEC) (No. P1751698), Thailand Graduate Institute of Science and Technology (TGIST) and Thailand Advanced Institute of Science and Technology-Tokyo Institute of Technology (TAIST-Tokyo Tech), National Science and Technology Development Agency, Thailand for their financial

Finally, I am thankful Sirindhorn International Institute of Technology (SIIT) for giving knowledge and scholarship and this research was partially supported by Hinode Laboratory, School of Environment and Society, Tokyo Institute of Technology, Japan.

Ms. Kanokwan Yamsomphong

## TABLE OF CONTENTS

	Page
ABSTRACT	(2)
ACKNOWLEDGEMENTS	(5)
TABLE OF CONTENTS	(6)
LIST OF TABLES	(8)
LIST OF FIGURES	(10)
LIST OF SYMBOLS/ABBREVIATIONS	(13)
CHAPTER 1 INTRODUCTION	1
1.1 Statement of problems	1
1.2 Research objectives	3
CHAPTER 2 LITERATURE REVIEW	4
2.1 Pesticide use in Thailand	4
2.2 Glyphosate	6
2.3 Analytical techniques for the determination of glyphosate	12
2.4 Titanium dioxide (TiO <sub>2</sub> ) photocatalysis	14
2.5 Photocatalytic degradation of glyphosate by using TiO <sub>2</sub> photocatalysts	19
2.6 Commercial TiO <sub>2</sub> pellets	21
2.7 Clay and TiO <sub>2</sub> photocatalysts	22
CHAPTER 3 METHODOLOGY	25
3.1 Pellet Preparation	26

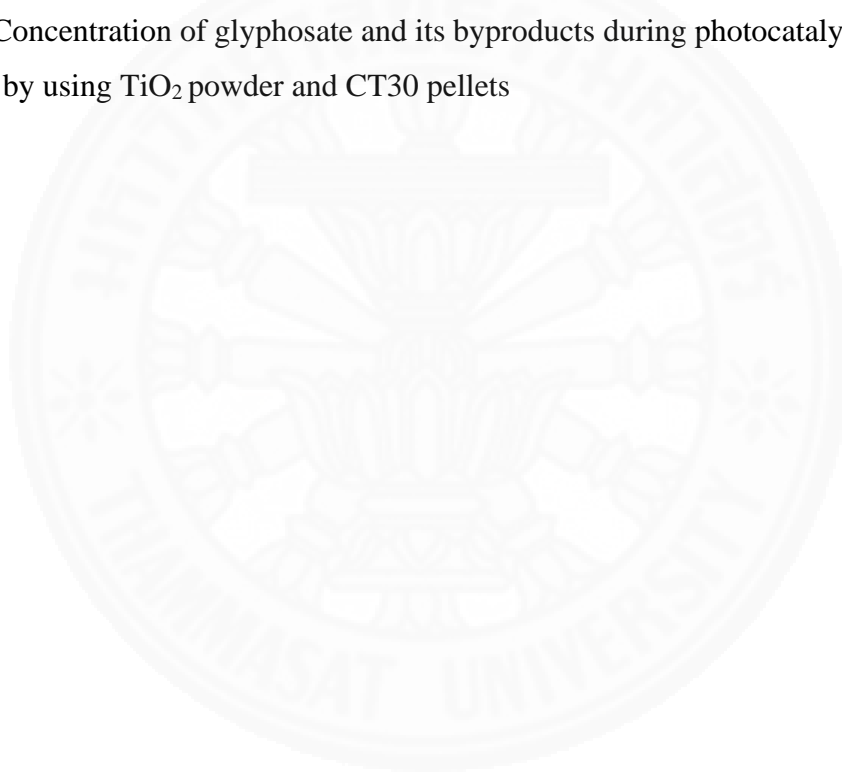


	(7)
3.2 Catalyst Characterization	26
3.3 Preliminary test of PE-TiO <sub>2</sub> and clay TiO <sub>2</sub> pellets	27
3.4 Photocatalytic degradation of glyphosate	29
3.5 Mechanisms of the photocatalytic degradation of glyphosate	34
CHAPTER 4 RESULTS AND DISCUSSION	37
4.1 TiO <sub>2</sub> pellet preparation	37
4.2 Catalyst characterization	39
4.3 Preliminary Test of PE-TiO <sub>2</sub> and Clay TiO <sub>2</sub> pellets	49
4.4 Photocatalytic degradation of glyphosate	59
4.5 Mechanisms of the photocatalytic degradation of glyphosate	72
CHAPTER 5 CONCLUSION	76
REFERENCES	77
BIOGRAPHY	85

## LIST OF TABLES

Tables	Page
2.1 The most imported pesticides by active ingredient into Thailand in 2018	5
2.2 Physical/chemical properties of glyphosate	7
2.3 The maximum admissible level of glyphosate in drinking water	8
2.4 The major breakdown products of glyphosate	11
2.5 Characteristics of TiO <sub>2</sub> powder (Degussa P-25)	14
2.6 Current-Commercial TiO <sub>2</sub> pellets	21
2.7 Properties and clay minerals constitute of clay	23
3.1 Weight ratios of white clay and TiO <sub>2</sub> powder in clay TiO <sub>2</sub> pellets	26
4.1 Characteristics of pellets	38
4.2 BET surface area, pore volume and pore size of TiO <sub>2</sub> samples	41
4.3 The ratio of anatase and rutile phases of TiO <sub>2</sub> samples	43
4.4 EDX analysis of clay TiO <sub>2</sub> pellets	44
4.5 MB concentration during the adsorption test by using PE-TiO <sub>2</sub> pellets	49
4.6 MB concentration during photocatalytic reaction by using PE-TiO <sub>2</sub> pellets	51
4.7 MB concentration during the adsorption test by using clay TiO <sub>2</sub> pellets	52
4.8 MB concentration during the photocatalytic reaction by using clay TiO <sub>2</sub> pellets	55
4.9 L*a*b* color values of MB on clay TiO <sub>2</sub> pellets	56
4.10 L*a*b* color values of adsorbed CT30 pellets After stirring for 240 mins	58
4.11 Glyphosate concentration during the adsorption test by using TiO <sub>2</sub> powder	59
4.12 Glyphosate concentration during photocatalytic reaction by using TiO <sub>2</sub> powder under UVA and UVC light	60
4.13 Glyphosate concentration during the adsorption test by using clay TiO <sub>2</sub> pellets	62
4.14 Glyphosate concentration during the photocatalytic reaction by using clay TiO <sub>2</sub> pellets with pre-adsorption	65

4.15 Glyphosate concentration during the photocatalytic degradation of glyphosate by using clay TiO <sub>2</sub> pellets without pre-adsorption	67
4.16 The kinetics constants ( <i>k</i> ) for the photocatalytic degradation of glyphosate in CT30, CT40 and CT50 pellets	68
4.17 Glyphosate concentration during the adsorption test by using CT30 pellets, PE-TiO <sub>2</sub> pellets and TiO <sub>2</sub> powder	69
4.18 Glyphosate concentration during the photocatalytic reaction by using CT30 pellets, PE-TiO <sub>2</sub> pellets and TiO <sub>2</sub> powder	70
4.19 Concentration of glyphosate and its byproducts during photocatalytic degradation by using TiO <sub>2</sub> powder and CT30 pellets	73



## LIST OF FIGURES

Figures	Page
2.1 The imported pesticides between 2010 to 2018	5
2.2 How glyphosate works	7
2.3 Chemical structure of glyphosate	7
2.4 Glyphosate biodegradation pathways	10
2.5 Possible physical and chemical degradation pathways of glyphosate	11
2.6 Structure of TiO <sub>2</sub>	15
2.7 Mechanism of Photocatalysis	16
3.1 The experimental set up and procedure	25
3.2 UV enclosure box for photocatalytic degradation of MB	28
3.3 UV enclosure box for photocatalytic degradation of glyphosate	30
3.4 Emission spectra for the UV lamp	30
3.5 Photocatalytic degradation set-up for TiO <sub>2</sub> pellets	32
3.6 Photocatalytic degradation set-up of TiO <sub>2</sub> powder	33
3.7 Chromatogram of glyphosate standard with concentration of 1 mgL <sup>-1</sup>	33
3.8 Calibration curve of glyphosate standard with concentration of 0- 1.25 mgL <sup>-1</sup>	34
3.9 Chromatogram of PO <sub>4</sub> <sup>3-</sup> standard with concentration of 0.6 mgL <sup>-1</sup>	35
3.10 Calibration curve of PO <sub>4</sub> <sup>3-</sup> standard with concentration of 0- 0.6 mgL <sup>-1</sup>	35
3.11 Chromatogram of AMPA standard with concentration of 0.5 mgL <sup>-1</sup>	35
3.12 Calibration curve of AMPA standard with concentration of 0-0.6 mgL <sup>-1</sup>	36
4.1 The appearance of TiO <sub>2</sub> pellets	37
4.2 The stability of clay TiO <sub>2</sub> pellets in water by observed the turbidity for 10 mins	39
4.3 TGA-DTA curves	40
4.4 XRD diffraction patterns of the TiO <sub>2</sub> powder	42

4.5 XRD diffraction patterns of the TiO <sub>2</sub> white clay	42
4.6 XRD diffraction patterns of PE-TiO <sub>2</sub> pellets and clay TiO <sub>2</sub> pellets	43
4.7 SEM and EDX mapping images of clay TiO <sub>2</sub> pellets	45
4.8 Surface roughness by AFM	48
4.9 Effect of PE-TiO <sub>2</sub> Pellet loading on the removal of MB under dark condition	50
4.10 Effect of PE-TiO <sub>2</sub> pellet loading on the removal of MB under UVA light	51
4.11 Effect of weight percentage of TiO <sub>2</sub> in clay TiO <sub>2</sub> pellets on the removal of MB under dark condition	53
4.12 The removal efficiency of MB (10 mgL <sup>-1</sup> ) under the dark condition	54
4.13 Effect of weight percentage of TiO <sub>2</sub> in clay TiO <sub>2</sub> pellets on the removal of MB under UVA condition	55
4.14. MB on clay TiO <sub>2</sub> pellets	57
4.15 MB on clay TiO <sub>2</sub> pellets under dark condition for 90 mins	57
4.16 The removal efficiency of glyphosate by using TiO <sub>2</sub> powder	60
4.17 Effect of weight percentage of TiO <sub>2</sub> in clay TiO <sub>2</sub> pellets on the removal of glyphosate under dark condition	63
4.18 The removal efficiency of glyphosate (10 mgL <sup>-1</sup> ) under the dark condition by using 0.035 gL <sup>-1</sup> of TiO <sub>2</sub> powder and 0.25 gL <sup>-1</sup> of clay powder	64
4.19 The concentration of glyphosate during the adsorption test and photocatalytic reaction on clay TiO <sub>2</sub> pellets	65
4.20 Effect of weight percentage of TiO <sub>2</sub> in clay TiO <sub>2</sub> pellets on the removal of glyphosate under UVA condition with pre-adsorption	66
4.21 Effect of weight percentage of TiO <sub>2</sub> in clay TiO <sub>2</sub> pellets on the removal of glyphosate under UVA condition without pre-adsorption:	67
4.22 Photocatalytic degradation kinetic of glyphosate	68
4.23 Concentration of glyphosate during the adsorption test and photocatalytic reaction	70

4.24 Removal efficiency of glyphosate under Dark and UVA Conditions	73
4.25 Concentration of glyphosate and its byproducts during photocatalytic degradation	73
4.26 Effects of illumination time on the photocatalytic degradation of glyphosate and its byproducts by using CT30 pellets	75



## LIST OF SYMBOLS/ABBREVIATIONS

Symbols/Abbreviations	Terms
SIIT	Sirindhorn International Institute of Technology
TU	Thammasat University
IARC	International Agency for Research on Cancer
TiO <sub>2</sub>	Titanium dioxide
PE	Polyethylene
PP	Polypropylene
MB	Methylene blue
AMPA	Aminomethylphosphonic acid
PO <sub>4</sub> <sup>3-</sup>	Phosphate
UV/VIS	Ultraviolet-visible spectrophotometry
HPLC	High performance liquid chromatography
GC	Gas chromatography
IC	Ion chromatography
e <sup>-</sup>	Electron
h <sup>+</sup>	Positive hole
h <sub>VB</sub> <sup>+</sup>	Valance band
e <sub>CB</sub> <sup>-</sup>	Conduction band
•OH	Hydroxyl radical
•O <sub>2</sub> <sup>-</sup>	Superoxide ion
ROS	Reactive oxygen species

## CHAPTER 1

### INTRODUCTION

#### 1.1 Statement of problems

Agricultural sector in Thailand has played an important role in terms of serving agricultural products for its own population and contributing to the global demand. In order to protect and increase agricultural production, most Thai farmers excessively use pesticides (e.g., herbicide, insecticide and other) and other agricultural chemicals. According to the Department of Agriculture, about 115,246,509 kg of the pesticides was imported into Thailand in 2018 (Office of Agricultural Regulation, 2019). Among the imported pesticides, glyphosate-isopropyl ammonium was the most imported herbicide with 53,699,528 kg of product, followed by paraquat dichloride, 2,4-D-dimethylammonium, and Ametryn. The studies indicated that pesticides, which contain at least atrazine, glyphosate and paraquat, are found in water resource, drinking water and tap water in Thailand (Patsiriwong, 2015; Pattarasiriwong, 2016).

In focus, glyphosate (N-(phosphonomethyl) glycine) is an organophosphate herbicide widely used to preventing food crops in agriculture, Thailand. It is a common substance used to controls broadleaf weeds and grass prior to planting or after wheat is harvested, as well as probably carcinogenic to human reported by the International Agency for Research on Cancer (IARC) in March 2015. Due to its high polarity, glyphosate is practically soluble in water, but insoluble in most organic solvents. In addition, glyphosate adsorbs strongly to soil and organic matter particles (Baylis, 2000). Based on the previous study, glyphosate ranged between 2 and 197 days to break down its half-life in soil. The usual half-life of glyphosate in water differed from 2 to 91 days (Henderson, 2010). Its remaining is also environmentally contaminated while the use of water is cycled. When people use contaminated water, pollutants can expose into the body. According to the Office of Agricultural Economics, 64.1 million of Thai people risk to receive pesticide more than 2.6 kilograms per person per year in 2017 (Office of Agricultural Economics, 2013). Pesticides contaminate the environment through runoff and leaching into groundwater. The contaminated water can affect everyone who uses water which is surrounding those agricultural area.



Therefore, the wastewater treatment system within the farm is necessary for pesticides mitigation in wastewater before releasing to natural water resources.

During recent decades, the photocatalytic degradation has been an effective process to degrade organic pesticide including glyphosate in water. Normally, photocatalysis is a reaction which utilizes light to the active catalyst. The photocatalyst is used to absorb light, generating reactive oxygen species (ROS) to degrade or transform the organic compounds into carbon dioxide ( $\text{CO}_2$ ), water and mineral byproducts (Carp, Huisman, & Reller, 2004; Dârjan, Drăghici, Perniu, & Duță, 2013; Umar & Aziz, 2013). A number of photocatalysts such as Titanium dioxide ( $\text{TiO}_2$ ), Tin dioxide ( $\text{SnO}_2$ ), Zinc oxide ( $\text{ZnO}$ ), Tungsten trioxide ( $\text{WO}_3$ ), etc. have been studied due to its ability to degrade organic pollutants (Devipriya & Yesodharan, 2005; Hao & Jiaqiang, 2010; Rabindranathan, Devipriya, & Yesodharan, 2003). Among the photocatalysts,  $\text{TiO}_2$  is the most commonly used in photocatalytic processes due to its non-toxic, commercial availability, relatively cheap material, high stability and efficient photoactivity, etc. Additionally, a large amount of studies has been performed on  $\text{TiO}_2$  photocatalysts applied for degradation of pesticide contaminants in water (Carp et al., 2004; Chatterjee & Mahata, 2001; J. Q. Chen, Hu, & Wang, 2012; Y. Chen et al., 2007; Dârjan et al., 2013; Echavia, Matzusawa, & Negishi, 2009; Muneer & Boxall, 2008). For example, J. Q. Chen et al. (2012) studied the  $\text{TiO}_2$  photocatalysis for glyphosate degradation in a circulating upflow photochemical reactor photocatalysts under UV light. As a result, the photocatalytic degradation efficiency of glyphosate was reached 90.87%. Chlorpyrifos insecticide can be also degraded by using  $\text{TiO}_2$  photocatalyst in the presence of UV light and sunlight.  $4.0 \text{ gL}^{-1}$  of  $\text{TiO}_2$  showing photocatalytic activity for chlorpyrifos was achieved 90%.

Although  $\text{TiO}_2$  has been popularly applied for the photocatalytic degradation of pesticides, the using commercial  $\text{TiO}_2$  powder as catalyst causes difficulties during the separation of photocatalyst from water for the applications in real life. Despite the wide availability of post-treatment processes, such as filtration, precipitation and other, the consequence is expensive technique and time needed to remove these fine- $\text{TiO}_2$  particles from the treated water. Considering the practical application,  $\text{TiO}_2$  industries have transformed  $\text{TiO}_2$  powder into larger pellets i.e. polypropylene (PP) white masterbatch (Soltex petro products Ltd.) and polyethylene (PE)- $\text{TiO}_2$  pellet

(Shandong longsheng masterbatch) for commercial and research applications, whereas few studies relating with the degradation of  $\text{TiO}_2$  pellet are presented. Furthermore, the photocatalytic degradation of glyphosate in water has been rarely studied.

Hence, the present study aims to investigate the applicability of the  $\text{TiO}_2$  powder (Degussa P-25) and  $\text{TiO}_2$  pellets under UV light to degrade glyphosate herbicide in water, specifically, the extent of its products formed during the degradation process. Thereby, the possible degradation mechanisms of the glyphosate will be represented. Significantly, the results of the application of  $\text{TiO}_2$  pellets will be responsible for ensuring that water is safe from glyphosate and its harmful by-products contamination. In the long run, to be able to eliminate glyphosate contaminated substance by using  $\text{TiO}_2$  pellets will lead to a good practice in agricultural water usage, which is considered as an important factor of sustainable agro-ecosystems and practically help to preserve critical habitats, as well as improve water quality as a whole.

## **1.2 Research objectives**

1.2.1 To determine the photocatalytic degradation of glyphosate in water using  $\text{TiO}_2$  powder for the photocatalytic degradation of glyphosate in water.

1.2.2 To fabricate and characterize of prepared clay  $\text{TiO}_2$  pellets.

1.2.3 To investigate the photocatalytic activity and mechanism of photocatalytic degradation of glyphosate in water  $\text{TiO}_2$  powder and prepared  $\text{TiO}_2$  pellets

## CHAPTER 2

### LITERATURE REVIEW

#### 2.1 Pesticide use in Thailand

Agricultural sector in Thailand has played an important role in terms of serving agricultural products for its own population and contributing to the global demand due to its suitable climate for growing many crops and high-quality agriculture stocks. In addition, it has also provided employment for Thai people, representing 30% of labor force in 2018 (Ministry of Digital Economy and Society, 2019). In order to prevent crop losses caused by agricultural pests and weeds as well as increase agricultural production, most Thai farmers excessively use pesticides (e.g., herbicide, insecticide and other) and other agricultural chemicals.

In fact, Thailand was ranked fourth out of the world in annual pesticide use whereas the total land area for agricultural purposes was relatively small, when compared with other countries, approximately forty-seventh out of the world (Food and Agriculture Organization, 2017). Mostly, pesticides used in Thailand are imported only. The Office of Agriculture Economics (OAE) showed that the imported quantity of pesticides was 103,828 tons in year 2010 and has continued to increase for the last 9 years (Department of Agriculture, 2019). Obviously, herbicides were the largest category of import in Thailand 2017, accounting for 148,979 tons of all imported herbicides. Moreover, the increasing trend of herbicides imported was obviously observed from about 68,825 tons totally in 2010 to approximately 125,280 tons totally in 2018 (Figure 2.1). The most imported pesticides including herbicides, insecticides and fungicides by active ingredient into Thailand in 2018 are represented in Table 2.1. Glyphosate isopropylammonium and paraquat dichloride were the most intense used herbicides with 26 and 8 million kilogram in 2018, respectively. In fact, both pesticides have been remained for the first and second ranks over the last decade. Additional pesticides, such as 2,4-D-dimethylammonium, atrazine, ametryn, 2,4-D-sodium, diuron, propineb, chlorpyrifos and mancozeb were also consumed intensively in Thailand with over a 2 million kilogram of each one per year.

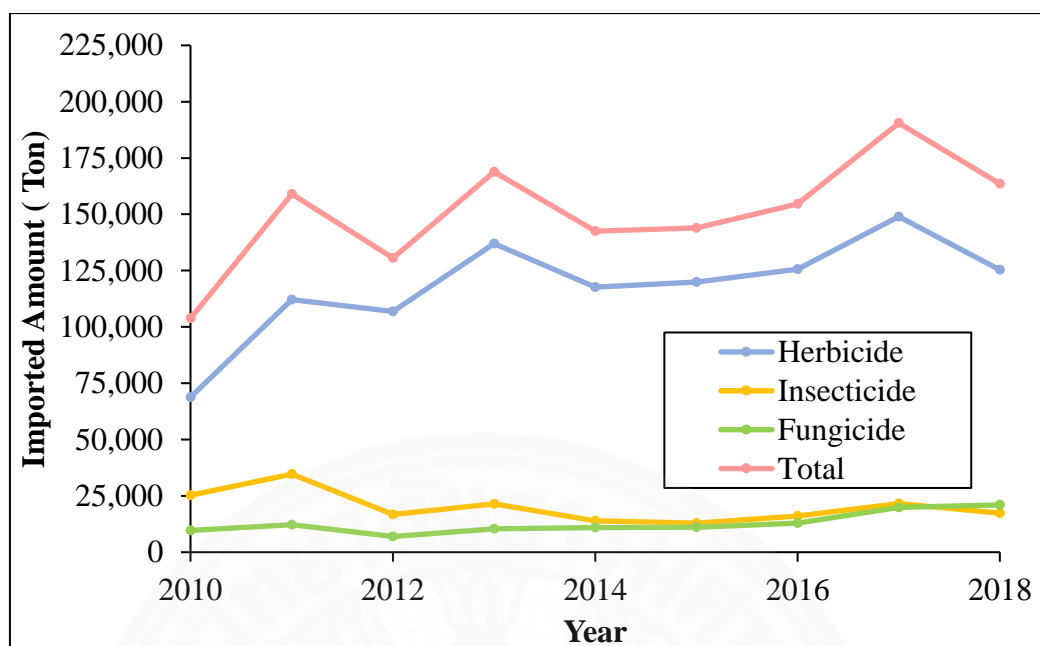


**Figure 2.1** The imported pesticides between 2010 to 2018

(Department of Agriculture, 2019)

**Table 2.1** The most imported pesticides by active ingredient into Thailand in 2018

(Office of Agricultural Regulation, 2019)

Rank	Pesticides	Imported amount (Kg)	Active ingredient (Kg)
1	glyphosate-isopropylammonium	53,699,528.30	26,685,770.12
2	paraquat dichloride	22,162,440.58	8,943,828.58
3	2,4-D-dimethylammonium	9,209,580.40	7,737,259.54
4	Ametryn	8,246,160.00	6,278,658.00
5	Propineb	5,940,771.00	4,719,689.70
6	Atrazine	4,284,036.00	3,559,040.76
7	Butachlor	3,550,035.40	2,726,177.24
8	diuron	2,575,253.00	2,446,490.35
9	2,4-D-sodium	2,789,352.25	2,231,481.80
10	mancozeb	2,789,352.25	2,231,481.80

Generally, a wide variety of crops (including tree plantations and rice paddy fields) are grown predominantly in the northern regions of Thailand. Considerable variation in pesticide is used in order to prevent these agricultural products. The most used pesticides are organophosphate i.e., glyphosate, chlorpyrifos, methomyl

methidathion, parathion-methyl, paraquat etc. As a result, the northern part of Thailand has a high potential to be affected by chemical usage and is sensitive to environmental degradation (Patsiriwong, 2015; Pattarasiriwong, 2016). Also, two or more pesticides were regularly mixed together while spraying chemicals in one application in order to save labor costs (Tagun, 2014). These extensive uses of pesticides can be contaminated the environment, especially, water resource. Its remaining is also environmentally contaminated while the use of water is cycled. When people use contaminated water, pollutants can expose into the body. Unfortunately, pesticides are poisons and they can cause a wide range of serious diseases in humans from respiratory problems to cancer. For example, 2,4-D and glyphosate herbicides probably, cause cancer in humans. Additionally, paraquat is very toxic to human skin and it is one of factor to significantly increase the risk of Parkinson's disease (Tawatsin, 2015). Recently, department of Environmental Quality Promotion (DEQP), Ministry of Natural Resources and Environment (Thailand) reported that eleven chemicals are detected in the soil, water and plant samples collected in Chiang Rai and Nan provinces, i.e. glyphosate, AMPA, paraquat, chlorpyrifos, methamidophos, triazophos, methomyl, carbofuran, carbendazim, fenobucarb and carbaryl. Most of the chemicals were found in the level of less than 1 mg/l or 1 mg/kg, except for paraquat that was found with maximum concentration of 18 mg/kg in soil. Furthermore, glyphosate was found in drinking water and tap water in Nan provinces, Thailand with concentration 10.1 and 11.26 µg/l, respectively. However, no standard values have been established for these chemicals in Thailand (Patsiriwong, 2015; Pattarasiriwong, 2016).

## 2.2 Glyphosate

Glyphosate is an organophosphate herbicide extensively used to prevent food crops all over the world. First patented glyphosate was produced in 1974 by the Monsanto Company. It is a common substance used to controls broadleaf weeds and grass prior to planting or after wheat is harvested, which is usually initially taken up via leaves and shoots, as well as transported throughout the whole plant. When glyphosate is adsorbed by plant, glyphosate blocks an enzyme enolpyruvylshikimate-3-phosphate synthase (EPSPS) that plants need to produce amino acids and proteins.

The insufficiency, in amino acids and proteins finally lead to the plant's death by starvation (Figure 3.3) (Baylis, 2000).



**Figure 2.2** How glyphosate works (Baylis, 2000)

For characteristics of glyphosate, glyphosate is a very polar compound and thus practically soluble in water, but insoluble in most organic solvents (Baylis, 2000). The chemical structure and physical/chemical properties of glyphosate are given in Figure 2.3 and Table 2.2, respectively. Glyphosate has been used extensively for agricultural practices. Thereby, glyphosate is being detected surface waters and groundwater which cause serious harmful effects on environment and human health (Torretta, Katsoyiannis, Viotti, & Rada, 2018). Moreover, glyphosate has been classified as “probably carcinogenic” to humans reported by the International Agency for Research on Cancer (IARC) in March 2015.

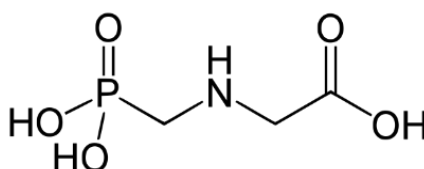


**Figure 2.3** Chemical structure of glyphosate (Ibrahim, 2015)

**Table 2.2** Physical/chemical properties of glyphosate (National Center for Biotechnology Information, 2018)

Trade name	Roundup
Chemical Name	Glyphosate
IUPAC name	N-(phosphonomethyl) glycine
Molecular formula	C <sub>3</sub> H <sub>8</sub> NO <sub>5</sub> P
Molecular weight (g mol <sup>-1</sup> )	169.08
Characteristics	Odorless, Colorless crystalline powder
Stability	Stable, Incompatible with metals
Density (g L <sup>-3</sup> )	1.74
Water Solubility at 25°C (g L <sup>-1</sup> )	12
Vapour pressure at 20°C (Pa)	<1 × 10 <sup>-5</sup>
Decomposition (°C)	230

### 2.2.1 Glyphosate standard in water

Glyphosate can be directly discharged into the water resource. Therefore, some countries have established the Maximum Contaminant Level (MCL) in surface water for glyphosate as shown in Table 2.3. However, in Thailand, no quality standards have been set or proposed in Hessen for glyphosate.

**Table 2.3** The maximum admissible level of glyphosate in drinking water (Grandcoin, Piel, & Baures, 2017; NHMRC, 2016; Health Canada, 2014; US EPA, 2016).

Organization	Maximum contaminant level (mgL <sup>-1</sup> )	Country
United States Environmental Protection Agency (US.EPA)	0.7	USA
National Health and Medical Research Council (NHMRC)	1	Australia
Health Canada	0.28	Canada



## 2.2.2 Glyphosate degradation pathways

For environmental fate of glyphosate, based on the previous study, glyphosate is highly water-soluble with an usual half-life of 45 to 60 days, whereas it is strongly adsorbed by inorganic soil components and needs 2 to 91 days to break down its half-life (Henderson, 2010). Its remaining is also environmentally contaminated while the use of water is cycled. Additionally, glyphosate is relatively resistant to degrade by chemical reaction, stable in the sunlight, and very low mobility. Rueppel, Brightwell, Schaefer, and Marvel (1977) also reported that glyphosate is not affected by sunlight, however, previous studies found glyphosate can be destroyed with a half-life of 4 days by UV light. Recently, several possible reaction pathways— biodegradation and Physical and chemical degradation— have been studied for the degradation of glyphosate.

### 2.2.2.1 Biodegradation pathways

Glyphosate consists of two main biodegradation pathways, consisting of the formation of sarcosine and glycine as well as the formation of aminomethylphosphonic acid (AMPA) (Figure 2.4) (Al-Rajab & Hakami, 2014; Al-Rajab & Schiavon, 2010; S. Wang et al., 2016). Duke (2010) investigated that glyphosate can be already broken down into AMPA after adsorbed by crops and weeds. Then, AMPA can pass into soil (Mamy, Barriuso, & Gabrielle, 2016). S. Wang et al. (2016) indicated that the major degradation of glyphosate pathway occurring in sediments. Furthermore, firstly, the sarcosine occurred due to microbial degradation, and then the AMPA occurred under conditions of starvation (lack of nutriment). The formation sarcosine and AMPA can be occurred from glyphosate degradation in both water and sediment systems. Sviridov et al. (2015) also studied the degradation glyphosate in soil and water. Both soil and water also occurred glyphosate degradation which is mostly assisted by each microorganism and AMPA is produced most (S. Wang et al., 2016). Kertesz, Elgorriaga, and Amrhein (1991) investigated that glyphosate is lost from water through sediment adsorption and especially microbial degradation. The degradation rate in water was normally slower due to fewer micro-organisms in water than in soil particles. In almost all studies of glyphosate degradation, the main biodegradation pathway in environment leads to the formation of the intermediate AMPA. AMPA is higher



persistent in soil with typical half-life varying from 76 to 240 days. Glyphosate also provides mainly a phosphorus source, whereas, the microorganisms investigated not able to use it as carbon or nitrogen source.

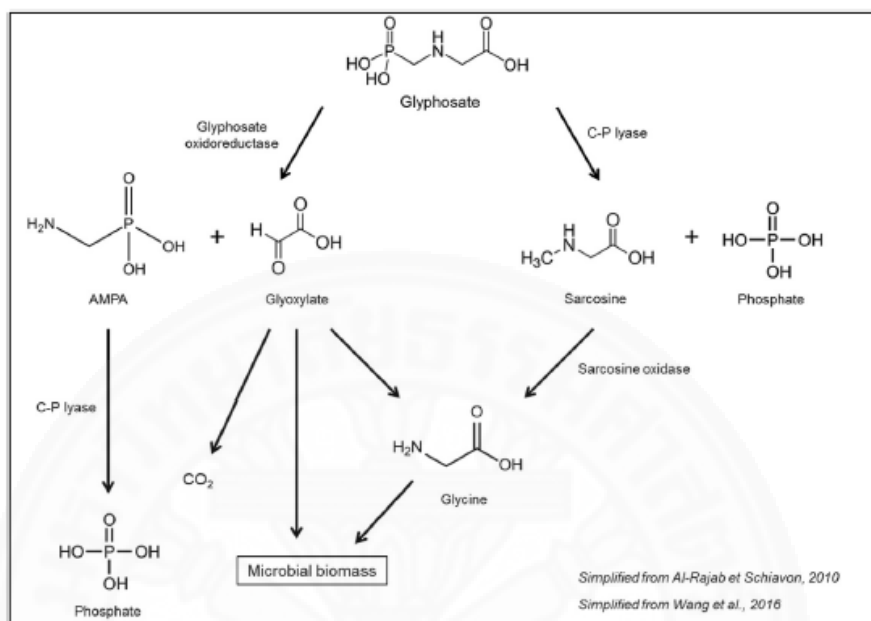


**Figure 2.4** Glyphosate biodegradation pathways  
(Grandcoin, Piel, & Baures, 2017)

#### 2.2.2.2 Physical and chemical degradation

Physical and chemical degradation of glyphosate are minor degradation pathways occurred in the environment. Several possible metabolic pathways have been studied for the degradation of glyphosate in previous studies. In one of them, glyphosate can be broken down in water by using manganese oxide in the absence of microorganisms. The degradation was successfully achieved, and the intermediate product was sarcosine. After that sarcosine was degraded into formic acid and glycine (Barrett & McBride, 2005). In a different work, Y. Chen et al. (2007) purposed two degradation paths of glyphosate in the Fe (III)/ $\text{H}_2\text{O}_2$ /UV process. Due to the presence of hydroxyl radicals ( $\bullet\text{OH}$ ), glyphosate was degraded into sarcosine and phosphoric acid. Also, glyphosate was degraded into AMPA and then the acetic acid. Additionally, Muneer and Boxall (2008) revealed that different pathways occurred at different pH values. As a result, two plausible pathways to break down glyphosate—the direct generation of glycine and indirect generation of glycine—at low and high pH were

investigated. In a recent research,  $\text{TiO}_2$  immobilized was used for the photocatalytic degradation of glyphosate herbicides, degradation path of glyphosate was conducted. In one of them, the sarcosine was produced directly and, as the other path, the glycolic acid and AMPA generation (Echavia et al., 2009). The previous studies on degradation pathways of glyphosate under different reactions is concluded in Figure 2.5.

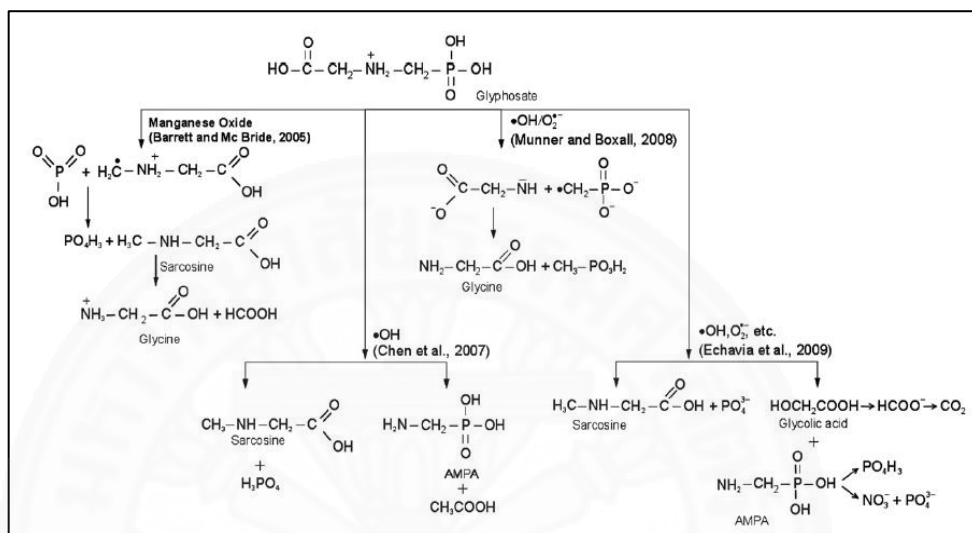


**Figure 2.5** Possible physical and chemical degradation pathways of glyphosate (Manassero, Passalia, Negro, Cassano, & Zalazar, 2010)

Therefore, based on the literature reviews, the main breakdown products of glyphosate are AMPA, sarcosine, glycine and phosphate. Their toxicity is illustrated in Table 2.4.

**Table 2.4** The major breakdown products of glyphosate (Grandcoin et al., 2017; Li, Wallace, Sun, Reardon, & Jaisi, 2018; Razzaque, 2011)

Name of by-product	Toxicity	Half life
AMPA	<ul style="list-style-type: none"> <li>Effect on human erythrocytes</li> <li>Cause neonatal cells death</li> </ul>	76 to 240 days
Sarcosine	<ul style="list-style-type: none"> <li>No toxicity</li> </ul>	~13.6 h
Glycine	<ul style="list-style-type: none"> <li>Low toxicity and effect on the develop central nervous system (large amounts)</li> </ul>	14 days
Phosphate	<ul style="list-style-type: none"> <li>Very Low toxicity and increase cell death and Vascular calcification (Long-term exposure)</li> </ul>	Not available

### 2.3 Analytical techniques for the determination of glyphosate

The different analytical techniques e.g. Ultraviolet-visible (UV/VIS) spectrophotometry, High performance liquid chromatography (HPLC), Gas chromatography (GC) etc. are being developed in order to analyze these compounds in water samples. However, glyphosate has high polarity and lacks the chromophores or fluorescent molecules, making it difficult to determine. Accordingly, in many cases, it is required derivatization of these compounds, in order to make them proper for analysis. However, Ion chromatography (IC) has been a useful technique for measuring glyphosate quickly and conveniently. IC method can separate and quantitate glyphosate without derivatization or preparation of complex compound.

#### 2.3.1 Determination of glyphosate by IC

IC separation has been a convenient tool for determination glyphosate. Zhu, Zhang, Tong, and Liu (1999) reported an uncomplicated detection using IC for glyphosate. IC was carried out by suppressed conductivity detection (DX-100) with Na CO and NaOH eluents. The technique was suitable, convenient and sensitive determination of glyphosate. Recently, IC method to analyze glyphosate was purposed for improved detection. For example, Coutinho, Coutinho, Mazo, Nixdorf, and Camara (2008) developed an IC with coulometric detector to measure glyphosate in aqueous solution without derivatization step. Marques et al. (2009) improved an IC technique that can measure of glyphosate with the other anions such as sulphate ( $\text{SO}_4^{2-}$ ), phosphate ( $\text{PO}_4^{3-}$ ), fluoride ( $\text{F}^-$ ), chloride ( $\text{Cl}^-$ ), nitrite ( $\text{NO}_2^-$ ), and so on.

#### 2.3.2 Determination of glyphosate by UV–visible spectrophotometry

The glyphosate molecule lacks the chromophores or fluorescent groups in the structure that would be necessary for colorimetric, UV ( $> 200 \text{ nm}$ ), or fluorimetric detection. Therefore, glyphosate cannot be detected by Spectrophotometric and fluorometric determination of method directly. Sirotiak (2015) presented the derivatization method by using carbon disulphide ( $\text{CS}_2$ ) and copper (Cu). The amine group in glyphosate was transform by  $\text{CS}_2$  into dithiocarbamic acid. Then, dithiocarbamic acid reacted with Cu, leading to the yellow colored of copper dithiocarbamate complex. As a result, the derivative solution was measured at 435 nm.

However, the derivatization method by using 9-fluorenyl methoxycarbonyl chloride (FMOC-Cl) has been the most frequently applied method for the determination of glyphosate. The amine group in glyphosate will react with FMOC-Cl in acetonitrile to give the derivatized glyphosate (FMOC–glyphosate) which was measured at 265 nm (Waiman, Avena, Garrido, Band, & Zanini, 2012).

### 2.3.3 Determination of glyphosate by HPLC

HPLC method can be used to determine glyphosate with different detectors i.e., UV-Vis and fluorescence detectors. Also, pre-column and post-column derivatization methods are being applied to increase detection sensitivity, modifying the chemical properties of glyphosate (i.e., structure and polarity). This can help to improve separation and stabilization of its labile analytes. used FMOC to form fluorescent derivatives and facilitate the Most pre-column methods commonly chromatographic retention time. In addition, derivatization p-toluenesulphonyl with UV detector (Khrolenko & Wieczorek, 2005) and NBD-Cl (4- chloro-7-nitrobenzofurazan) with fluorescence detector have been used. In post-column procedures in HPLC method, the post-column derivatization required after chromatographic separation (Miles, Wallace, & Moye, 1986). To reduce the formation of other by product, the post-column derivatization was used. The most common reaction used o-phthalaldehyde (OPA) with N, N-dimethyl-2-mercaptoethylamine (Piriyapittaya, Jayanta, Mitra, & Leepipatpiboon, 2008).

### 2.3.4 Determination of glyphosate by GC

Glyphosate, being high polar and non-volatile compound, is requires the derivatization method for GC analyses in order to convert them to less polar and more volatile forms. A widely used for the determination of glyphosate, the technique for quantification by GC requires derivatization usually involves mixing trifluoroacetic anhydride (TFAA) and trifluoroethanol (TFE) in excess. These mixtures ere known to transform glyphosate into AMPA with only a single reaction step, which derivatives are adequately volatile for GC/ MS (Roy & Konar, 1989). Acetic acid and trimethyl orthoacetate (Tsuji, Akiyama, & YANo, 1997) as well as N-methyl-N-(tertbutyldimethylsilyl) trifluoroacetamide (MTBSTFA) with tert-

butyldimethylchlorosilane (TBDMCS) have been used for derivatization of glyphosate (Motojyuku et al., 2008).

## 2.4 Titanium dioxide (TiO<sub>2</sub>) photocatalysis

### 2.4.1 Titanium dioxide (TiO<sub>2</sub>)

TiO<sub>2</sub> has been commonly used in photocatalytic functions from long time ago. They are chemically stable, inexpensive, highly efficient photoactivity and nontoxicity. Its chemical reaction cannot be occurred in the dark condition, whereas UV light illumination can cause some chemical reactions in TiO<sub>2</sub>. Crystallinity TiO<sub>2</sub> is consisted of rutile, anatase, and brookite; however, the most significant used as a photocatalyst is rutile and anatase. Rutile and anatase were intensively utilized in photocatalysis, but anatase generally has more actively than rutile. Moreover, it has been widely reported that mixed-phase photocatalysts with anatase/rutile compositions enhance photocatalytic activity, relative to single phase TiO<sub>2</sub>, through improved electron-hole separation in TiO<sub>2</sub> interfaces. Thereby, this electron-hole separation process has effectively increased excited electrons and positive holes moving. Interestingly, commercial TiO<sub>2</sub> powder (Degussa P-25) have been commonly used in many studies. The TiO<sub>2</sub> powder has been frequently used as a benchmark for photocatalysis applications because of its highly active in several photocatalytic reaction systems. The TiO<sub>2</sub> powder consists of anatase and rutile crystallites, showing ratios typically of 70:30 or 80:20 (Ohtani, Prieto-Mahaney, Li, & Abe, 2010) (Table.2.5).

**Table 2.5** Characteristics of TiO<sub>2</sub> powder (Degussa P-25) (Ohno, Sarukawa, Tokieda, & Matsumura, 2001)

<b>TiO<sub>2</sub> powder</b>	<b>Characteristic</b>
<b>Preparties</b>	
Specific surface area(m <sup>2</sup> /g)	50 ± 15
PH	3.5 – 4.5
Tamped density (g/l)	approx. 130
Particles diameter	21±5 nm
TiO <sub>2</sub> phrase	Anatase: Rutile 70:30
Manufacturer	Evonik industries

In all three structures, they have the same basic structural unit in the form of octahedral network structure. Each distorted octahedron can be considered as one titanium atom surrounded by six oxygen atoms ( $\text{TiO}_6$ ). Among of these  $\text{TiO}_2$  phases, rutile is the more stable than anatase and brookite. Rutile crystalline structure is tetragonal symmetry. Each octahedron is linked to ten other octahedrons by sharing two edge oxygen pairs and eight corner oxygen atoms). Anatase crystal structure are slender tetragonal prisms. The octahedron in anatase contains eight surrounded octahedrons, sharing four edges and four corners with each other. However, brookite has the least stable phase. Brookite crystal structure is built up of flat orthorhombic plates. Each distorted octahedron with a titanium ion at its the center shares three edges and six corners with each other. Figure 2.6 shows the phase diagram for  $\text{TiO}_2$ . Additionally, rutile phase is the high temperature form, whereas brookite and anatase phases are low temperature forms. rutile  $\text{TiO}_2$  can be successfully transformed into brookite and anatase in low temperatures (Bourikas, Kordulis, & Lycourghiotis, 2014).

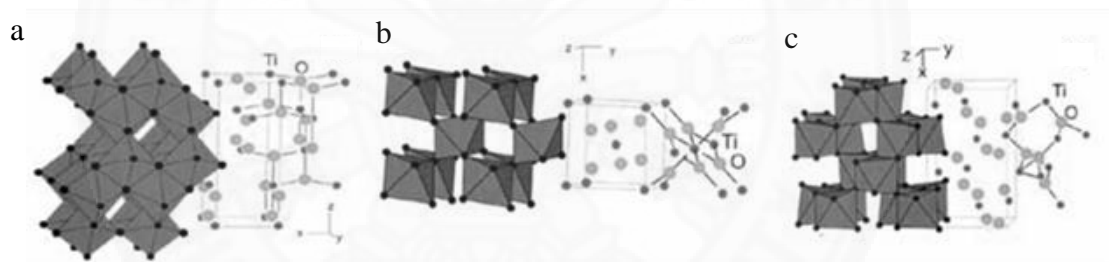


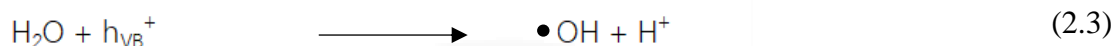
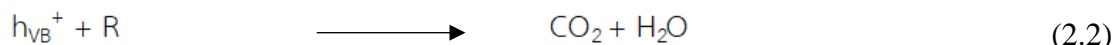
**Figure 2.6** Structure of  $\text{TiO}_2$ : (a) rutile, (b) anatase and (c) brookite  
(Bourikas et al., 2014)

#### 2.4.2 Photocatalysis

Photocatalysis is a reaction which utilizes light to the photocatalyst. When photocatalysts are activated by adsorbing light of appropriate energy (e.g. ultraviolet light), leading in the electron hole pair separation on to the photocatalyst surface. These electron-hole pairs are strong oxidizing and reducing agents.

During recent decades, a number of catalysts such as Copper(I)oxide ( $\text{Cu}_2\text{O}$ ), Titanium dioxide ( $\text{TiO}_2$ ), Tin dioxide ( $\text{SnO}_2$ ), etc. have been increasingly focused due to its potentiality to degrade organic and inorganic pollutants from water(Devipriya & Yesodharan, 2005; Hao & Jiaqiang, 2010; Rabindranathan et al., 2003). Among the

photocatalysts, TiO<sub>2</sub> is the most frequently used in photocatalytic processes owing to its non-toxic, commercial availability, relatively cheap material, high stability and efficient photoactivity, etc. The significant processes taking place in TiO<sub>2</sub> photocatalysis as follows:



Once TiO<sub>2</sub> photocatalyst is illuminated with light having energy equal or higher than 3.2 eV contributing to the initial charge separation event in the energy-band gap of TiO<sub>2</sub>. Therefore, electron (e<sup>-</sup>) from the valance band (h<sub>VB</sub><sup>+</sup>) leaves to the conduction band (e<sub>CB</sub><sup>-</sup>). Also, a hole (h<sup>+</sup>), having a positive charge, appears in the h<sub>VB</sub><sup>+</sup> as shown in equation 2.1. The h<sub>VB</sub><sup>+</sup> is a strong oxidizing equivalent, whereas the e<sub>CB</sub><sup>-</sup> are a strong reducing equivalent. After this initial event, the h<sub>VB</sub><sup>+</sup> oxidizes either organic substances directly or H<sub>2</sub>O to generate hydroxyl radical (•OH) as shown in equation 2.2 to 2.3. •OH can non-selectively degraded most of organic compounds, finally converting them into by product, CO<sub>2</sub> and water as shown in equation 2.4. As part of the conduction band, the e<sup>-</sup> react with oxygen (O<sub>2</sub>) forming a superoxide ion (•O<sub>2</sub><sup>-</sup>) as shown in equation 2.5. The •O<sub>2</sub><sup>-</sup> is highly reactive species, also able to oxidize organic substances. The electron-hole pairs generation process can be represented in Figure 2.7 (Carp et al., 2004; Dârjan et al., 2013; Umar & Aziz, 2013)

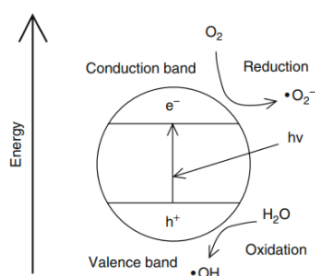


**Figure 2.7** Mechanism of Photocatalysis (Umar & Aziz, 2013)



### 2.4.3 Factors affecting the degradation performance

Various influencing factors, such as catalyst loading and size, irradiation time, light intensity, UV types, pH and reaction temperature can affect the water photocatalytic process. These influencing factors will bring about changes in efficient photocatalysis process, ultimately making a difference in performance.

#### 2.4.3.1 Catalyst loading and size

The amount of  $\text{TiO}_2$  is a significant factor for an efficient photocatalysis process. This can be directly affected to the photocatalytic degradation rate. An increase in the catalyst loading leads to an increase in the number of active sites on the  $\text{TiO}_2$  surface, resulting in the generation of highly reactive oxygen species (i.e.,  $\bullet\text{O}_2^-$  radicals). However, as the amount of  $\text{TiO}_2$  is beyond an optimum level, the degradation rate is slightly decreased. Due to the fact that the number of photons adsorbed on the photocatalyst decreases and the light penetration depth into the solution can consequently create a light scattering and screening effect.

The previous studies revealed that the optimum dosage of  $\text{TiO}_2$  purposed varied obviously, from 0.07 to 12 g/L because of the differences in the working condition, the amount of radiation, wavelengths etc. The photocatalytic activity mostly occurs at the surface of the catalyst. The catalyst must have sufficient surface area to adsorb and also destruct pollutants. Therefore, the increase of catalyst loading leads to the increase of photocatalytic rate (Dârjan et al., 2013; Umar & Aziz, 2013).

#### 2.4.3.2 Initial concentration of organic compound

The initial concentration the concentration of pollutants also influences the degradation performance including reaction rate. The high concentration of organic compound can reduce the photocatalytic degradation efficiency. More organic substances are adsorbed on the surface of  $\text{TiO}_2$ , and thereby less number of photons are available to adsorb the photocatalyst surface and less  $\bullet\text{OH}$  is formed. Therefore, the small amount of organic pollutant can be degraded (Dârjan et al., 2013; Umar & Aziz, 2013).



#### 2.4.3.3 Irradiation time

Time of irradiation affects the organic pollutants degradation. For the pseudo first-order kinetics, the reaction rate decreases with irradiation time and a competition for degradation may also occur among the intermediate products. After certain time, the slow kinetics of pollutant degradation is mainly led to the difficulty in the reaction of hydroxyl radicals with short chain aliphatics, and photocatalyst deactivation by active site coverage with strong by-products deposition. The by-products may also give a toxic equal or higher than the initial pollutant. Therefore, the optimal irradiation time should be selected for pesticides photocatalytic degradation and its mineralization. Moreover, the irradiation time should be as low as possible in a cost-effective process (Dârjan et al., 2013; Umar & Aziz, 2013).

#### 2.4.3.4 Light intensity

As the irradiated light has energy equal or higher than the band gap of photocatalyst, the  $e^-$  in the valence band leaves to the conduction band. Meantime, the  $h^+$  and a free radical are formed. From previously studies, higher light intensity would increase electron-hole pair generation rate and photocatalytic activity, leading to high removal efficiency. On the other hand, when light intensity is increased up to a certain point, the electron-hole pair separation may undergo with electron-hole recombination, thereby effecting on lower reaction rate (Dârjan et al., 2013; Umar & Aziz, 2013).

#### 2.4.3.5 UV types

Due to large band-gap energy ( $\sim 3.2\text{eV}$ ) of  $\text{TiO}_2$  photocatalyst,  $\text{TiO}_2$  photocatalysis for the degradation of organic compounds is required ultraviolet (UV) light to activate. According to the difference in wavelengths, UV light can be categorized into three groups.  $\text{UV}_A$  light has wavelengths close to visible light (320 to 400 nm in wavelength);  $\text{UV}_B$  light is in the range from 290 to 320 nm and  $\text{UV}_C$  light has a short wavelength (100 to 290 nm in wavelength). The wavelength of the light has an effect on the photocatalytic degradation speed with shorter wavelengths leading to faster degradation.  $\text{UV}_C$  has the highest potential to degrade for water contaminated with organic pollutant. The  $\text{UV}_C$  wavelength has better performance compared with

UV<sub>B</sub> and UV<sub>A</sub> (Cortés, Alarcón-Herrera, Villicaña-Méndez, González-Hernández, & Pérez-Robles, 2011).

#### 2.4.3.6 pH

pH is a significant factor in the photocatalytic degradation of organic compounds, which affects the electrostatic interactions between the photocatalyst and the pollutant compounds. Based on the previous studies, the point of zero charge (PZC) of TiO<sub>2</sub> differs from 4.5 to about 7. However, the most typically used PZC of TiO<sub>2</sub> powder (Degussa -P25) is 6.9. At pH below PZC, the surface of TiO<sub>2</sub> showed positively charged, whereas, pH above PZC, the surface showed negatively charged. When the pH is near PZC, the TiO<sub>2</sub> particles have a tendency to agglomerate, forming large clusters. The number of active sites on TiO<sub>2</sub> is decreased and, so, the photocatalytic degradation rate is reduced (Dârjan et al., 2013; Kosmulski, 2006; Umar & Aziz, 2013).

#### 2.4.3.7 Reaction temperature

The reaction temperature also influences the degradation performance. An increase in reaction temperature generally leads to increase photocatalytic degradation efficiency. When reaction temperature is more than 80°C, the recombination of charge is occurred, and small amount of organic compounds can be adsorbed on TiO<sub>2</sub> surface. Therefore, the reaction temperature should be 20-80 °C in order to achieve a high photocatalytic activity (Gaya & Abdullah, 2008; Kumar & Pandey, 2017).

### 2.5 Photocatalytic degradation of glyphosate by using TiO<sub>2</sub> photocatalysts

Echavia et al. (2009) prepared TiO<sub>2</sub> immobilized on silica gel for the photocatalytic degradation of glyphosate herbicide. Silica gel particles were coated by pure anatase TiO<sub>2</sub> through sol–gel technique. As a result, glyphosate was completely removed within 60 min by immobilized TiO<sub>2</sub> (14 g) and UV<sub>A</sub> lamp (6 w). Glyphosate was removed by both adsorption and photocatalytic processes, fitted by the first-order Langmuir–Hinshelwood kinetics. Also, photocatalytic degradation of glyphosate released PO<sub>4</sub><sup>3-</sup> and NO<sub>3</sub><sup>-</sup> which are non-toxic byproducts.

Muneer and Boxall (2008) investigated the photocatalytic degradation of a derivative glyphosate by using TiO<sub>2</sub> powder. As a result, glyphosate ( $1 \times 10^{-3}$  molL<sup>-1</sup>)

can be adsorbed on the TiO<sub>2</sub> surface under dark condition at ~pH 3 and the adsorption of glyphosate decreased when pH values increased. Glyphosate consists of phosphate group showing negatively charged. The TiO<sub>2</sub> surface showed positively charged at low pH values (~pH 3) and thereby glyphosate can be adsorbed on TiO<sub>2</sub> surface. When the pH of solution increased, the degradation rate of glyphosate increased. The highest degradation rate was observed at pH 11. In addition, the different photocatalytic degradation pathways were observed between low and high pH values. At ~pH 3, sarcosine was formed as the intermediate product, whereas no sarcosine was formed at ~pH 11. At ~pH 11, the formation of glycine was observed as the main intermediate product.

Y. Chen et al. (2007) investigated the most appropriate condition i.e., the TiO<sub>2</sub> loading, pH value, illumination time, electron acceptors, and ions for the degradation of glyphosate on TiO<sub>2</sub>/UV in aqueous suspensions. As a result, 6.0 gL<sup>-1</sup> TiO<sub>2</sub> showed the highest photocatalytic degradation efficiency, reaching 92.0% at 3.5 h. However, with increase in TiO<sub>2</sub> concentration beyond 6.0 gL<sup>-1</sup>, the photocatalytic degradation efficiency of glyphosate was slightly decreased. Acidic and alkaline conditions showed the different result in the degradation efficacy of glyphosate. With pH 2.0, the photodegradation efficiency was 66.9%, whereas the photocatalytic degradation efficiency was lower (36.2%) at pH 6.0. With adding small amount of Ions (0.001 to 1.0 mM) such as Na<sup>+</sup>, K<sup>+</sup>, Cl<sup>-</sup> and SO<sub>4</sub><sup>2-</sup> had no significance effects on the photocatalytic performance. In addition, the formation of PO<sub>4</sub><sup>3-</sup> can be observed as an indicator for the complete degradation of glyphosate. The complete degradation was carried out at least 3.5 h.




J. Q. Chen et al. (2012) used TiO<sub>2</sub> powder/UV in a circulating upflow photochemical reactor for the degradation of glyphosate. As a result, the photocatalytic degradation efficiency of glyphosate (2.0×10<sup>-4</sup> molL<sup>-1</sup>) increased with increasing the amount of TiO<sub>2</sub> from 0 to 0.8 g L<sup>-1</sup> within 80 mins. Also, the optimal TiO<sub>2</sub> concentration was 0.4 g L<sup>-1</sup>, reaching a maximum efficiency of glyphosate (2.0 ×10<sup>-4</sup> mol L<sup>-1</sup>) of 90.87% within 80 mins. Also, as the amount of glyphosate increased to 8.0 × 10<sup>-4</sup> mol L<sup>-1</sup>, the degradation efficiency decreased to 65.08%. The photocatalytic degradation rate was fitted by the first-order kinetics.

Xue et al. (2011) prepared titania nanotubes doped with cerium (Ce–TiO<sub>2</sub> nanotubes) for the degradation of glyphosate herbicide under UV light. The rutile TiO<sub>2</sub> nanoparticles was mixed with NaOH solution (10 mol L<sup>-1</sup>) at 130 °C for 24 h to fabric TiO<sub>2</sub> nanotubes. Then, cerium was doped on prepared TiO<sub>2</sub> nanotubes. The cerium helped to generate more electron–hole pairs. Hence the photocatalytic degradation efficiency of glyphosate (1.0×10<sup>-4</sup> molL<sup>-1</sup>) was reached 76% by using 0.1 g of Ce–TiO<sub>2</sub> nanotubes within 1 h.

## 2.6 Commercial TiO<sub>2</sub> pellets

Practically, the commercial TiO<sub>2</sub> powder is the most active photocatalyst used in water decontamination. However, TiO<sub>2</sub> powder easily agglomerates which reduces photocatalytic degradation efficiency and requires expensive water filtration process for removing these nanoparticles from treated water. Accordingly, TiO<sub>2</sub> companies have transformed TiO<sub>2</sub> powder into larger pellets for commercial and research applications (Table 2.6).

**Table 2.6** Current-Commercial TiO<sub>2</sub> pellets

Picture	Product Name	Remarks	Manufacturer
	PE-TiO <sub>2</sub> Pellet	Color: White Anatase TiO <sub>2</sub> : 70 % Polyethylene (PE) :30 % Pellet Size :2.5-3mm	Shandong longsheng masterbatch
	PP White Masterbatch	Color: White Poly Propylene:50 % Rutile TiO <sub>2</sub> : 50 % Pellet Size: 2.5mm	Soltex Petro Products Ltd.
	TiO <sub>2</sub> White Masterbatch	Color: White Polyethylene Carrier (LLDPE) :15 % Rutile TiO <sub>2</sub> : 70 % Pellet Size: 2.5mm	Yiangmen Yixing Plastic Raw Material Co. Ltd

## 2.7 Clay and TiO<sub>2</sub> photocatalysts

Many researchers have used clay to exhibit larger specific surface areas with TiO<sub>2</sub> (Bouna et al., 2011; Kutlákova et al., 2011; C. Wang, Shi, Zhang, & Li, 2011). Also, previous studies have shown that using clay with TiO<sub>2</sub> as photocatalyst offers several advantages: They can easily separate and recover from decontaminated water; increase adsorption ability and enhance photocatalytic activity for removing organic pollutants.




### 2.7.1 Definition of Clay

Clay refers to natural fine-grained soil and rock that consists of primarily fine-grained clay minerals and other minerals such as hydrated aluminium silicate, carbonate, quartz, and metal oxides. Generally, clay is smaller than 0.004 mm and easy to disperse in water. Clay are divided into three common types i.e., stoneware, earthenware (or common clay), and kaolin. Stoneware is tough and durable clay. Its natural colors are often light gray, dark gray or brown. Earthenware consists of many minerals and many impurities such as sand. Its natural colors are often white or gray. Kaolin contains few impurities and thus it is the purest clay. Also, Kaolin shows larger particle size and tougher than other clays (Bergaya & Lagaly, 2006; C. Wang et al., 2011).

Interestingly, clay has clay minerals as the major constituent. The clay minerals are significant constituent to identify the properties of a clay such as plasticity. Therefore, the properties of clay do not consistency. However, most clay can be molded into many versatile products when it is moist and either become strong and hard when it is dried naturally, or it is fired in high temperatures, adsorption ability, ion-exchange capacity, good binder (Bergaya & Lagaly, 2006). Therefore, clay has been known to, and utilized for industrial applications and domestic products worldwide including ceramics, cosmetics, plastics, paints, and paper. Clay minerals are classified into four main groups (i.e., Kaolinite, Montmorillonite/Smectite, and Illite groups) depending on their structure and composition. The Kaolinite group consists of kaolinite, dickite and nacrite. The common structure is aluminum hydroxide (Al<sub>2</sub>(OH)<sub>4</sub>) layers or gibbsite layer linking with silicate (Si<sub>2</sub>O<sub>5</sub>) layers. The Montmorillonite/Smectite group consists of talc, pyrophyllite, montmorillonite, saponite, nontronite, vermiculite, and sauconite.

Their common structure is gibbsite /or brucite layer linking between two silicate layers. The Illite group consists of illite (or the Clay-mica). The structure is also similar to montmorillonite group. The water molecules and potassium ions can be place between the layer. Base on the previous studies, some clay minerals listed above are belong to different of the clay groups (Table 2.7).

**Table 2.7** Properties and clay minerals constitute of clay (Bergaya & Lagaly, 2006)

Picture	Clays	Main clay minerals	Properties
	Pyrophyllite Clay	Pyrophyllite	Removal of heavy metal ions and dyes
	Bentonite	Montmorillonite	Hydration, swelling, water absorption,
	Bleaching earth	Montmorillonite	High adsorption capacity
	Kaolin	Kaolinite	Plastic, white burning
	Fire clay	Kaolinite	Plastic, fire resistance
	Nano clay	Mostly montmorillonite	Use for nanocomposites



### 2.7.2 The photocatalytic degradation by using clay with TiO<sub>2</sub>

Recently, many researchers have used clay with TiO<sub>2</sub>. Clay TiO<sub>2</sub> composites offer several advantages including make dealing with photocatalysts easier and enhance the photocatalytic efficiency of the materials (C. Wang et al., 2011) .

C. Wang et al. (2011) successfully prepared Kaolinite/TiO<sub>2</sub> nanophotocatalysts through Titanium tetrachloride (TiCl<sub>4</sub>) hydrolysis method. Kaolinite powders were stirred with TiCl<sub>4</sub> solution at 70 °C for 4 h. This prepared sample was filtrated and then dried at 80 °C for 2 h. To obtain final kaolinite/TiO<sub>2</sub> nano-photocatalysts, the dries mixtures were calcined for 2 h with various temperature from 200 °C to 600 °C in a muffle furnace. As a result, the samples calcined at 200 °C showed the maximum photocatalytic degradation efficiency than other samples. The degradation efficiency of methyl orange reached 45% after 7 h.

KutlÁková et al. (2011) prepared kaolinite/TiO<sub>2</sub> nanocomposite using titanyl sulfate (TiOSO<sub>4</sub>) with kaolin. Kaolin was mixed with TiOSO<sub>4</sub>. And then dried at 105 °C. The dried mixtures were calcined at 600 °C for 2 h. The result showed that samples calcined at 600 °C showed the maximum photocatalytic degradation efficiency. The 57.2 wt.% of TiO<sub>2</sub> content in kaolinite/TiO<sub>2</sub> nanocomposite represented the highest photoactivity, with approximately 60% within 1 hr.

Bouna et al. (2011) synthesized TiO<sub>2</sub> supported palygorskite clay and utilized it to remove orange G pollutant from wastewater. Organo-clay sample was mixed with hexadecyltrimethylammonium bromide and titanium tetraisopropoxide to form the gel through ion exchange reaction. The mixtures were dried at 60 °C for 2 days. Then, the dries mixtures were heated with various temperature and times. The sample calcined at 600 °C for 1 h showed the maximum degradation efficiency, with 89%. However, the photocatalytic performance decreased with increasing the calcined temperature. The sample calcined at 900 °C showed the low degradation efficiency of Orange G with 25%..

## CHAPTER 3

### METHODOLOGY

The photocatalytic degradation of glyphosate was carried out by using TiO<sub>2</sub> pellets. Firstly, the effect of UV types (UVA or UVC light) on photocatalytic degradation of glyphosate was purposed by using TiO<sub>2</sub> powder. Simultaneously, 2 types of TiO<sub>2</sub> pellets—prepared clay TiO<sub>2</sub> pellets and commercial polyethylene (PE)-TiO<sub>2</sub> pellets — have been focused. These pellets were characterized by X-ray diffraction (XRD), Brunauer-Emmett-Teller (BET) and scanning electron microscopy with energy dispersive X-ray spectroscopy (SEM/EDX) and Atomic force microscope (AFM). Next, TiO<sub>2</sub> pellets were preliminarily applied for the photocatalytic degradation of methylene blue (MB). Finally, the photocatalytic degradation of glyphosate and the possible mechanism of photocatalytic degradation of glyphosate were investigated by using TiO<sub>2</sub> pellets (Figure 3.1).

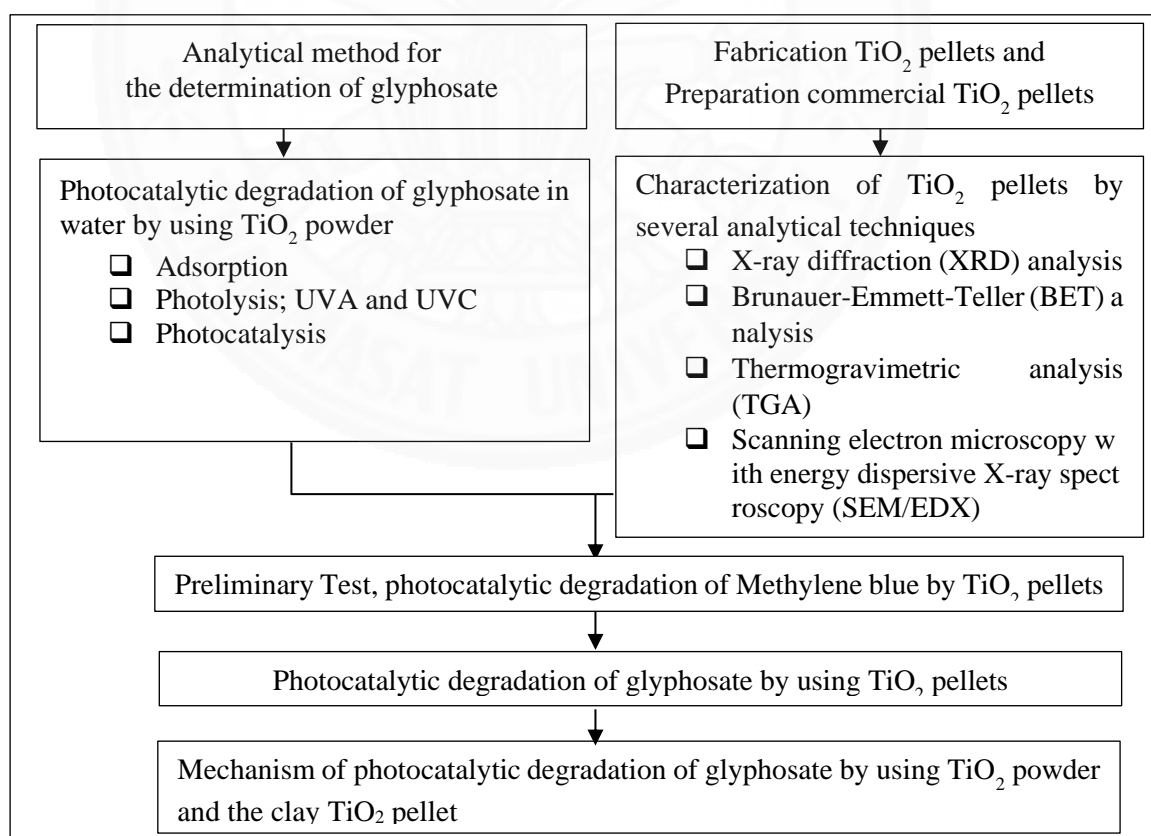


**Figure 3.1** The experimental set up and procedure



### 3.1 Pellet Preparation

The PE-TiO<sub>2</sub> pellets were purchased commercially from Shandong Longsheng Masterbatch Co. (China), whereas the clay TiO<sub>2</sub> pellets were prepared in this experiment. For TiO<sub>2</sub> Clay pellets fabrication, white clays (FUJIFILM Wako pure chemical Co., Japan) and TiO<sub>2</sub> powders (Degussa P25 Titanium Dioxide 99.9%, Evonik industries) were mixed up with 50-60 % distilled water and vigorously stirred at room temperature. Subsequently, these mixtures were heated up to 110 °C for 5 h and added distilled water until it is soft. Then, the product was formed into 4-7 mm of clay TiO<sub>2</sub> pellets. The prepared samples were finally calcined at 600 °C for 2 h in a muffle furnace. The clay TiO<sub>2</sub> pellets containing different TiO<sub>2</sub> content (0, 5, 10, 20, 30, 40 and 50 weight%) were prepared (Table 3.1).

**Table 3.1** Weight ratios of white clay and TiO<sub>2</sub> powder in clay TiO<sub>2</sub> pellets

Clay TiO <sub>2</sub> pellets	TiO <sub>2</sub> powder (%wt)	White clay (%wt)
CT0 pellet	0	100
CT5 pellet	5	95
CT10 pellet	10	90
CT20 pellet	20	80
CT30 pellet	30	70
CT40 pellet	40	60
CT50 pellet	50	50

### 3.2 Catalyst Characterization

#### 3.2.1 Thermogravimetric analysis (TGA)

The thermal behavior of the commercial PE-TiO<sub>2</sub> pellets was carried out with a Thermo plus TG 8120 (Rigaku Corp., Japan) from 20 °C to 800 °C. A heating rate of 10 °C/minute was used under air atmosphere and at a flow rate of 20 mL/minute.

#### 3.2.2 Brunauer-Emmett-Teller (BET) analysis

The specific surface area, pore size and pore volume of clay TiO<sub>2</sub> and PE-TiO<sub>2</sub> pellets were investigated with BELSORP-max apparatus (BEL Japan Inc., Japan) after the samples degassed at 110 °C for 1.5 h.

### 3.2.3 X-Ray diffraction (XRD) analysis

The crystalline structures of clay TiO<sub>2</sub> pellets were determined by x-ray diffraction at room temperature using Bruker D8 Venture diffractometer with CuK $\alpha$  radiation. The diffractometer was operated at 40 kV and 40 mA. The diffractograms were recorded in the range of  $2\theta$  from 15° to 80°.

### 3.2.4 Scanning electron microscopy/energy dispersive X-ray spectroscopy (SEM/EDX) analysis

The morphology and the elemental distribution of Titanium (Ti) in the clay TiO<sub>2</sub> and PE-TiO<sub>2</sub> pellets were evaluated by a scanning electron microscope (SEM, HITACHI SU-5000, Japan) that was equipped with an energy dispersive X-ray spectroscopy (EDX, Horiba, Hitachi High-Technologies, Japan).

### 3.2.5 Atomic force microscope (AFM)

The surface roughness of clay TiO<sub>2</sub> pellets were obtained by using Hitachi AFM5500M system (Hitachi High-Technologies, Japan).

## 3.3 Preliminary test of PE-TiO<sub>2</sub> and clay TiO<sub>2</sub> pellets

In this experiment, methylene blue (MB) was selected as the deputy of organic pollutants. Initially, TiO<sub>2</sub> pellets (PE-TiO<sub>2</sub> and clay TiO<sub>2</sub> pellets) were studied in the absence of light to determine the amount of time that would be necessary to saturate the TiO<sub>2</sub> pellets with MB before exposing under the UV light. In the adsorption experiment, 10 mgL<sup>-1</sup> of MB solutions were mixed with TiO<sub>2</sub> pellets in beakers. A magnetic multi-stirrer or air bubbles pump were used to stir the samples in the darkness. For the photocatalytic activity test, the UV enclosure box which was consisted of an enclosure box with six blacklight (UVA) lamps with the wavelength range of 315-400 nm and peak intensity at 355 nm was used as shown in Figure 3.2.



**Figure 3.2** UV enclosure box for photocatalytic degradation of MB

### 3.3.1 Photocatalytic degradation test of PE-TiO<sub>2</sub> pellets

In this experiment, the varied amounts of PE-TiO<sub>2</sub> pellets (0.5, 1 and 2 gL<sup>-1</sup>) were mixed with 100 mL MB solution (10 mg L<sup>-1</sup>) in 100 ml beaker and placed on top of magnetic stirrer inside a UV enclosure box. Prior to an UV illumination, the solution was magnetically stirred in the dark for 60 mins in order to saturate the MB on PE-TiO<sub>2</sub> pellet surface. The mixture was continued stirring during the photocatalysis reaction under an UVA irradiation at 1700  $\mu\text{W}/\text{cm}^2$  within 120 mins. A 2 mL of sample was collected using a syringe at certain time intervals and then centrifuged with speed 10,000 rpm for 5 mins. Each experiment was repeated three times.

### 3.3.2 Photocatalytic activity test of clay TiO<sub>2</sub> pellets

In this experiment, 2.5 g of clay TiO<sub>2</sub> pellets was mixed with 100 mL MB solution (10 mg L<sup>-1</sup>) in 100 ml beaker and used an air bubbles pump for stirring the solution inside a UV enclosure box. Prior to an UV illumination, the mixture was stirred in the dark for 90 mins in order to saturate the MB on clay TiO<sub>2</sub> pellet surface. The mixture was continued stirring during the photocatalytic process under an UVA irradiation at 1700  $\mu\text{W}/\text{cm}^2$  within 120 mins. A 2 mL of sample was collected using a syringe at certain time intervals and then centrifuge with speed 10,000 rpm for 5 mins. TiO<sub>2</sub> clay pellets comprising of 30, 40 and 50 wt% of TiO<sub>2</sub> (CT30, CT40 and CT50 pellets) were used in this experiment. Each experiment was repeated three times.

### 3.3.3 The reusability of CT30, CT40 and CT50 pellets

Initially, the adsorption of MB on CT30, CT40 and CT50 pellets were studied. In the experiment, 2.5 g of CT30, CT40 or CT50 pellets was mixed with 10 mgL<sup>-1</sup> of MB solution in 100 ml beaker and used an air bubbles pump for stirring the solution. The mixture was stirred in the darkness for 90 mins in order to saturate the clay TiO<sub>2</sub> pellets with MB. Then, only adsorbed pellets were withdrawn from the beaker and placed in dry chamber under UVA light (2497 μw/cm<sup>2</sup>) for 240 mins. Next, these adsorbed pellets were remixed with fresh MB solution (10 mgL<sup>-1</sup>) in 100 ml beaker and continuously stirred in the darkness for 90 mins. All clay TiO<sub>2</sub> pellets at 90 mins under dark condition, at 240 mins under UVA condition dark condition and after remixing for 90 mins under dark condition were measured their surface color. The color of clay TiO<sub>2</sub> pellets were measured by using a HunterLab UltraScan Pro spectrophotometer (UltraScan Pro, Hunter Lab, USA). The values of color were recorded in the CIE LAB color system i.e., L\*, a\* and b\*. The L\* value represents the brightness and L\* value of a perfect black object was 100. The a\* value represents redness (positive a\*) and greenness (negative a\*). The b\* value represents yellowness (positive b\*) and blueness (negative b\*). For MB color on clay TiO<sub>2</sub> pellets, the negative number of b\* value was focused. More negative value indicates that the measured pellets show much more blue (dark blue). Each experiment was repeated three times.

### 3.3.4 Analytical method

The concentration of MB solution was directly determined using Shimadzu UV-1800 UV-Vis spectrophotometer. The methylene blue is measured at 665 nm. The removal efficiency for each sample was calculated from the following equation 3.1:

$$\eta\% = (C_0 - C_t)/C_0 \times 100 \quad (3.1)$$

where  $\eta\%$  is the photodegradation efficiency of MB;  $C_t$  is the amount of MB in solution after  $t$  illumination and  $C_0$  is the initial concentration of MB before illumination.

### 3.4 Photocatalytic degradation of glyphosate

In this experiment, TiO<sub>2</sub> photocatalysts were utilized to investigate the photocatalytic degradation of glyphosate herbicides. The solution was stirred inside the

UV enclosure box. The UV enclosure box was consisted of an enclosure box with six UV lamps as shown in Figure 3.3.



**Figure 3.3** UV enclosure box for photocatalytic degradation of glyphosate

### 3.4.1 Effect of UV types on photocatalytic degradation of glyphosate by $\text{TiO}_2$ powder

Two different types of UV on photocatalytic degradation of glyphosate was studied. Figure 3.4 shows the spectra of the UV lamps i.e., UVA and UVC obtained by using HR4000CG-UV-NIR, ocean optics spectrometers. UVA lamps (Philips TL-D 18W BLB) and UVC lamps (TOKIVA G20T8) showed a significant difference of emission spectra patterns with various wavelengths, represented by the decrease in the intensity of each main emission band.

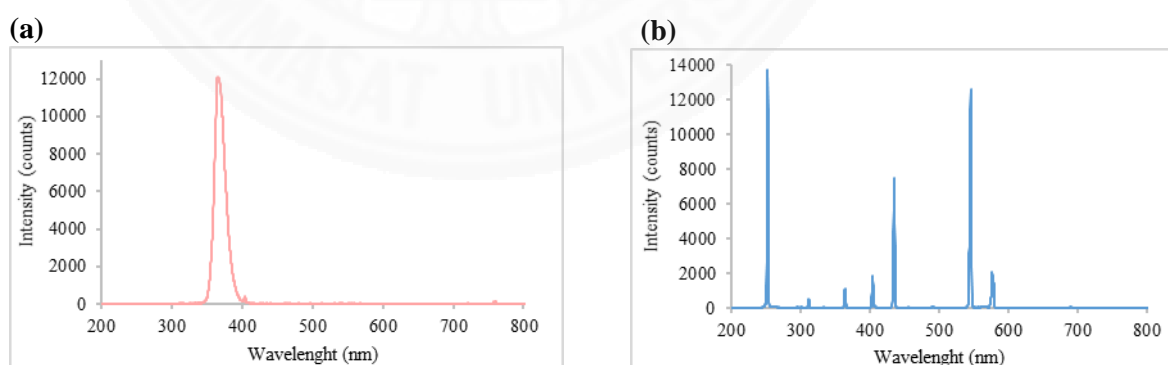


**Figure 3.4** Emission spectra for the UV lamps: (a) UVA (b) UVC

Measure by HR4000CG-UV-NIR, ocean optics spectrometers

The UVA lamp ( $2497 \mu\text{w}/\text{cm}^2$ ) showed only a main band of 368 nm of maximum spectra (Figure 3.4a). However, the UVC lamp ( $1648 \mu\text{w}/\text{cm}^2$ ) emitted three main spectra bands and other additional bands at greater wavelengths. The maximum

spectra was at 253 nm; the main spectra band was at 435 nm and the additional spectra band was at 545 nm (Figure 3.4b).

In the photocatalytic test for glyphosate degradation, the suspension solution was test under the dark and UV light conditions separately. Initially, 0.25 g of  $\text{TiO}_2$  powder was mixed with 400 mL glyphosate solution ( $30 \text{ mgL}^{-1}$ ) in 600 ml beaker. The suspension solution was magnetically stirred in the darkness for 240 mins. For the photocatalytic experiment, the suspension solution was also magnetically stirred in the dark until well-mixed. Then, the suspension solution was continue placed on top of magnetic stirrer inside a UV enclosure box under UVA or UVC light for 240 mins. The 10 mL of sample was withdrawn using a syringe at certain time intervals and then separate the  $\text{TiO}_2$  particles using a  $0.22 \mu\text{m}$  filter paper. Each experiment was repeated three times.

#### **3.4.2 Photocatalytic degradation of glyphosate by clay $\text{TiO}_2$ pellets under UVA irradiation**

In this experiment,  $\text{TiO}_2$  powder and pellets were studied in the absence of light to determine the amount of time that would be necessary to saturate the clay  $\text{TiO}_2$  pellets with glyphosate before exposing under the UV light. Initially, 8 g of clay  $\text{TiO}_2$  pellets i.e., CT30, CT40 or CT50 pellets were mixed with 400 mL glyphosate solution ( $1 \text{ mgL}^{-1}$ ) in 600 ml beaker. Prior to an UV illumination, the solution was stirred by using air bubbles pump in the darkness for 180 mins in order to saturate the clay  $\text{TiO}_2$  pellets surface with glyphosate. Then, the mixture of clay  $\text{TiO}_2$  pellets was continue stirring by using air bubbles pump inside a UV enclosure box. The 10 mL of sample was withdrawn using a syringe at certain time intervals and then separated  $\text{TiO}_2$  particles using a  $0.22 \mu\text{m}$  filter paper. This experiment was proceeded under an UVA illumination ( $2497 \mu\text{W/cm}^2$ ) within 240 mins. Each experiment was repeated three times.

#### **3.4.3 Comparison of photocatalytic activities of $\text{TiO}_2$ powder, CT30 pellets and PE- $\text{TiO}_2$ pellets**

In this experiment, two types of  $\text{TiO}_2$  pellets— CT30 pellets and PE- $\text{TiO}_2$  pellets— were studied for photocatalytic degradation of glyphosate in water. Also, the



removal efficiency of glyphosate by using  $\text{TiO}_2$  pellets was compared to the removal efficiency of glyphosate by using  $\text{TiO}_2$  powder. Considering the practical application, thereby, there no pre-adsorption of glyphosate on the  $\text{TiO}_2$  photocatalysts was performed in this part. The mixture of  $\text{TiO}_2$  photocatalysts was test under the dark and UVA light conditions separately. For  $\text{TiO}_2$  pellets, 8 g of  $\text{TiO}_2$  pellets was mixed with 400 mL glyphosate solution in 600 ml beaker. For the adsorption test, the mixture of  $\text{TiO}_2$  pellets was test under the dark condition for 240 mins. For the photocatalytic experiment, the suspension solution was stirred inside a UV enclosure box for 240 mins. The mixture of clay  $\text{TiO}_2$  pellets was stirred by using air bubble pump, while the mixture of PE- $\text{TiO}_2$  pellets was stirred by using magnetic stirrer (Figure 3.5).



**Figure 3.5** Photocatalytic degradation set-up for  $\text{TiO}_2$  pellets

As part of  $\text{TiO}_2$  powder, 14 mg of  $\text{TiO}_2$  powders was mixed with 400 mL glyphosate solution in 600 ml beaker and placed on top of magnetic stirrer inside a UV enclosure box. Prior to an UV illumination, the suspension solution was magnetically stirred in the dark until well-mixed. Then, the suspension solution was continue stirring during the photocatalysis process for 240 mins. The 10 mL of sample was withdrawn using a syringe at certain time intervals and then separate the  $\text{TiO}_2$  particles using a  $0.22\ \mu\text{m}$  filter paper (Figure 3.5). This part was proceeded under an UVA illumination at  $2497\ \mu\text{w}/\text{cm}^2$  within 240 mins. The initial concentration of glyphosate and were  $1\ \text{mgL}^{-1}$ . Each experiment was repeated three times.



**Figure 3.6** Photocatalytic degradation set-up of TiO<sub>2</sub> powder

### 3.4.4 Glyphosate Analysis

The amount of glyphosate was directly determined using IC (Ion chromatography). The IC used was a Dionex Model ICS-5000 connected with a Variable Wavelength Detector (VWD), Ion Pac AG11 (4 x 50 mm), AS11 (4 x 250 mm) guard, ASRS-300 (4 mm) self-regenerating suppressor, EG Eluent Generator, and AS-HV auto sampler. Under this condition the retention time for glyphosate was around 10.50 min (Figure 3.7). The removal efficiency for each sample was calculated using the following equation 3.2:

$$\eta\% = (C_0 - C_t)/C_0 \times 100 \quad (3.2)$$

where  $\eta\%$  is the removal efficiency of glyphosate;  $C_t$  is the concentration of glyphosate in the solution after  $t$  illumination and  $C_0$  is the initial concentration of glyphosate before illumination.

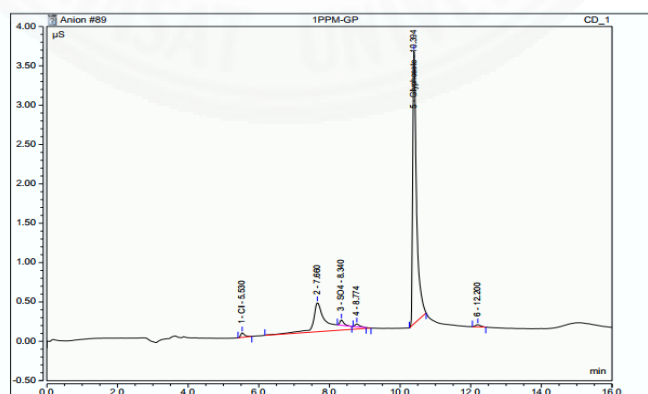


**Figure 3.7** Chromatogram of glyphosate standard with concentration of 1 mgL<sup>-1</sup>



The calibration curve of glyphosate standard was constructed by using peak area versus glyphosate concentration (Figure 3.8). The response is linear from 0 to 1.25 mgL<sup>-1</sup>.

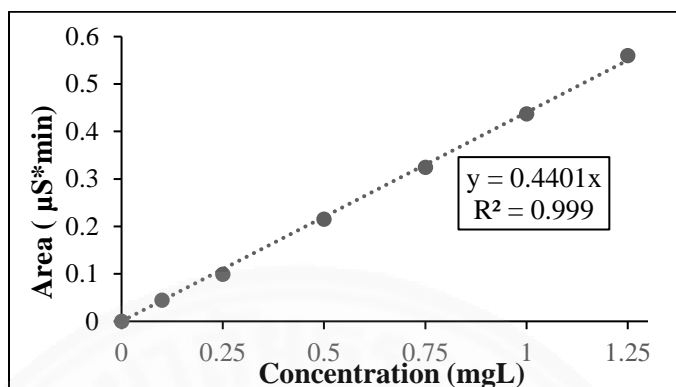


**Figure 3.8** Calibration curve of glyphosate standard with concentration of 0- 1.25 mgL<sup>-1</sup>

### 3.5 Mechanisms of the photocatalytic degradation of glyphosate

The mechanisms of the photocatalytic degradation of glyphosate were investigated by using TiO<sub>2</sub> powder and clay TiO<sub>2</sub> pellet. The procedure set-up in this part was similar to 3.4.2. The sample was withdrawn using a syringe at certain time intervals to determine by-products of glyphosate.

Through the possible degradation pathways, it is presumed that decomposition of glyphosate released AMPA, glycolic acid, sarcosine, phosphoric acid (H<sub>3</sub>PO<sub>4</sub>), carbon dioxide (CO<sub>2</sub>) and, inorganic anions i.e. phosphate (PO<sub>4</sub><sup>3-</sup>) and nitrate (NO<sub>3</sub><sup>-</sup>). Among these byproducts AMPA is initially produced and frequently occurs within glyphosate decomposition, while (PO<sub>4</sub><sup>3-</sup>) is stable major byproduct. In relation to glyphosate decomposition pathway, the products monitored were AMPA and PO<sub>4</sub><sup>3-</sup>. PO<sub>4</sub><sup>3-</sup> which could be identified under the same operation of glyphosate. The retention time for PO<sub>4</sub><sup>3-</sup> was around 11 min (Figure 3.9). Meanwhile, AMPA determination was examined by using 6495 Triple Quadrupole Liquid chromatography–mass spectrometry (LC–MS, Agilent Technologies, USA) which was carried out using Agilent Poroshell 120 HILIC-Z, (2.7 μm, 2.1 mm × 100 mm) with a HILIC guard column (2.7 μm, 2.1 mm × 5 mm). Under this condition, the retention time for glyphosate was around 1.40 mins (Figure 3.11).

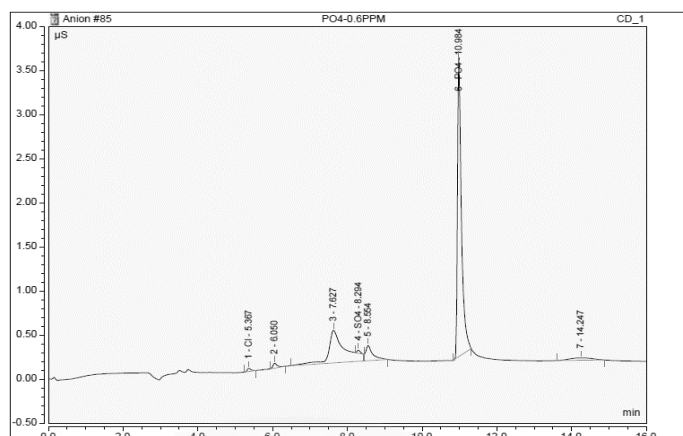


**Figure 3.9** Chromatogram of  $\text{PO}_4^{3-}$  standard with concentration of  $0.6 \text{ mgL}^{-1}$

The calibration curve of  $\text{PO}_4^{3-}$  standard was constructed by using peak area versus glyphosate concentration (Figure 3.9). The response is linear from 0 to  $0.6 \text{ mgL}^{-1}$ .

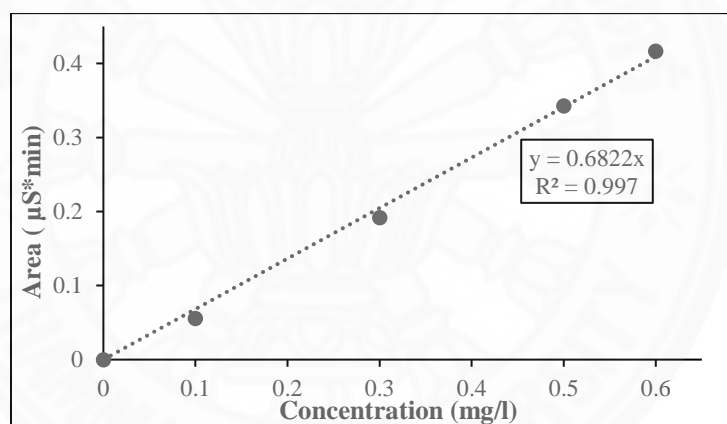


**Figure 3.10** Calibration curve of  $\text{PO}_4^{3-}$  standard with concentration of 0-  $0.6 \text{ mgL}^{-1}$

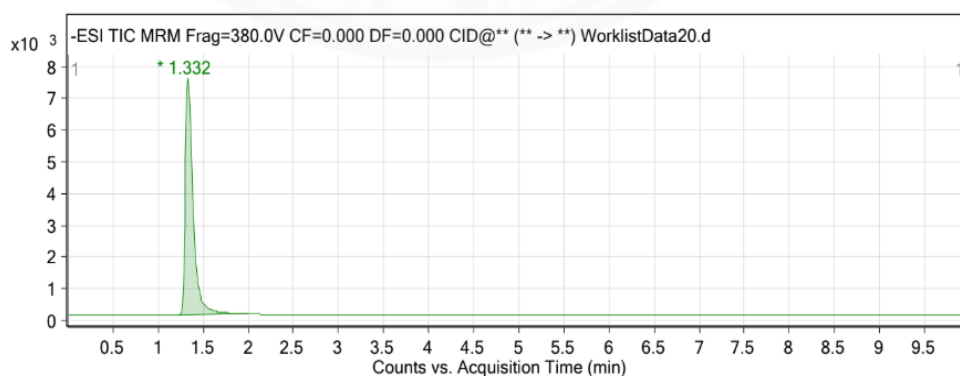


**Figure 3.11** Chromatogram of AMPA standard with concentration of  $0.5 \text{ mgL}^{-1}$

The calibration curve of AMPA standard was constructed by using peak area versus glyphosate concentration (Figure 3.12). The response is linear from 0 to 0.6 mgL<sup>-1</sup>.

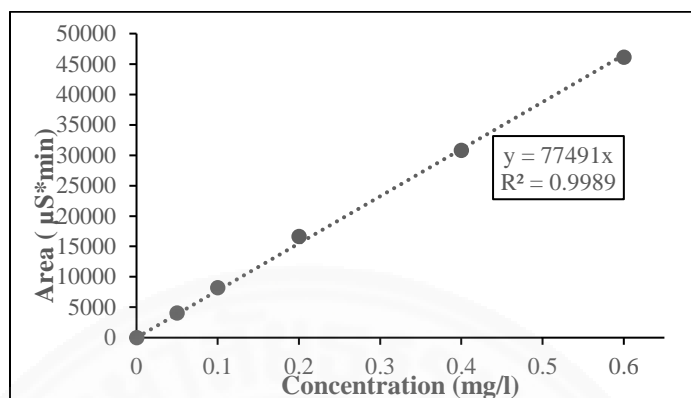


**Figure 3.12** Calibration curve of AMPA standard with concentration of 0-0.6 mgL<sup>-1</sup>

## CHAPTER 4

### RESULTS AND DISCUSSION

#### 4.1 TiO<sub>2</sub> pellet preparation

In the experiment, 2 types of TiO<sub>2</sub> pellets—prepared clay TiO<sub>2</sub> pellets and commercial TiO<sub>2</sub> pellets— have been focused. The clay TiO<sub>2</sub> pellets were prepared in this experiment, whereas the PE-TiO<sub>2</sub> pellets were purchased commercially.

##### 4.1.1 The appearance of TiO<sub>2</sub> Pellets

In the experiment, 2 types of TiO<sub>2</sub> pellets—prepared TiO<sub>2</sub> pellets and commercial TiO<sub>2</sub> pellets— are shown in Figure 4.1. All clay TiO<sub>2</sub> pellets comprising of 0, 5, 10, 20, 30, 40 and 50 wt% of TiO<sub>2</sub> (CT0, CT5, CT910, CT20, CT30, CT40 and CT50 pellets, respectively) had a similar external appearance (Figure 4.1b-h). The Characteristics of TiO<sub>2</sub> Pellets are shown in Table 4.1.

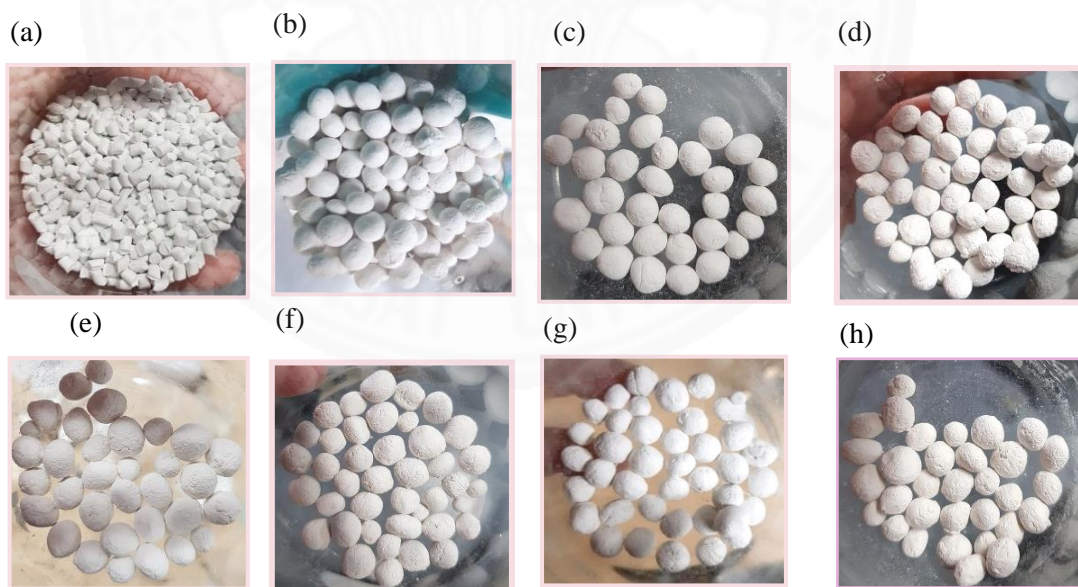


**Figure 4.1** The appearance of TiO<sub>2</sub> pellets: (a) PE-TiO<sub>2</sub> pellets, (b) CT0 pellets, (c) CT5 pellets, (d) CT10 pellets, (e) CT20 pellets, (f) CT30 pellets, (g) CT40 pellets and (h) CT50 pellets

**Table 4.1** Characteristics of pellets

TiO <sub>2</sub> pellets	Diameter (mm)	Weight (g/ 1 unit)	Shape	Color	Stability
PE-TiO <sub>2</sub> Pellet	2.7 ± 0.1	0.02±0.00	cylinder	White	√
CT0 pellet	5.97± 0.96	0.22±0.04	Sphere	White	X
CT5 pellet	5.97± 0.96	0.22±0.04	Sphere	White	X
CT10 pellet	5.97± 0.96	0.22±0.04	Sphere	White	X
CT20 pellet	5.97± 0.96	0.22±0.04	Sphere	White	X
CT30 pellet	5.97± 0.96	0.22±0.04	Sphere	White	√
CT40 pellet	5.97± 0.96	0.22±0.04	Sphere	White	√
CT50 pellet	5.97± 0.96	0.22±0.04	Sphere	White	√

Note: √ Pellets were stable in water

X Pellets were unstable in water.

#### 4.1.2 The stability of TiO<sub>2</sub> pellets in water

After immersion in water for 10 mins, the CT0, CT5 and CT10 pellets broke down immediately (Figure 4.2b-d)). Clay- TiO<sub>2</sub> particles on CT0 pellets spread out more quickly than CT5 and CT10 pellets, respectively. It can be seen that the stability of the clay TiO<sub>2</sub> pellets in water decreases with the increasing clay content. This is because that the calcination temperature at 600 °C does not enough to produce strong clay TiO<sub>2</sub> pellets. Generally, calcination temperature should be over 1000 °C to produce strong clay TiO<sub>2</sub> pellets. All water molecules are removed from clay particles. Neighboring clay particles become connecting to each other, with strong oxygen bridge (Breuer, 2012). Also, clay- TiO<sub>2</sub> particles of CT20 pellets gradually broke down after immersion (Figure 4.2e). However, the CT30, CT40 and CT50 pellets were stable in water for a long time, and the loss of clay- TiO<sub>2</sub> particles was minimal (Figure 4.2f-h). The stability was depended on the weight ratio of TiO<sub>2</sub> and clay. As calcination at 600 °C, new chemical bonds are generated between clay and TiO<sub>2</sub>. TiO<sub>2</sub> connects to clay via Si–O–Ti and Al–O–Ti bonds, resulting in improved the stability of the pellets in water (B. Wang, Ding, & Deng, 2010; Q. Zhang et al., 2013). Thereby, CT30, CT40 and CT50 pellets will be applied for the photodegradation of glyphosate.

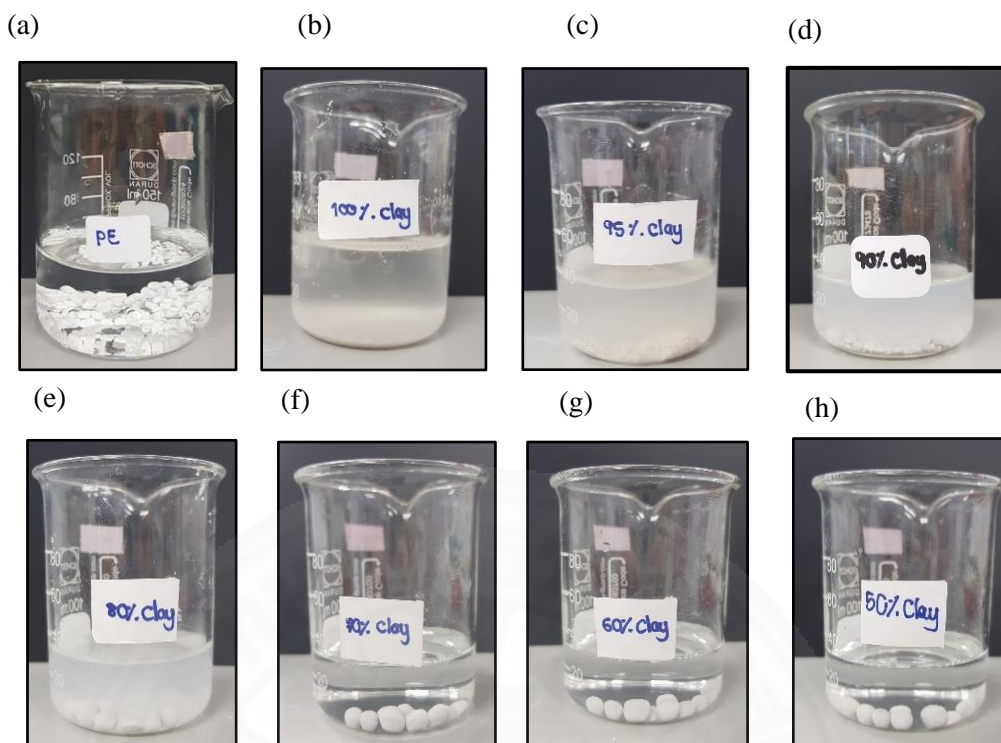


**Figure 4.2** The stability of clay TiO<sub>2</sub> pellets in water by observed the turbidity for 10 mins: (a) PE-TiO<sub>2</sub> pellets, (b) CT0 pellets, (c) CT5 pellets, (d) CT10 pellets, (e) CT20 pellets, (f) CT30 pellets, (g) CT40 pellets and (h) CT50 pellets

## 4.2 Catalyst characterization

In this experiment, TiO<sub>2</sub> pellets were characterized by X-ray diffraction (XRD), Brunauer-Emmett-Teller (BET) and scanning electron microscopy with energy dispersive X-ray spectroscopy (SEM/EDX) and Atomic force microscope (AFM).

### 4.2.1 Thermogravimetric analysis and Differential thermal analysis (TGA/DTA)

TGA/DTA is widely used to measure the thermal decomposition of material as a function of temperature or mass loss in a controlled atmosphere. The measurement was used fundamentally to confirm the component of PE-TiO<sub>2</sub> pellets through the thermal properties of material.



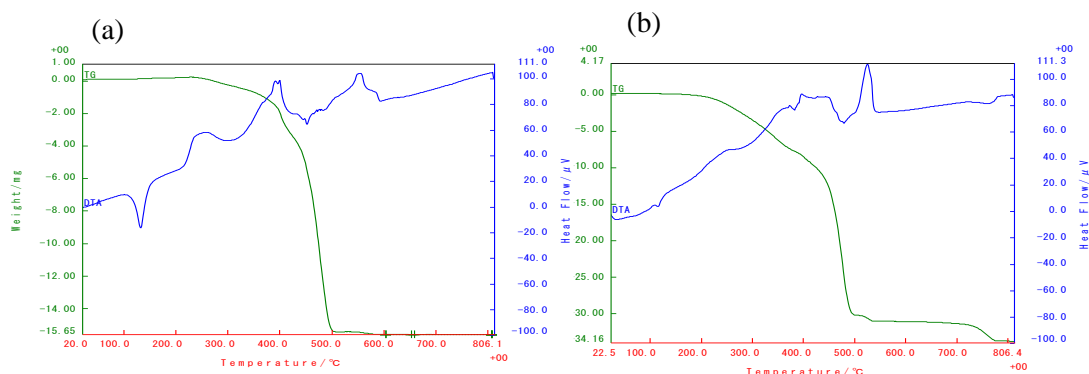


**Figure 4.3** TGA-DTA curves: (a) PE Pellets and (b) PE-TiO<sub>2</sub> Pellets

From the TGA curve of PE pellets, it can be seen that the PE pellets were undergone thermal degradation beginning from 200 °C to 500 °C with a mass loss of 98.16%. Above this temperature the TGA curve did not exhibit any peak (Figure 4.3a). Also, the PE-TiO<sub>2</sub> pellets showed four decomposition steps in the temperature from 20 to 800°C. In the first weight loss stage below 200 °C, the weight loss was due to the loss of water molecules in the PE-TiO<sub>2</sub> pellets with 0.37 wt%. As part of second step, the high weight loss, approximately 38.68% was observed in the TGA curve, assigned to the combustion of PE. For the third step, it can be observed that the DTA curve of PE-TiO<sub>2</sub> pellets showed exothermic peaks at the temperature ranges from 500 and 550°C corresponding to the phase transformation of TiO<sub>2</sub> from anatase to rutile. Above this temperature, the weight loss over 800 °C was around 41.66 wt% (Figure 4.3b). Thereby, PE was confirmed in the PE-TiO<sub>2</sub> pellets, as claimed by the manufacturer.

#### 4.2.2 BET analysis

The surface area, pore volume and pore size of PE-TiO<sub>2</sub> and clay TiO<sub>2</sub> pellets were investigated (as shown in Table 4.2). In the manufacturers specifications, TiO<sub>2</sub> powder showed a large surface area, and its value reaches  $50 \pm 15$  m<sup>2</sup>/g (Evonik Industries, Thailand). Also, Raj and Viswanathan (2009) investigated that TiO<sub>2</sub> powder has pore volume 0.177 cm<sup>3</sup>/g and pore size 17.5 nm. As a result, the surface area and pore volume of the clay TiO<sub>2</sub> pellets decreased, compared with TiO<sub>2</sub> powder.

Moreover, the CT30, CT40 and CT50 pellets had quite similar surface areas, pore volumes and pore sizes, whereas the surface area, pore volume and pore size of the PE-TiO<sub>2</sub> pellets were considerably less than clay TiO<sub>2</sub> pellets. This result indicates

that such large surface areas, pore volume and pore size of clay TiO<sub>2</sub> pellets were presumably better candidate material for photocatalytic activity than PE-TiO<sub>2</sub> pellets.

**Table 4.2** BET surface area, pore volume and pore size of TiO<sub>2</sub> samples

Sample	Surface area (m <sup>2</sup> /g)	Pore volume (cm <sup>3</sup> /g)	Pore size (nm)
<b>TiO<sub>2</sub> powder</b>	50 ± 15*	0.250*	17.500*
<b>PE-TiO<sub>2</sub> Pellet</b>	2.160	0.005	7.541
<b>CT30 pellet</b>	30.710	0.145	20.465
<b>CT40 pellet</b>	36.989	0.203	24.493
<b>CT50 pellet</b>	33.124	0.153	18.836

Note: \* cite from Raj & Viswanathan, 2009

#### 4.2.3 XRD analysis

XRD patterns of the TiO<sub>2</sub> powder is shown in Figure 4.4. The obtained XRD pattern of calcined and non-calcined TiO<sub>2</sub> powders were not different (Figure 4.4). It can be seen that both rutile and anatase phases obviously appeared in both TiO<sub>2</sub> powder samples. A strong peak of TiO<sub>2</sub> Powder appearing at 25.30°, 38.56°, 48.04°, 53.89°, 57.06°, 70.29° and 76.03° corresponded to anatase TiO<sub>2</sub>. On the other hand, the peaks of rutile phase were detected at 2θ = 27.41°, 36.04°, 41.19°, 43.99°, 63.97°, 71.33° and 73.31°. The percentage of crystalline phases of the calcined TiO<sub>2</sub> powder is quite similar to non-calcined TiO<sub>2</sub> powder (Table 4.3). Also, previously reported by Bayan, Lupeiko, Kolupaeva, Pustovaya, and Fedorenko (2017); (Raj & Viswanathan, 2009) revealed that the phase transition from anatase to rutile in TiO<sub>2</sub> occurred at temperatures of above 700 °C. Bowering, Croston, Harrison, and Walker (2007) similarly investigate that after calcination at 600 °C for 2 h, the relative intensity of anatase to rutile phases increased slightly. With increasing temperature above 600 °C, the intensities of anatase diffraction peaks decreased gradually, and no anatase peaks was observed at 800 °C. However, increasing calcination time also caused the considerable change in the anatase to rutile transformation. After calcination TiO<sub>2</sub> powders at 600°C for 4 h, the content of rutile reached 44.8%, while the content of rutile was 55.2% (G. Wang, Xu, Zhang, Yin, & Han, 2012).



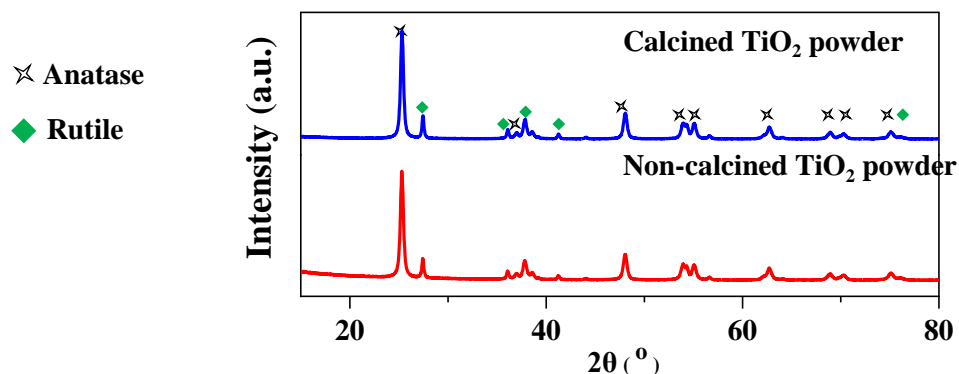


**Figure 4.4** XRD diffraction patterns of the  $\text{TiO}_2$  powder

For XRD patterns of the white clay, quartz and pyrophyllite represented as typical mineral mixtures of white clay (Figure 4.5). No phase transformation of calcined clay was observed at 600 °C for 2 h. These mineral clays started transforming after being heated to over 1000 °C (Sanchez-Soto & Perez-Rodriguez, 1989; Zheng, Ren, Gao, Zhang, & Bian, 2018). The overall result indicated calcination at 600 °C for 2 h does not have significant in transforming the composition of  $\text{TiO}_2$  and the white clay.

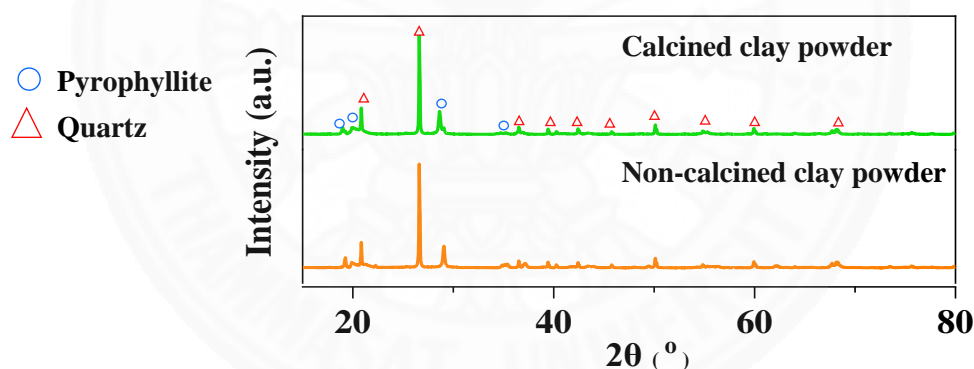


**Figure 4.5** XRD diffraction patterns of the  $\text{TiO}_2$  white clay

Figure 4.6 confirms that in the PE- $\text{TiO}_2$  pellets, only anatase phase obviously appeared, as claimed by the manufacturer. XRD patterns exhibited strong diffraction peaks at 25.65°, 38.27°, 48.38°, 54.23°, 55.66°, 63.20°, 68.99°, 70.78°, 75.37°, and 76.81° indicating  $\text{TiO}_2$  in the anatase phase. Meanwhile, the presence of quartz, pyrophyllite, rutile and anatase  $\text{TiO}_2$  was also detected in all the clay  $\text{TiO}_2$  pellets. The phase contents of  $\text{TiO}_2$  in clay  $\text{TiO}_2$  pellets are also shown in Table 4.3. The percentage of anatase and rutile contents in CT30, CT40 and CT50 pellets were similar. The result was also similar to the non-calcined  $\text{TiO}_2$  powder. Evidently, these mineral mixtures of white clay had no obvious effect on any composition change in  $\text{TiO}_2$  of clay  $\text{TiO}_2$

pellets. Also, the decrease of the TiO<sub>2</sub> weight ratios in clay TiO<sub>2</sub> pellet was related to a decrease in the peak intensity of anatase and rutile phases. Overall, all obtained TiO<sub>2</sub> pellets were observed rutile and anatase TiO<sub>2</sub> which were presumably good materials for photocatalytic activity.

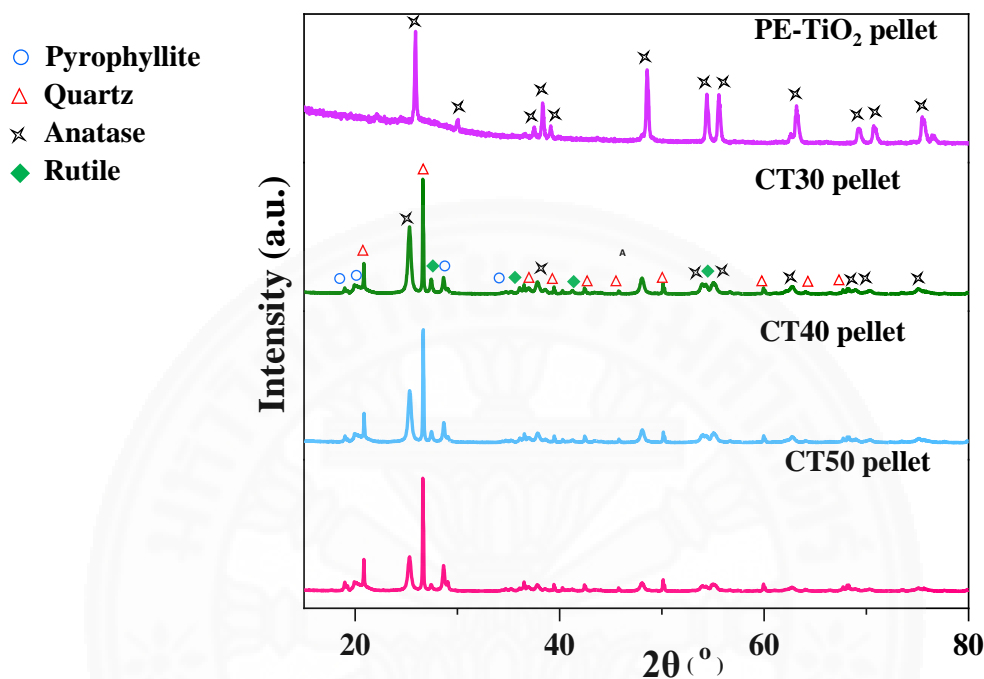


**Figure 4.6** XRD diffraction patterns of PE-TiO<sub>2</sub> pellets and clay TiO<sub>2</sub> pellets

**Table 4.3** The ratio of anatase and rutile phases of TiO<sub>2</sub> samples

Sample	TiO <sub>2</sub> phase (wt%)	
	Anatase	Rutile
Non-calcined TiO <sub>2</sub> powder	80.35±4.31	19.65±4.31
Calcined TiO <sub>2</sub> powder	80.50±0.42	19.50±0.42
PE-TiO <sub>2</sub> Pellet	79.20±2.83	20.80±2.83
CT30 pellet	79.20±2.83	20.05±0.66
CT40 pellet	78.45±2.62	21.55±2.62
CT50 pellet	80.35±4.31	19.65±4.31

Note: Each value represents the mean ± S.D

#### 4.2.4 SEM/EDX analysis

SEM images and results of EDX analysis of clay TiO<sub>2</sub> pellets are shown in Figure 4.7. CT50 pellets exhibited a smoother surface than CT 30 and CT40 pellets (Figure 4.7). Obviously, as the amount of the TiO<sub>2</sub> increased, surface of the clay TiO<sub>2</sub> pellets became smooth. Also, EDX mapping analysis revealed that the Titanium (Ti), Silica (Si) and Aluminum (Al) were uniformly distributed either throughout the entire external or internal surface of CT 30, CT40 and CT50 pellets. Furthermore, EDX results showed that Ti was found in both external and internal surfaces of CT30, CT40 and CT50 pellets in the range from 15.5 to 15.9 %wt, 21.1 to 25.4%wt and 25.3 to 35.4 %wt, respectively (Table 4.4).

**Table 4.4** EDX analysis of clay TiO<sub>2</sub> pellets

Sample	Al (%wt)	Si (%wt)	Ti (%wt)
<b>CT30 pellet</b>	5.62±0.50	15.50±0.95	15.68±1.73
<b>CT40 pellet</b>	4.58±0.59	13.63±0.63	23.2±2.98
<b>CT50 pellet</b>	3.73±0.91	11.63±2.04	30.33±5.88

Note: Each value represents the mean ± S.D.

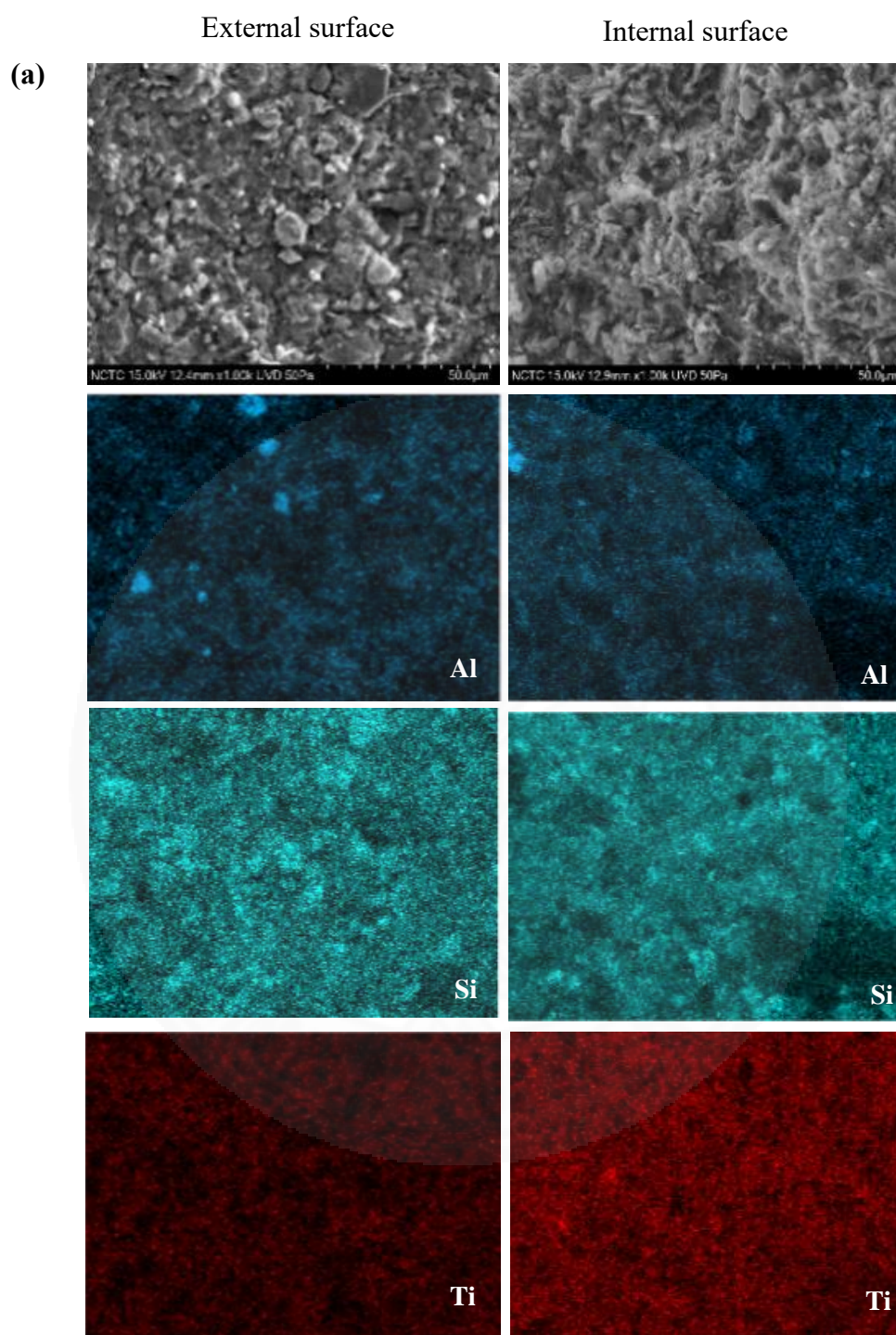


**Figure 4.7** SEM and EDX mapping images of clay TiO<sub>2</sub> pellets:  
 (a) CT30 pellets, (b) CT40 pellets and (c) CT50 pellets



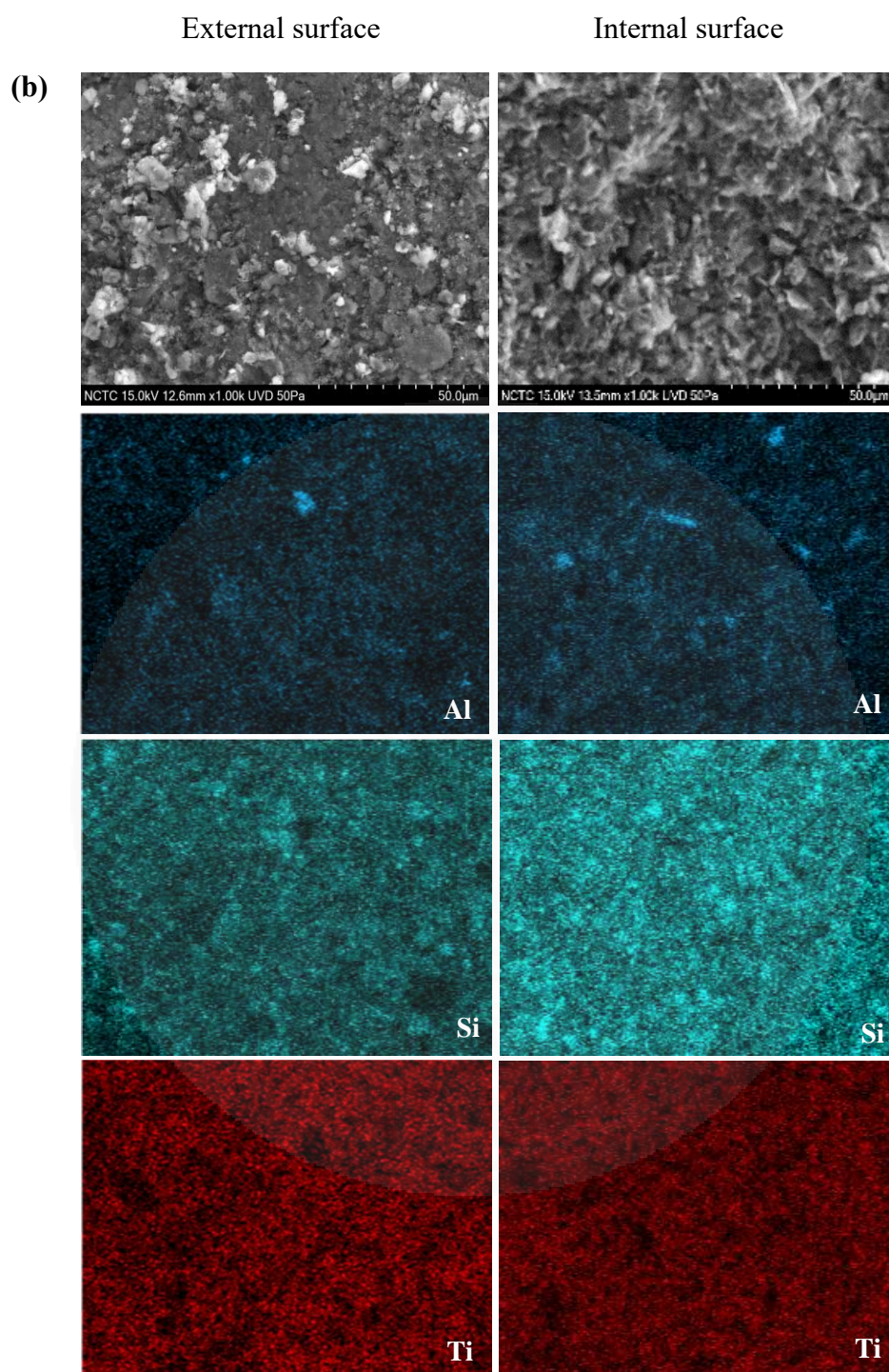


**Figure 4.7** SEM and EDX mapping images of clay TiO<sub>2</sub> pellets:  
 (a) CT30 pellets, (b) CT40 pellets and (c) CT50 pellets

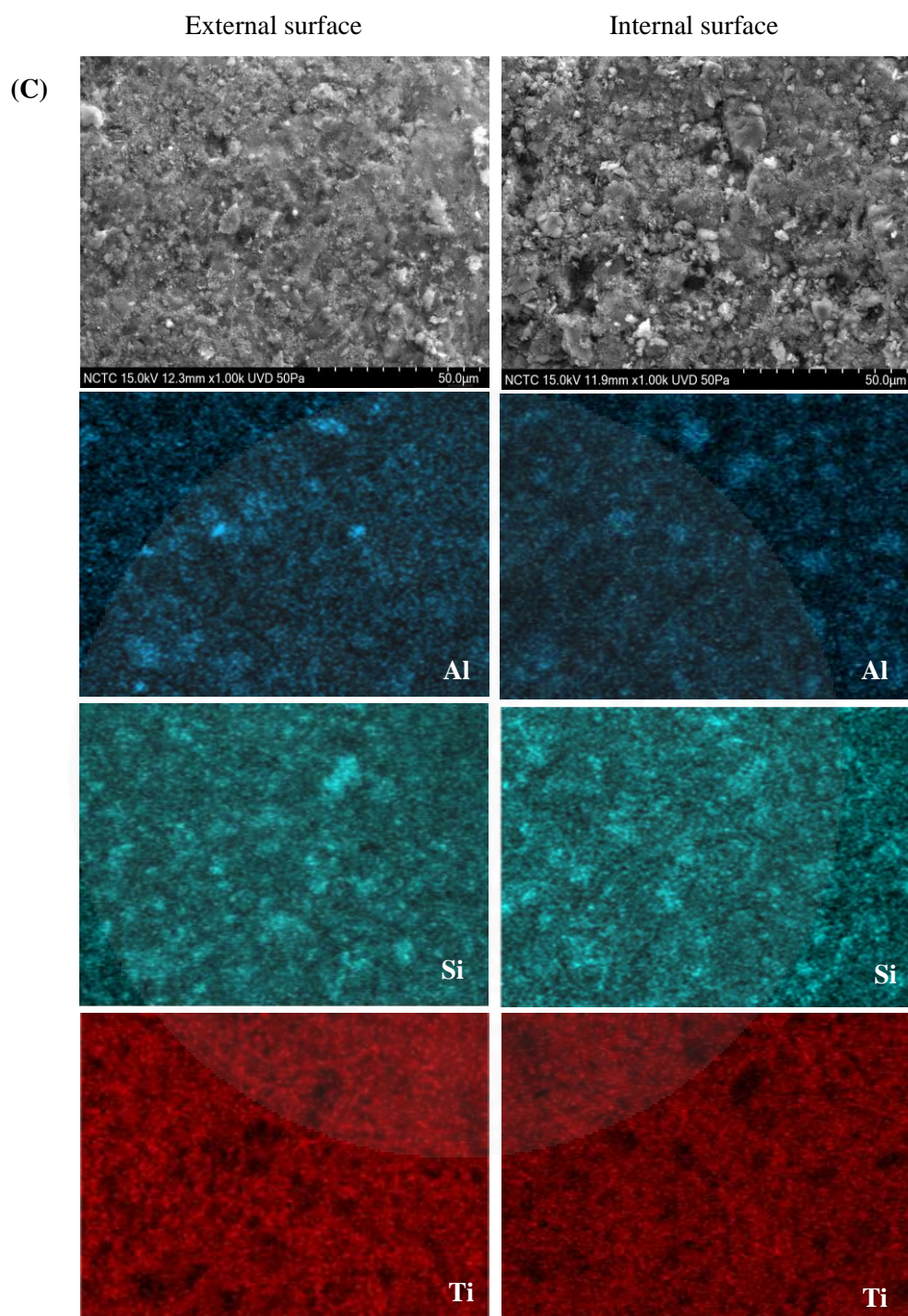


**Figure 4.7** SEM and EDX mapping images of clay TiO<sub>2</sub> pellets:  
 (a) CT30 pellets, (b) CT 40 pellets and (c) CT50 pellets



#### 4.2.4 Atomic force microscope (AFM)

The AFM images of clay TiO<sub>2</sub> pellets are shown in Figure 4.8. Figure 4.8a-c shows two dimensional (2D) and three dimensional (3D) of surface roughness CT30, CT40 and CT50 pellets, respectively.

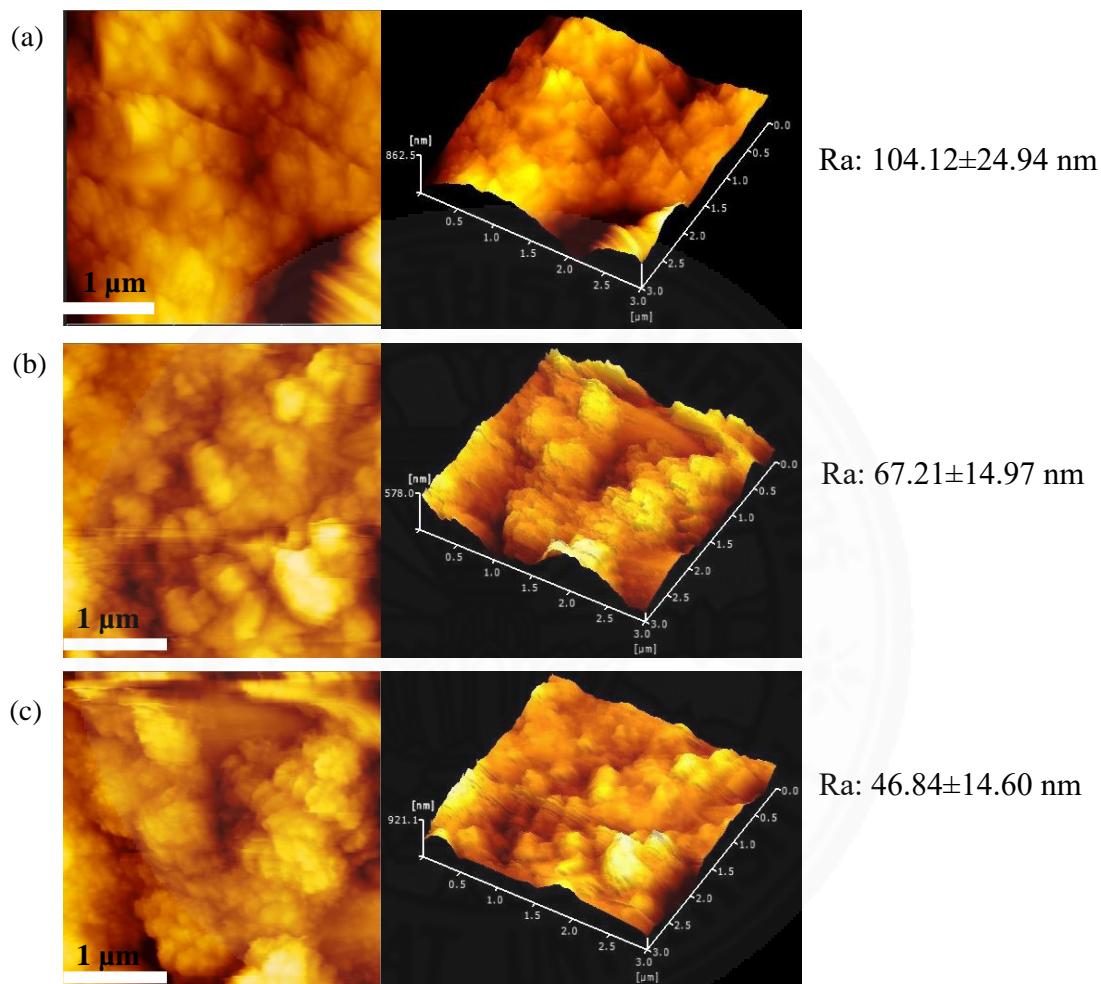


**Figure 4.8** Surface roughness by AFM

(a) CT30 pellets, (b) CT 40 pellets and (c) CT50 pellets

With the increase of clay content, the surface of the pellet became smoother. According to AFM analysis, the roughness values (Ra) of CT30, CT40 and CT50 pellets were  $104.12 \pm 24.94$  nm,  $67.21 \pm 14.97$  nm and  $46.84 \pm 14.60$  nm, respectively. CT30 pellets exhibited a rougher surface than CT 40 and CT50 pellets

### 4.3 Preliminary Test of PE-TiO<sub>2</sub> and Clay TiO<sub>2</sub> pellets

Preliminary, the photocatalytic activities of PE-TiO<sub>2</sub> pellets and clay TiO<sub>2</sub> pellets i.e., CT30, CT40 and CT50 pellets were studied by using methylene blue (MB) as a model organic pollutant. The different amount of PE-TiO<sub>2</sub> pellets was studied on photocatalytic degradation of MB. Also, CT30, CT40 and CT50 pellets were used for the photocatalytic degradation of MB.

#### 4.3.1 Photocatalytic degradation test of PE-TiO<sub>2</sub> pellets

The different amount of PE-TiO<sub>2</sub> pellet was studied for influencing on efficiency of photocatalytic reaction. Prior to an UV illumination, PE-TiO<sub>2</sub> pellets were studied in the absence of light to determine the amount of time that would be necessary to saturate the TiO<sub>2</sub> photocatalysts with MB before exposing under the UV light. Also, the concentration of MB adsorbed on PE-TiO<sub>2</sub> pellets and removal efficiency of MB under the dark condition were calculated as shown in Table 4.5 and Figure 4.9.

**Table 4.5** MB concentration during the adsorption test by using PE-TiO<sub>2</sub> pellets

Under the dark condition				
Sample	2 gL <sup>-1</sup> of PE pellet	0.5 gL <sup>-1</sup> of PE- TiO <sub>2</sub> pellet	1 gL <sup>-1</sup> of PE- TiO <sub>2</sub> pellet	2 gL <sup>-1</sup> of PE- TiO <sub>2</sub> pellet
Time (min)	Conc. (mgL <sup>-1</sup> )	Conc. (mgL <sup>-1</sup> )	Conc. (mgL <sup>-1</sup> )	Conc. (mgL <sup>-1</sup> )
0	8.56±0.33	9.05±0.31	9.34±0.53	8.79±0.02
30	8.04±0.36	8.80±0.32	9.19±0.37	8.62±0.05
60	7.71±0.46	8.76±0.32	8.74±0.73	8.49±0.14
90	7.65±0.45	8.70±0.40	8.69±0.67	8.44±0.09
120	7.53±0.36	8.59±0.26	8.60±0.71	8.27±0.13
180	7.43±0.15	8.39±0.17	8.41±0.46	8.11±0.06
240	7.20±0.03	8.14±0.37	8.22±0.52	7.74±0.16

Note: Each value represents the mean ± S.D. (n = 3)



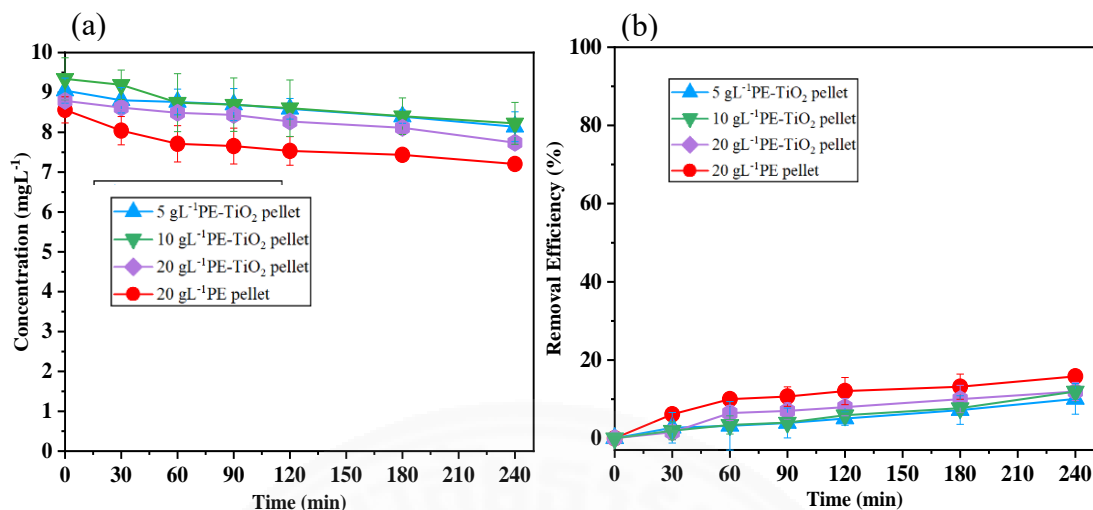


**Figure 4.9** Effect of PE-TiO<sub>2</sub> pellet loading on the removal of MB under dark condition: (a) concentration of MB and (b) removal efficiency of MB

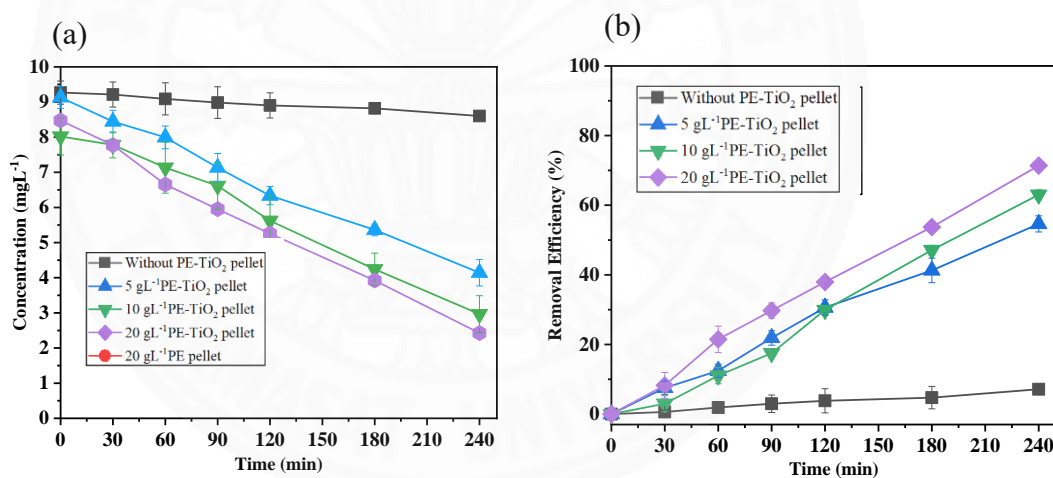
In the presence of PE pellets with MB under the dark condition, the concentration of MB was decreased from 8.56 to 7.20 mgL<sup>-1</sup>, with 15.87% removal efficiency within 240 mins (Figure 4.9). In the presence of PE-TiO<sub>2</sub> pellets, the concentration of MB adsorbed by using 5, 10 and 20 gL<sup>-1</sup> of PE-TiO<sub>2</sub> pellets were decreased from 9.05 to 8.14 mgL<sup>-1</sup>, 9.34 to 8.22 mgL<sup>-1</sup> and 8.79 to 7.74 mgL<sup>-1</sup>, respectively as shown in Table 4.5 and Figure 4.9a. The removal efficiencies at different PE-TiO<sub>2</sub> pellets loading of 5, 10 and 20 gL<sup>-1</sup> were 10.05%, 11.99%, 11.95%, respectively (Figure 4.9b). Also, it can be seen that the concentration of MB adsorbed by different PE-TiO<sub>2</sub> pellets loading became quite stable after 60 mins. Therefore, the PE-TiO<sub>2</sub> pellet was stirred in MB solution under the dark condition for 60 mins in order to saturate the PE-TiO<sub>2</sub> pellet with MB before exposing under the UV light. For photocatalytic reaction of MB, the concentration of MB and removal efficiency of MB were calculated as shown in Table 4.6 and Figure 4.10.

**Table 4.6** MB concentration during photocatalytic reaction by using PE-TiO<sub>2</sub> pellets

Under the UVA light condition				
Sample	Without pellet*	0.5 gL <sup>-1</sup> of PE- TiO <sub>2</sub> pellet	1 gL <sup>-1</sup> of PE- TiO <sub>2</sub> pellet	2 gL <sup>-1</sup> of PE- TiO <sub>2</sub> pellet
Time(min)	Conc. (mgL <sup>-1</sup> )	Conc. (mgL <sup>-1</sup> )	Conc. (mgL <sup>-1</sup> )	Conc. (mgL <sup>-1</sup> )
0	9.27±0.63	9.13±0.03	8.02±0.06	8.47±0.14
30	9.21±0.67	8.44±0.15	7.78±0.13	7.77±0.19
60	9.09±0.51	7.99±0.15	7.13±0.13	6.65±0.21
90	8.98±0.38	7.13±0.17	6.62±0.13	5.95±0.09
120	8.90±0.28	6.34±0.18	5.62±0.05	5.26±0.16
180	8.82±0.30	5.63±0.30	4.24±0.08	3.92±0.12
240	8.60±0.49	4.14±0.20	2.97±0.09	2.43±0.07

Note: Each value represents the mean ± S.D. (n = 3)

\* MB solution was stirred under UVA light without PE- TiO<sub>2</sub> pellets.

**Figure 4.10** Effect of PE-TiO<sub>2</sub> pellet loading on the removal of MB under UVA light:

(a) concentration of MB and (b) removal efficiency of MB

In the absence of PE-TiO<sub>2</sub> pellets with MB under the UVA light, the concentration of MB was decreased from 9.27 to 8.60 mgL<sup>-1</sup>, with 7.23 % removal efficiency which even after 240 mins. The result was negligible when UVA was used alone which appeared lower value of degradation. For the photocatalytic reaction, the study found that the presence of PE-TiO<sub>2</sub> pellets significantly enhanced the removal efficiency of MB. As the number of PE-TiO<sub>2</sub> pellets increased from 5 to 20 gL<sup>-1</sup>, the removal efficiency of MB increased from 54.65% to 72.37%, respectively. After 240

mins, the concentration of MB adsorbed by 2 gL<sup>-1</sup> of PE-TiO<sub>2</sub> pellets was decreased from 8.47 to 2.43 mgL<sup>-1</sup> (Figure 4.10a). The removal efficiency of MB was reached a maximum at 72.37% (Figure 4.10b). The increase PE-TiO<sub>2</sub> pellets loading lead to increase of the number of active sites on the photocatalyst surface. This can also increase the number of reactive oxygen species (ROS) such as hydroxide ( $\bullet\text{OH}$ ) radicals and superoxide radical ions ( $\bullet\text{O}_2^-$ ) to remove MB. These  $\bullet\text{OH}$  and  $\bullet\text{O}_2^-$  are strong enough to remove MB adsorbed on the surface (J. Q. Chen et al., 2012; S. Chen & Liu, 2007; Umar & Aziz, 2013). As a result, PE-TiO<sub>2</sub> pellets can be immersed in water with easily to separate from the water and they had an efficient photocatalytic degradation of MB. Consequently, they can be used for on the photocatalytic degradation of glyphosate.

#### 4.3.2 Photocatalytic degradation test of clay TiO<sub>2</sub> pellets

Different weight percentage of TiO<sub>2</sub> in the range of 30, 40 and 50 wt% of TiO<sub>2</sub> (CT30, CT40 and CT50 pellets) were used to investigate for the photocatalytic degradation of MB. Prior to an UV illumination, clay TiO<sub>2</sub> pellets were studied in the absence of light to determine the amount of time that would be necessary to saturate the TiO<sub>2</sub> photocatalysts with MB before exposing under the UV light. Also, the concentration of MB adsorbed on clay TiO<sub>2</sub> pellets and removal efficiency of MB under the dark condition were calculated as shown in Table 4.7 and Figure 4.11.

**Table 4.7** MB concentration during the adsorption test by using clay TiO<sub>2</sub> pellets

Sample Time (min)	Under the dark condition			
	CT0 pellet** Conc. (mgL <sup>-1</sup> )	CT30 pellet Conc. (mgL <sup>-1</sup> )	CT40 pellet Conc. (mgL <sup>-1</sup> )	CT50 pellet Conc. (mgL <sup>-1</sup> )
0	9.39±0.07	9.19±0.06	9.25±0.13	9.12±0.32
30	8.60±0.07	8.77±0.05	8.68±0.52	8.70±0.17
60	8.21±0.07	8.49±0.33	8.04±0.41	8.14±0.02
90	7.92±0.07	7.80±0.26	7.70±0.35	7.53±0.52
120	7.71±0.05	7.80±0.24	7.36±0.45	7.10±0.29
180	7.26±0.06	7.00±0.25	6.67±0.22	6.59±0.07
240	6.88±0.06	6.78±0.11	6.39±0.24	5.81±0.03
P	-	NS*	NS*	NS*

Note: Each value represents the mean ± S.D. (n = 3)

\*Non-significant at probability level P > 0.01

\*\* CT0 pellet was calcined at 1000 °C for 2 h

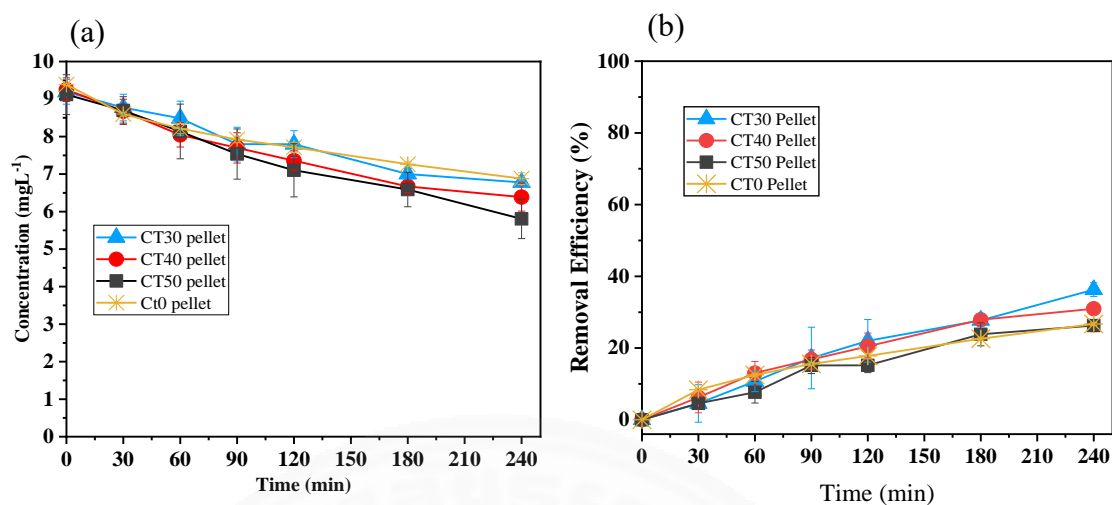


**Figure 4.11** Effect of weight percentage of TiO<sub>2</sub> in clay TiO<sub>2</sub> pellets on the removal of MB under dark condition: (a) concentration of MB and (b) removal efficiency of MB

In the absence of UV light, the concentration of MB adsorbed on CT30, CT40 and CT50 pellets at 240 mins were quite similar as shown in Table 4.7 and Figure 4.11a. MB can be adsorbed on CT30, CT40 and CT50 pellets, with approximately 31% (Figure 4.11b). Also, One-way ANOVA analysis showed that there were no significant differences on any adsorption of MB on CT30, CT40 and CT50 pellets (ANOVA,  $P=0.019$ ). Obviously, 26.71% of MB was decreased which even after 240 mins by using CT0 pellets. The decrease of MB under the dark condition was mainly adsorbed by clay (Figure 4.12). The total clay content of CT30, CT40 and CT50 pellets in MB solution test was approximately 10 to 14 gL<sup>-1</sup>. Also, the active clay on clay TiO<sub>2</sub> pellets can be performed only on the surface of the pellets (Figure 4.15). It can be seen in Figure 4.12b that 18.03% of MB removal was reached by using 0.0625 gL<sup>-1</sup> of clay powder within 240 mins in the darkness. With increasing the clay loading up to 14 gL<sup>-1</sup>, the removal efficiency of MB was reached 96.56% (Figure 4.11b). For TiO<sub>2</sub> powder, the removal of MB by using 0.0625 gL<sup>-1</sup> of TiO<sub>2</sub> powder was 4.66% removal efficiency and about 9 % removal efficiency was reached by using 10 gL<sup>-1</sup> of TiO<sub>2</sub> powder (Figure 4.12a). Therefore, the adsorption of MB by using TiO<sub>2</sub> could be negligible. The adsorption of MB on clay was affected by pH of the working solution. The pH of a solution can directly affect the electrical charge for the surface of pyrophyllite in clay as mentioned previously from XRD results in Figure 4.5. Based on previous study, the

zero point of charge in pyrophyllite is at about 2.3 (J. Zhang, Zhou, Jiang, Li, & Sheng, 2015). In this experiment, the pH of solution was about 6.07. Based on the zeta potential results at pH~7, zeta potential value of clay powder was -13.8 mV, while zeta potential value of  $\text{TiO}_2$  powder was +25.7 mV. Consequentially, the clay has become a net negative surface charge, thus, MB (cationic dye) in the solution can adsorb on clay surface through the electrostatic attractive interactions (Sheng, Xie, & Zhou, 2009; J. Zhang et al., 2015). The  $\text{TiO}_2$  has become a net positive surface charge, so it did not absorb MB.

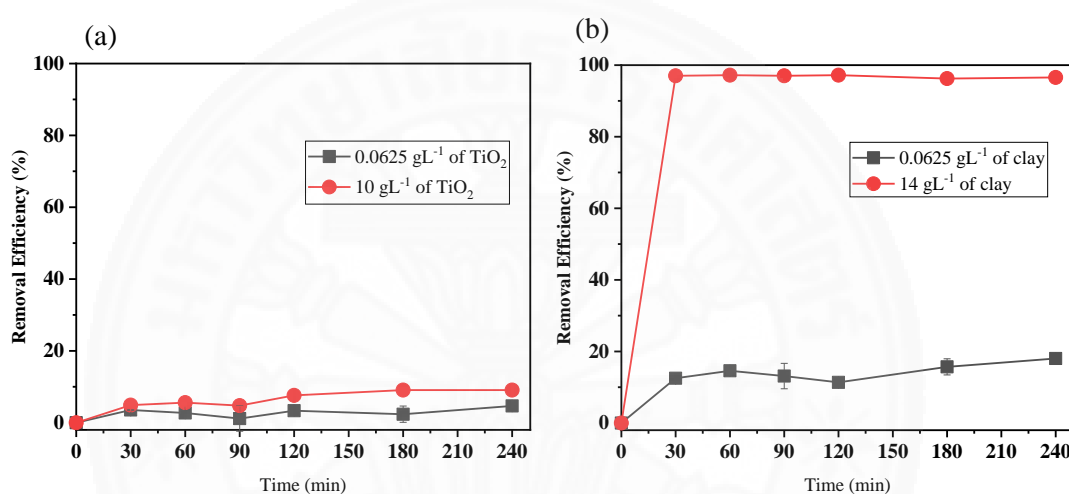


**Figure 4.12** The removal efficiency of MB (10 mgL<sup>-1</sup>) under the dark condition:

(a)  $\text{TiO}_2$  powder (b) Clay powder

It can be seen that the concentration of MB adsorbed by CT30, CT40 and CT50 pellets became quite stable after 90 mins. Therefore, the CT30, CT40 and CT50 pellets were stirred in MB solution under the dark condition for 90 mins in order to saturate the clay  $\text{TiO}_2$  pellets with MB before exposing under the UV light. For photocatalytic reaction of MB, the concentration of MB and removal efficiency of MB were calculated as shown in Table 4.8 and Figure 4.13.

**Table 4.8** MB concentration during the photocatalytic reaction by using clay TiO<sub>2</sub> pellets

Under the UVA light condition				
Sample	CT0 pellet**	CT30 pellet*	CT40 pellet	CT50 pellet
Time (min)	Conc. (mgL <sup>-1</sup> )	Conc. (mgL <sup>-1</sup> )	Conc. (mgL <sup>-1</sup> )	Conc. (mgL <sup>-1</sup> )
0	8.71±0.18	6.91±0.32	7.06±0.21	7.20±0.73
30	8.44±0.23	5.93±0.36	6.10±0.55	6.95±0.50
60	8.09±0.17	5.04±0.51	5.27±0.60	6.20±0.57
90	7.77±0.09	4.35±0.38	4.56±0.33	5.60±0.08
120	7.67±0.00	3.60±0.46	4.14±0.39	4.88±0.00
180	7.16±0.23	2.17±0.40	2.64±0.39	4.14±0.04
240	6.64±0.14	1.45±0.24	1.77±0.15	3.23±0.28

Note: Each value represents the mean ± S.D. (n = 3)

\*CT0 pellet was calcined at 1000 °C for 2 h.

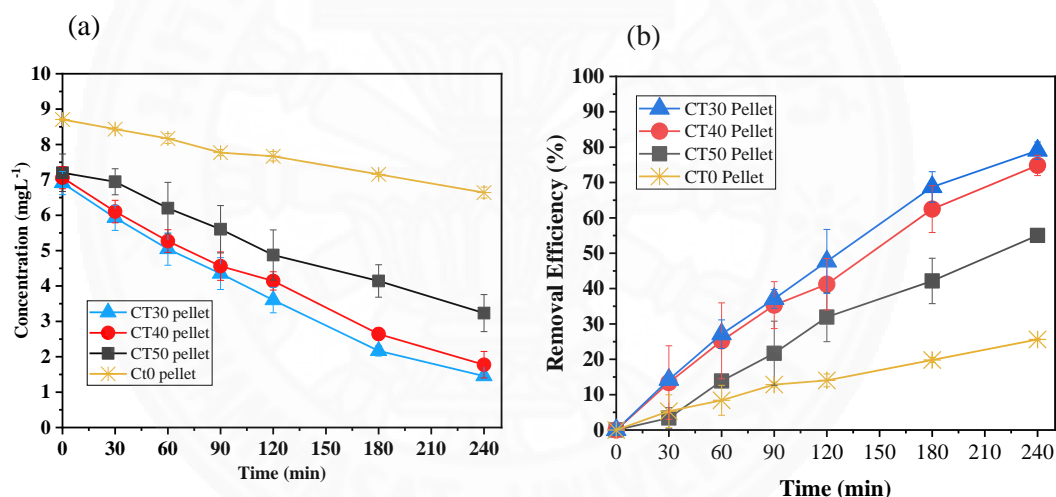


**Figure 4.13** Effect of weight percentage of TiO<sub>2</sub> in clay TiO<sub>2</sub> pellets on the removal of MB under UVA condition: (a) concentration of MB and (b) removal efficiency of MB

In the presence of UV light, CT30, CT40 and CT50 pellets obviously showed a drastic decrease of MB depending on the ratio of clay and TiO<sub>2</sub> (Figure 4.13a). The removal efficiencies of MB by using CT0, CT30, CT40 and CT50 pellets were 25.60%, 79.01%, 74.92%, and 55.13%, respectively within 240 mins (Figure 4.13b). The results indicate that CT30, CT40 and CT50 pellets exhibited the photocatalytic performance. However, CT0 pellets did not contain TiO<sub>2</sub>, therefore, removal of MB resulted from the

adsorption by clay. The removal efficiency of MB by using CT0 pellets in the absence of UV light was quite similar to the reaction in presence of UV light.

Among clay TiO<sub>2</sub> pellets, CT30 pellets showed the highest photocatalytic activity for MB. It can be seen that 30% wt of TiO<sub>2</sub> in clay TiO<sub>2</sub> pellets show the highest performance. Based on characterization results (Figure 4.7 and 4.8.), SEM and AFM images of clay TiO<sub>2</sub> pellets showed that CT30 exhibited a rougher surface than CT40 and CT50 pellets. The different surface roughness of clay TiO<sub>2</sub> pellet might affect the photocatalytic activity. A rough surface provides more contact area to adsorb pollutants on the surface of Cu-TiO<sub>2</sub> nanocomposites (Kumar & Pandey, 2017). Overall, CT30, CT40 and CT50 pellets showed a removal performance for MB. Consequently, CT30, CT40 and CT50 pellets were used for the photodegradation of glyphosate.

#### 4.3.3 The photocatalytic degradation of MB on CT50, CT40 and CT30 pellets

To confirm the results of 4.3.2, color determination of CT50, CT40 and CT30 pellets during the photocatalytic experiment was investigated (Figure 4.14). Also, the CIE Lab system was used to measure the color of clay TiO<sub>2</sub> pellets directly with precise results. The blue color of CT50, CT40 and CT30 pellets was reported as negative b\* (Table 4.9).

**Table 4.9** L\*a\*b\* color values of MB on clay TiO<sub>2</sub> pellets

Condition	Sample	L*	a*	b*
0 min	CT30 pellet	78.92±1.77	1.35±0.18	0.18±0.06
	CT40 pellet	77.42±0.92	0.26±0.08	1.36±0.18
	CT50 pellet	83.92±0.21	0.28±0.02	1.40±0.03
Dark (90 mins)	CT30 pellet	41.23±1.06	3.61±1.11	-32.06±2.21
	CT40 pellet	45.87±0.55	2.91±1.40	-29.20±1.34
	CT50 pellet	42.22±0.91	2.06±1.15	-32.33±1.38
UVA light (240 mins)	CT30 pellet	49.72±9.06	-3.69±2.12	-7.63±1.40
	CT40 pellet	65.16±5.47	-6.34±1.66	-12.45±1.67
	CT50 pellet	51.03±4.37	-5.42±1.69	-14.85±1.77
Dark (90 mins)	CT30 pellet	40.16±2.36	3.82±0.67	-30.36±10.0
	CT40 pellet	42.75±0.79	3.16±0.35	-28.40±4.00
	CT50 pellet	46.33±3.35	4.07±1.2	-30.26±1.22

Note: Each value represents the mean ± S.D. (n = 3)





**Figure 4.14.** MB on clay TiO<sub>2</sub> pellets: (a) under dark condition for 90 mins  
(b) under UVA light for 240 mins and (c) under dark condition for 90 mins

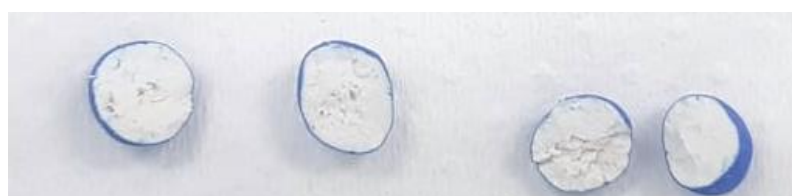


**Figure 4.15** MB on clay TiO<sub>2</sub> pellets under dark condition for 90 mins



The clay TiO<sub>2</sub> pellets were white in color as shown in Figure 4.1 and the b\* value was close to zero. After these clay TiO<sub>2</sub> pellets were immerse in MB solution for 90 mins, the color of clay TiO<sub>2</sub> pellets became dark blue and the b\* value showed more negative number. As mentioned previously, the MB was mainly adsorbed by clay in clay TiO<sub>2</sub> pellets, resulting in blue-colored pellets (Figure 4.14a). When these clay TiO<sub>2</sub> pellets were continue expose under the UVA light in the dry chamber, the color became pale blue as well as value of the b\* was less negative number (Figure 4.14b and Table 4.9). The color of the pellet changed due to photocatalytic reaction. Obviously, the increase of clay in clay TiO<sub>2</sub> pellets enhanced the removal of MB on the surface of the pellets. The color of CT30 pellets showed more pale color and less negative number than CT40 and CT30 pellets. The clay has played an important role in the photocatalysis, the photocatalytic reaction merely occurs on the surface of the pellets as shown in Figure 4.15. The enhance adsorption provided by the clay could be direct more contaminants to the surface of clay TiO<sub>2</sub> pellet prior to photocatalysis (Chong et al., 2009; Liu & Zhang, 2014). After the photocatalytic reaction, these pellets can further adsorbed MB on the surface as shown in Figure 4.14c.

Additionally, in order to reactivate clay TiO<sub>2</sub> pellets, clay TiO<sub>2</sub> pellet absorbed MB solution for 240 min in the darkness, then adsorbed clay TiO<sub>2</sub> pellet was separated and further applied in 3 different conditions: (a) deionized water under UVA light, (b) deionized water under the dark condition and (c) 70% alcohol under the dark condition. The result is showed in Table 4.10 that adsorbed clay TiO<sub>2</sub> pellets which was stirred in deionized water under UVA light showed the less negative number in b\* value, indicating that MB on clay TiO<sub>2</sub> pellets can removed by photocatalytic reaction. However, MB was still available (b\* value of -25.83 and -24.70) on clay TiO<sub>2</sub> pellets in both deionized water and 70% alcohol under the dark condition. Therefore, adsorbed clay TiO<sub>2</sub> pellet should add into deionized water under UVA light for 240 mins for reusability.

**Table 4.10** L\*a\*b\* color values of adsorbed CT30 pellets after stirring for 240 mins

Sample	L*	a*	b*
Water+Dark	46.48±7.16	2.96±2.42	-25.83±2.94
Water+Light	77.12±2.78	-5.18±0.66	-8.34±2.16
Alcohol+Dark	47.58±3.17	-4.14±2.42	-24.70±1.20

Note: Each value represents the mean ± S.D. (n = 3)

#### 4.4 Photocatalytic degradation of glyphosate

The photocatalytic degradation of glyphosate has been studied by using  $\text{TiO}_2$  photocatalysts. Firstly, the effect of UV types on photocatalytic degradation of glyphosate was investigated by using  $\text{TiO}_2$  powder. Also, CT50, CT40 and CT30 pellets were used to investigate on the photocatalytic degradation of glyphosate.

##### 4.4.1 Effect of UV types on photocatalytic degradation of glyphosate by $\text{TiO}_2$ powder

Two types of UV irradiation i.e., UVA and UVC light was used to investigate the photocatalytic degradation of glyphosate in the presence of  $\text{TiO}_2$  powder. Figure 16 presents removal efficiency of glyphosate ( $30 \text{ mgL}^{-1}$ ) with  $\text{TiO}_2$  powder ( $1 \text{ gL}^{-1}$ ) under dark condition and irradiation of UVA and UVC light within 120 mins. Also, photocatalytic degradation of glyphosate was investigated (Table 4.12 and Figure 4.16).

**Table 4.11** Glyphosate concentration during the adsorption test by using  $\text{TiO}_2$  powder under UVA and UVC light

Under the dark condition	
Sample Time (min)	Glyphosate+ $\text{TiO}_2$ powder
	Conc. ( $\text{mgL}^{-1}$ )
0	$30.45 \pm 0.33$
30	$16.01 \pm 0.14$
60	$16.31 \pm 0.01$
90	$16.28 \pm 0.00$
120	$16.34 \pm 0.09$

Note: Each value represents the mean  $\pm$  S.D. (n = 3)

**Table 4.12** Glyphosate concentration during photocatalytic reaction by using  $\text{TiO}_2$  powder under UVA and UVC light

Under the UV light condition				
Sample	Glyphosate +UVA+powder	Glyphosate+ UVA	Glyphosate +UVC+powder	Glyphosate+ UVC
Time (min)	Conc. ( $\text{mgL}^{-1}$ )	Conc. ( $\text{mgL}^{-1}$ )	Conc. ( $\text{mgL}^{-1}$ )	Conc. ( $\text{mgL}^{-1}$ )
0	$30.38 \pm 0.27$	30.69	$29.47 \pm 0.11$	30.01
30	$7.87 \pm 5.68$	30.88	$11.73 \pm 0.35$	30.19
60	$4.66 \pm 0.31$	30.90	$7.75 \pm 0.44$	30.22
90	$0.92 \pm 0.57$	30.99	$4.66 \pm 0.53$	30.30
120	$0.30 \pm 0.03$	31.24	$2.17 \pm 0.37$	30.54

Note: Each value represents the mean  $\pm$  S.D. ( $n = 3$ ) excluding glyphosate+UVA and glyphosate+UVC

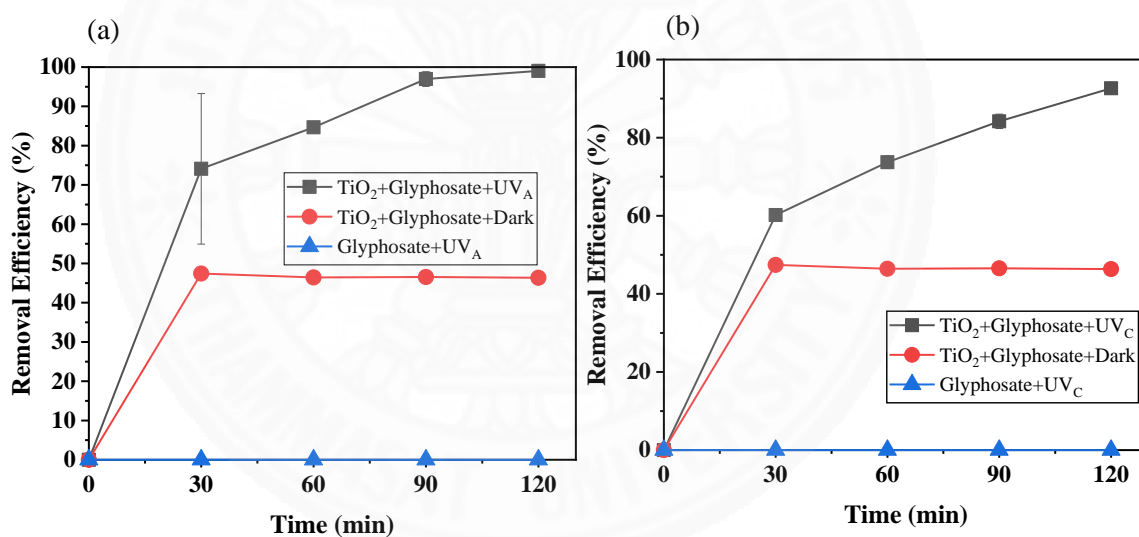


**Figure 4.16** The removal efficiency of glyphosate by using  $\text{TiO}_2$  powder:

(a) effect of UVA Light (b) effect of UVC Light

In the absence of  $\text{TiO}_2$ , there was no observable loss of glyphosate in both UVA and UVC irradiation (Table 4.11 and Figure 4.16). Additionally, when the  $\text{TiO}_2$  powder was employed under dark condition, glyphosate was immediately adsorbed on the surface of photocatalysts, approximately 47.42% removal of the glyphosate after stirring the solution, and there was no observable loss in the glyphosate concentration after 30 mins. The pH of a solution can directly affect the electrical charge for the surface of  $\text{TiO}_2$ . Due to the experiment condition occurring the solution pH around 5,

TiO<sub>2</sub> surface exhibited positively charged (Dârjan et al., 2013; Kosmulski, 2006; Umar & Aziz, 2013). Thereby, the negative charge of glyphosate molecule can be adsorbed on TiO<sub>2</sub> surface through electrostatic bonds.

In the presence of UV light without pre-adsorption of glyphosate on the TiO<sub>2</sub> powder, it can be seen that the presence of TiO<sub>2</sub> powder under UV irradiation significantly enhanced the removal efficiency (Table 4.12 and Figure 4.16). After 120 mins, the removal efficiency of glyphosate was reached 99.03 % and 92.67% under UVA and UVC irradiation, respectively. As mentioned previously, this experiment consisted of TiO<sub>2</sub>, and UV light which was necessary for the photocatalytic process. Generally, the photocatalytic degradation of glyphosate occurs mainly on the TiO<sub>2</sub> surface. When the TiO<sub>2</sub> surface adsorbs light to generate generating ROS such as •OH radicals and •O<sub>2</sub><sup>-</sup>. These •OH and •O<sub>2</sub><sup>-</sup> is strong enough to remove glyphosate adsorbed on the surface (J. Q. Chen et al., 2012; S. Chen & Liu, 2007; Umar & Aziz, 2013). Generally, UVC radiation has the higher energy than UVA radiation corresponding to the higher potential to degrade for water contaminated with organic pollutant (Cortés et al., 2011; Li Puma & Yue, 2002; L. H. Zhang, Xu, Chen, & Li, 2011). However, UVA had slightly better performance to degrade for water contaminated with glyphosate compared with UVC in Figure 4.16b. The previous studies indicated that the light intensity is also one of the major factors affecting photocatalytic degradation of glyphosate. In this experiment, the light intensity of UVA (2497 µW/cm<sup>2</sup>) had stronger influence for the glyphosate degradation than UVC (1648 µW/cm<sup>2</sup>). The higher light intensity of UVA results in a higher degradation rate and performance for glyphosate in photocatalysis process. Similar to the previous study, L. H. Zhang et al. (2011) indicated that glyphosate degrade faster in the UVA illumination due to the number of photons emitted by the UVA illumination is more than that of the UVC illumination. Considering the User's Safety, UVA irradiation was applied for the photocatalytic degradation of glyphosate by using TiO<sub>2</sub> pellets in this work.

#### 4.4.2 Photocatalytic degradation of glyphosate by clay TiO<sub>2</sub> pellets under UVA irradiation

Different weight percentage of TiO<sub>2</sub> in range from 30, 40 and 50 wt% (CT30, CT40 and CT50 pellets) were used to investigate on the photocatalytic degradation of glyphosate as shown in Table 4.9 and Figure 4.15. Prior to an UV illumination, CT30, CT40 and CT50 pellets were studied in the absence of light to determine the amount of time that would be necessary to saturate the pellets with glyphosate before exposing under the UV light. Also, the concentration of glyphosate adsorbed on clay TiO<sub>2</sub> pellet and removal efficiency of glyphosate under the dark condition were calculated as shown in Table 4.13 and Figure 4.17.

**Table 4.13** Glyphosate concentration during the adsorption test by using clay TiO<sub>2</sub> pellets

Under the dark condition				
Sample Time (min)	CT0 pellet* Conc. (mgL <sup>-1</sup> )	CT30 pellet Conc. (mgL <sup>-1</sup> )	CT40 pellet Conc. (mgL <sup>-1</sup> )	CT50 pellet Conc. (mgL <sup>-1</sup> )
0	1.01±0.01	1.15±0.00	1.16±0.03	1.15±0.04
30	1.02±0.00	1.08±0.13	1.00±0.02	1.03±0.04
60	1.01±0.01	0.99±0.00	0.95±0.00	0.78±0.08
90	1.01±0.01	0.90±0.07	0.84±0.01	0.76±0.08
120	0.99±0.01	0.81±0.04	0.73±0.04	0.70±0.07
180	0.99±0.01	0.64±0.03	0.63±0.05	0.60±0.03
240	0.98±0.01	0.59±0.06	0.59±0.01	0.58±0.01
P	-	NS**	NS**	NS**

Note: Each value represents the mean ± S.D. (n = 3)

\*CT0 pellet was calcined at 1000 °C for 2 h

\*\*Non-significance difference at probability level P > 0.01

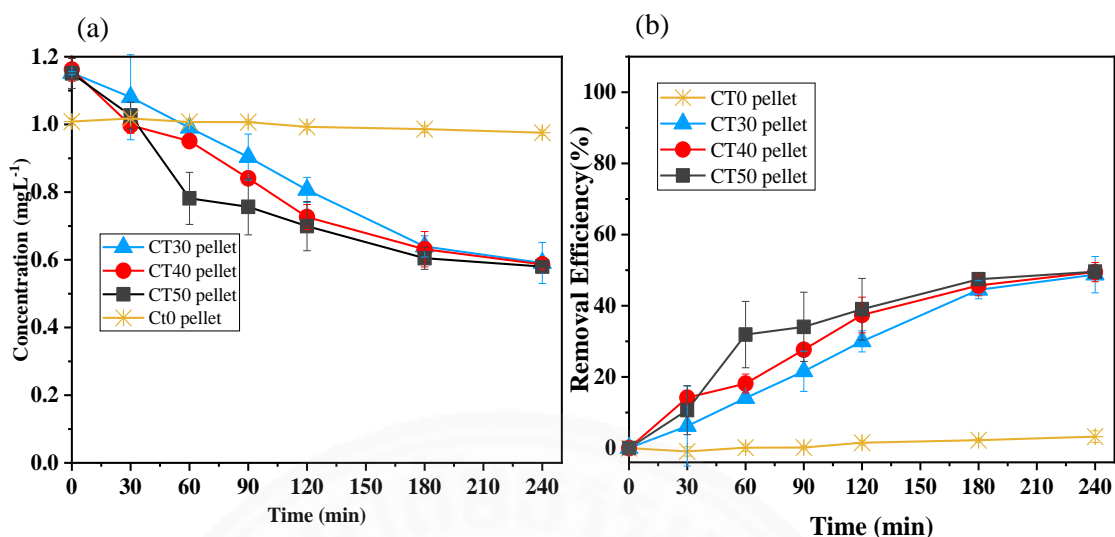


**Figure 4.17** Effect of weight percentage of TiO<sub>2</sub> in clay TiO<sub>2</sub> pellets on the removal of glyphosate under dark condition: (a) concentration of glyphosate and (b) removal efficiency of glyphosate

In the absence of UV light, the concentration of glyphosate adsorbed on CT30, CT40 and CT50 pellets at 240 mins were quite similar as shown in Table 4.12 and Figure 4.17a. Glyphosate can be adsorbed on clay TiO<sub>2</sub> pellets, with approximately 49.27%. (Figure 4.17b). Also, One-way ANOVA analysis showed that there were no significant differences on any adsorption of glyphosate on CT30, CT40 and CT50 pellets (ANOVA,  $P=0.653$ ). Also, only 1.69% of glyphosate was adsorbed by using CT0 pellets (without TiO<sub>2</sub>) (Figure 4.17a).

The decrease of glyphosate under the dark condition was mainly adsorbed by TiO<sub>2</sub> (Figure 4.18). Also, figure 4.18 confirmed that Glyphosate was adsorbed by TiO<sub>2</sub>, not clay. Small amount of TiO<sub>2</sub> powder (0.035 gL<sup>-1</sup>) can achieve 44.54% removal efficiency of glyphosate, while 0.25 gL<sup>-1</sup> of clay reached 4.66% removal efficiency of glyphosate. Therefore, the adsorption of glyphosate by using clay could be negligible. The adsorption of glyphosate on TiO<sub>2</sub> was affected by pH of the working solution. The pH of a solution can directly affect the electrical charge for the surface of TiO<sub>2</sub>. Based on previous studies, the zero point of charge in TiO<sub>2</sub> at about 6.9 (Dârjan et al., 2013; Kosmulski, 2006; Umar & Aziz, 2013). In this experiment, the pH of solution was about 5. From the zeta potential results at pH~7, zeta potential value of TiO<sub>2</sub> powder was +25.7 mV, while zeta potential value of clay powder was -13.8 mV.

Consequently, the  $\text{TiO}_2$  has become a net positive surface charge, thus, glyphosate (anionic molecule) in the solution can adsorb on  $\text{TiO}_2$  surface through the electrostatic attractive interactions. The clay has become a net negative surface charge, so it did not adsorb glyphosate.

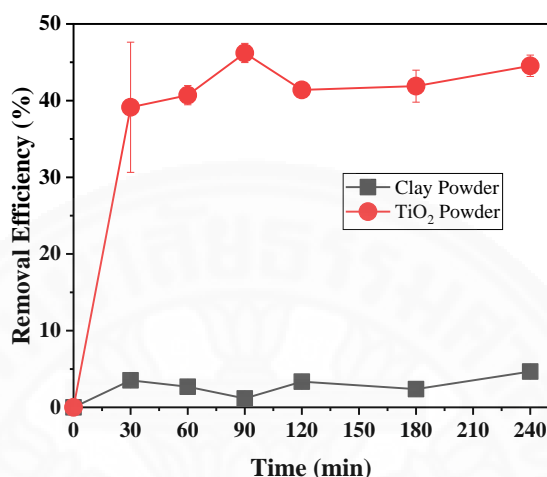


**Figure 4.18** The removal efficiency of glyphosate ( $10 \text{ mgL}^{-1}$ ) under the dark condition by using  $0.035 \text{ gL}^{-1}$  of  $\text{TiO}_2$  powder and  $0.25 \text{ gL}^{-1}$  of clay powder

It can be seen that the concentration of glyphosate adsorbed by CT30, CT40 and CT50 pellets became quite stable after 180 mins. Therefore, the CT30, CT40 and CT50 pellets were stirred in glyphosate solution under the dark condition for 180 mins in order to saturate the clay  $\text{TiO}_2$  pellets with glyphosate before exposing under the UV light. Then, the mixture was continued stirring during the photocatalytic process from 240 mins (Figure 4.19). For photocatalytic reaction of glyphosate, the concentration of glyphosate and removal efficiency of glyphosate were calculated as shown in Table 4.14 and Figure 4.20.



**Table 4.14** Glyphosate concentration during the photocatalytic reaction by using clay TiO<sub>2</sub> pellets with pre-adsorption

Under the UVA light condition				
Sample	Without pellet*	CT30 pellet	CT40 pellet	CT50 pellet
Time (min)	Conc. (mgL <sup>-1</sup> )	Conc. (mgL <sup>-1</sup> )	Conc. (mgL <sup>-1</sup> )	Conc. (mgL <sup>-1</sup> )
0	1.20±0.08	0.64±0.04	0.54±0.07	0.55±0.01
30	1.10±0.13	0.50±0.00	0.40±0.06	0.37±0.02
60	1.13±0.01	0.32±0.03	0.25±0.03	0.23±0.06
90	1.13±0.01	0.22±0.04	0.17±0.01	0.14±0.03
120	1.09±0.12	0.14±0.03	0.11±0.01	0.08±0.01
180	1.09±0.07	0.05±0.01	0.04±0.02	0.03±0.01
240	1.09±0.07	0.01±0.01	0.01±0.01	0.00±0.00

Note: Each value represents the mean ± S.D. (n = 3)

\* Glyphosate solution was stirred under UVA light without clay TiO<sub>2</sub> pellets.

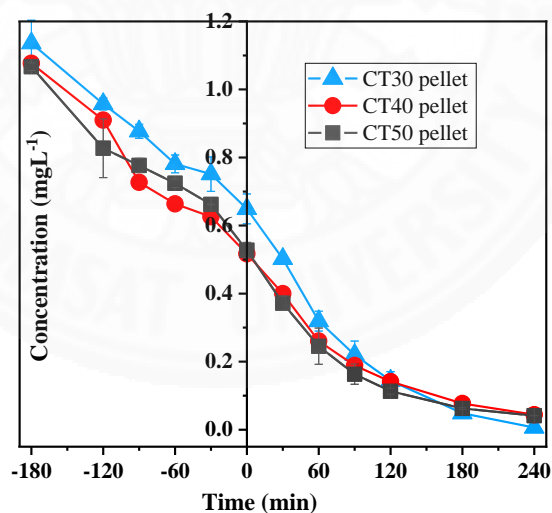


**Figure 4.19** The concentration of glyphosate during the adsorption test and photocatalytic reaction on clay TiO<sub>2</sub> pellets

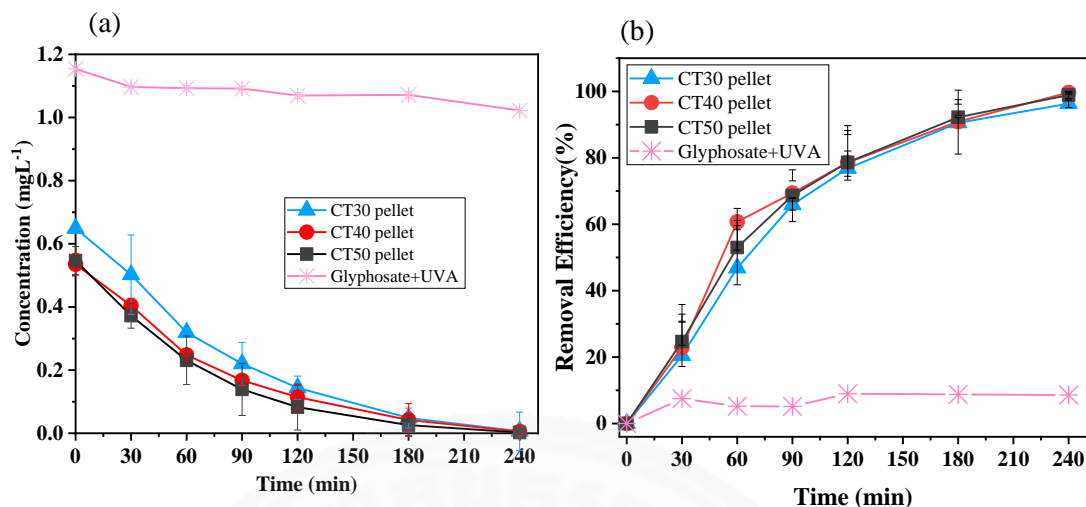


**Figure 4.20** Effect of weight percentage of TiO<sub>2</sub> in clay TiO<sub>2</sub> pellets on the removal of glyphosate under UVA condition with pre-adsorption: (a) concentration of glyphosate and (b) removal efficiency of glyphosate

When the CT30, CT40 and CT50 pellets were employed under UVA irradiation, CT30, CT40 and CT50 pellets showed the higher photocatalytic degradation efficiency of glyphosate. The concentration of glyphosate was decreased to nearly zero by using CT30, CT40 and CT50 pellets (Table 4.14 and Figure 4.20a). The removal efficiencies of glyphosate by using on CT30, CT40 and CT50 pellets were quite similar, with approximately 98.19% within 240 mins (Figure 4.20b). Without adsorption prior photocatalysis of glyphosate, the concentration of glyphosate was decreased from 1 mgL<sup>-1</sup> to near zero at 240 mins by using CT30, CT40 and CT50 pellets (Table 4.15 and Figure 4.21a). CT30, CT40 and CT50 pellets also showed quite similar performance for photocatalytic degradation of glyphosate, with approximately 98% (Figure 4.21b). However, CT0 pellets did not contain TiO<sub>2</sub>, therefore, only 3.61% of glyphosate was decreased which even after 240 mins (Figure 4.21). The removal efficiency of glyphosate by using CT0 pellets in the absence of UV light was quite similar to the reaction in presence of UV light.

**Table 4.15** Glyphosate concentration during the photocatalytic degradation of glyphosate by using clay TiO<sub>2</sub> pellets without pre-adsorption

Under the UVA light condition			
Sample Time (min)	CT30 pellet	CT40 pellet	CT50 pellet
	Conc. (mgL <sup>-1</sup> )	Conc. (mgL <sup>-1</sup> )	Conc. (mgL <sup>-1</sup> )
0	1.19±0.12	1.14±0.01	1.13±0.00
30	0.87±0.07	0.82±0.05	0.79±0.00
60	0.49±0.11	0.55±0.11	0.46±0.01
90	0.40±0.05	0.41±0.04	0.29±0.02
120	0.22±0.09	0.25±0.05	0.13±0.01
180	0.04±0.05	0.15±0.06	0.03±0.01
240	0.01±0.01	0.04±0.01	0.01±0.00

Note: Each value represents the mean ± S.D. (n = 3)

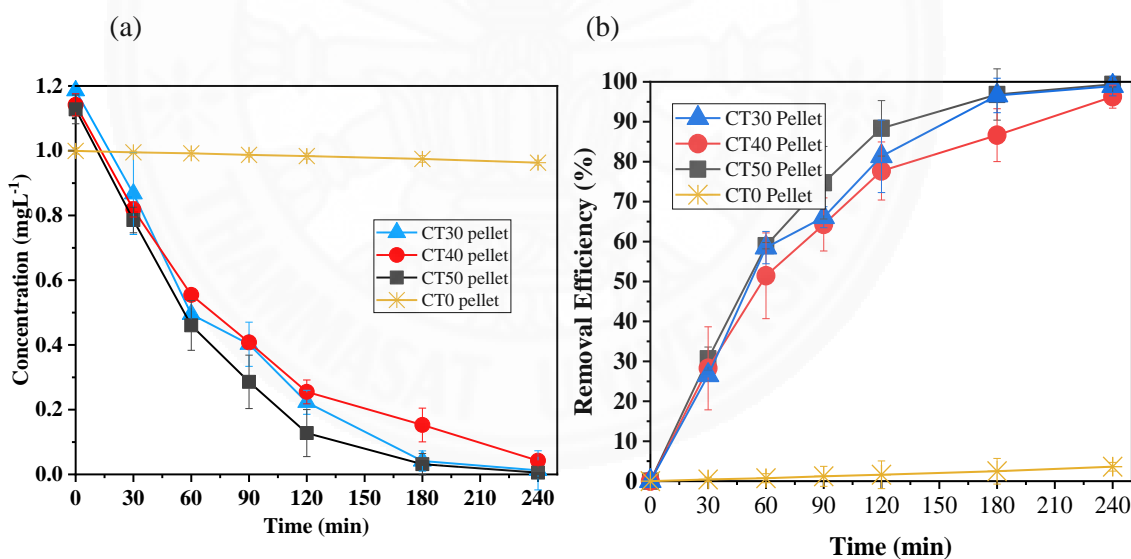


**Figure 4.21** Effect of weight percentage of TiO<sub>2</sub> in clay TiO<sub>2</sub> pellets on the removal of glyphosate under UVA condition without pre-adsorption: (a) concentration of glyphosate and (b) removal efficiency of glyphosate

For degradation rate constants in the present work, the kinetic data obtained was described by pseudo-first order kinetics. The plot of  $-\ln(C/C_0)$  versus time with different clay TiO<sub>2</sub> pellet types i.e., CT30, CT40 and CT50 pellets is shown in Figure 4.22. The figure shows that the photocatalytic degradation followed the pseudo-first

order kinetic with each clay TiO<sub>2</sub> pellet types. The rate constants and their corresponding R<sup>2</sup> values for CT30, CT40 and CT50 pellets are shown in Table 4.16. It can be seen that the photocatalytic degradation rate constant(*k*) were quite similar. The increase of TiO<sub>2</sub> content in clay TiO<sub>2</sub> pellet had no obvious effect on photocatalytic activity and photocatalytic degradation rate. Therefore, it can be concluded that CT30, CT40 and CT50 pellets showed the high-performance pellets for removal glyphosate.

**Table 4.16** The kinetics constants (*k*) for the photocatalytic degradation of glyphosate in CT30, CT40 and CT50 pellets

Sample	R <sup>2</sup>	Regression Equation	<i>k</i> x 10 <sup>-3</sup> (min <sup>-1</sup> )
CT30	0.9519	$y = 0.0186x + 0.1807$	18.6
CT40	0.9547	$y = 0.0182x + 0.4268$	18.2
CT50	0.9570	$y = 0.0217x + 0.3492$	21.7

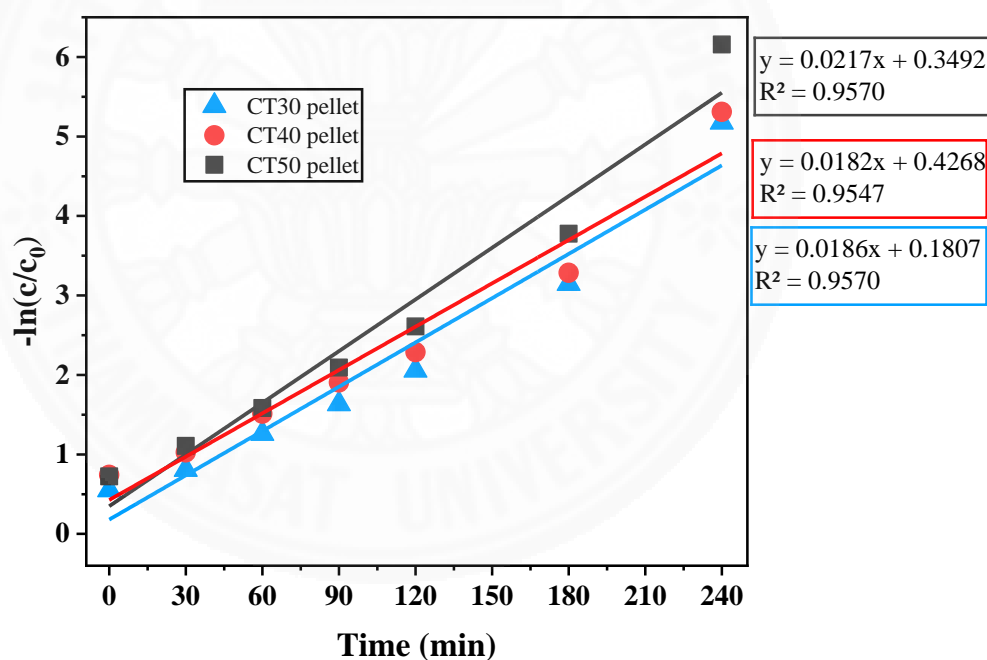


**Figure 4.22** Photocatalytic degradation kinetic of glyphosate

Overall, it can be obviously seen that CT30, CT40 and CT50 pellets can be performed to remove in both MB (cationic molecule) and glyphosate (anionic molecule). From preliminarily result, these clay TiO<sub>2</sub> pellets can removed MB efficiently. CT30 pellets showed the highest photocatalytic activity for MB than CT40 and CT50 pellets. When these clay TiO<sub>2</sub> pellets were used for the photocatalytic degradation of glyphosate. Also, they showed the high photocatalytic degradation

efficiency of glyphosate. Considering the high-performance removal in both MB (cationic molecule) and glyphosate (anionic molecule), thereby, CT30 pellets were continue used for comparing the activities with TiO<sub>2</sub> powder and commercial PE-TiO<sub>2</sub> pellets. Also, the mechanisms of the photocatalytic degradation of glyphosate by using CT30 pellets was investigated.

#### 4.4.3 Photocatalytic degradation of glyphosate by TiO<sub>2</sub> pellets

CT30 pellets, PE-TiO<sub>2</sub> pellets and TiO<sub>2</sub> powder were used to investigate the photocatalytic degradation of glyphosate. Considering the practical application, there no pre-adsorption of glyphosate on the TiO<sub>2</sub> photocatalysts was performed in this experiment. The mixture of TiO<sub>2</sub> photocatalysts was test under the dark and UV light conditions separately. Also, the concertation of glyphosate adsorbed on TiO<sub>2</sub> photocatalysts and removal efficiency of glyphosate by using CT30 pellets, PE-TiO<sub>2</sub> pellets and TiO<sub>2</sub> powder under the dark condition were calculated as shown in Table 4.17, Figure 4.23 and Figure 4.24.

**Table 4.17** Glyphosate concentration during the adsorption test by using CT30 pellets, PE-TiO<sub>2</sub> pellets and TiO<sub>2</sub> powder

Under the dark condition			
Sample Time (min)	CT30 pellet	PE pellet	TiO <sub>2</sub> Powder
	Conc. (mgL <sup>-1</sup> )	Conc. (mgL <sup>-1</sup> )	Conc. (mgL <sup>-1</sup> )
0	1.15±0.00	1.06±0.01	1.06±0.00
30	1.08±0.13	1.10±0.00	0.64±0.09
60	0.90±0.07	1.06±0.07	0.63±0.01
90	0.81±0.04	1.09±0.01	0.57±0.01
120	0.99±0.00	1.04±0.00	0.62±0.01
180	0.64±0.03	0.99±0.00	0.62±0.02
240	0.57±0.99	1.00±0.03	0.59±0.01

Note: Each value represents the mean ± S.D. (n = 3)

**Table 4.18** Glyphosate concentration during the photocatalytic reaction by using CT30 pellets, PE-TiO<sub>2</sub> pellets and TiO<sub>2</sub> powder

Under the UVA light condition			
Sample	CT30 pellet	PE pellet	TiO <sub>2</sub> Powder
Time (min)	Conc. (mgL <sup>-1</sup> )	Conc. (mgL <sup>-1</sup> )	Conc. (mgL <sup>-1</sup> )
0	1.26±0.12	1.17±0.01	1.06±0.00
30	1.10±0.00	0.94±0.02	0.55±0.01
60	1.05±0.01	1.01±0.01	0.00±0.01
90	0.98±0.04	0.84±0.04	0.00±0.01
120	0.90±0.02	0.70±0.02	0.00±0.00
180	0.77±0.00	0.48±0.01	0.00±0.00
240	0.73±0.03	0.30±0.01	0.00±0.00

Note: Each value represents the mean ± S.D. (n = 3)

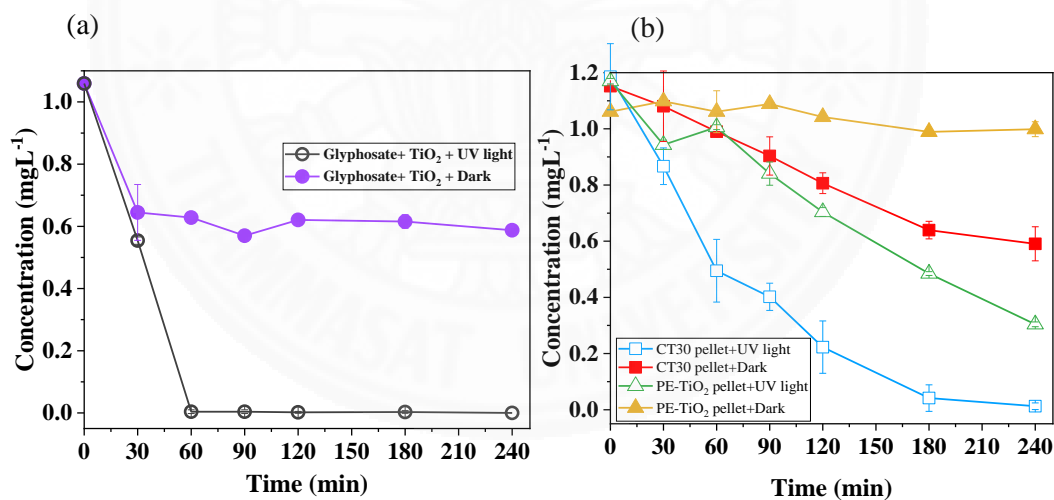


**Figure 4.23** Concentration of glyphosate during the adsorption test and photocatalytic reaction (a)TiO<sub>2</sub> Powder and (b) CT30 Pellet and PE-TiO<sub>2</sub> Pellet

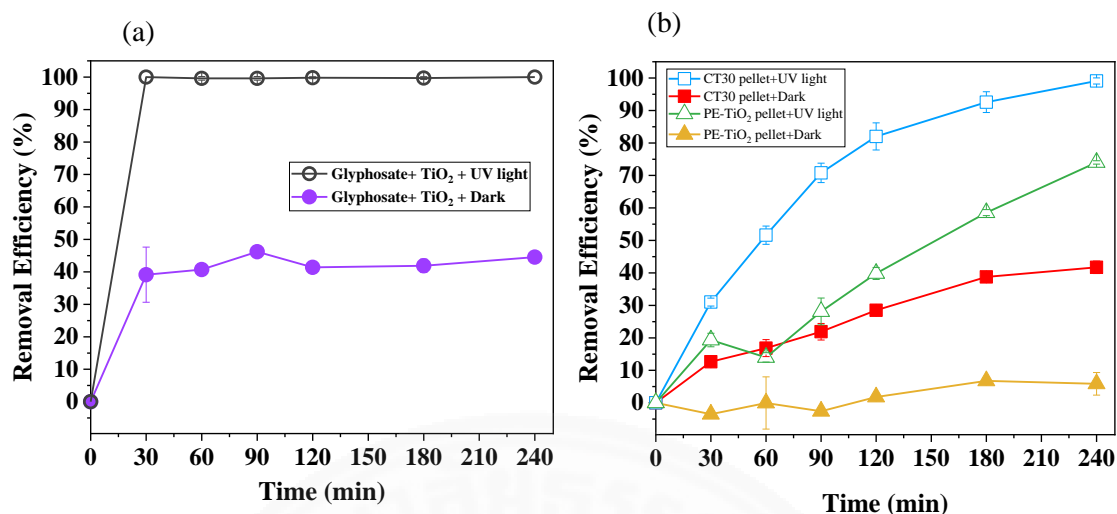


**Figure 4.24** Removal efficiency of glyphosate under Dark and UVA Conditions:

(a)TiO<sub>2</sub> Powder and (b) CT30 Pellet and PE-TiO<sub>2</sub> Pellet

When the TiO<sub>2</sub> powder was employed under dark condition, glyphosate was adsorbed on the TiO<sub>2</sub> powder. The concentration of glyphosate decreased from 1 to 0.59 mgL<sup>-1</sup> (approximately 39.62% removal efficiency) within 30 mins (Table 4.17) and then the concentration became stable until the end of experiment. Upon UV irradiation, glyphosate rapidly decreased and completely disappeared by TiO<sub>2</sub> powder within 30 mins (Table 4.18, Figure 4.23a and Figure 4.24a).

Apart from TiO<sub>2</sub> powder, PE-TiO<sub>2</sub> and CT30 pellets also can remove glyphosate effectively (Figure 4.24a and Figure 4.24b). The removal efficiency of glyphosate using both PE-TiO<sub>2</sub> and CT30 pellets under UV irradiation represented a considerable increase with time. For CT30 pellets, the concentration of glyphosate was reduced from 1.19 to 0.01 mgL<sup>-1</sup> (Table 4.18), with 99.15% removal efficiency, whereas the concentration of glyphosate was reduced from 1.17 to 0.30 mgL<sup>-1</sup> (Table 4.18), with 74.36% removal efficiency by using PE-TiO<sub>2</sub> pellets after 240 mins. Although both PE-TiO<sub>2</sub> and CT30 pellets a lower performance than TiO<sub>2</sub> powder, they were much easier to separate from water than TiO<sub>2</sub> powder. As mentioned previously, clay TiO<sub>2</sub> pellets showed a higher removal efficiency of glyphosate, compared with PE-TiO<sub>2</sub> pellets. Also, clay TiO<sub>2</sub> pellets had a mixture of anatase-rutile phase, while the PE-TiO<sub>2</sub> pellets only have anatase phase (Figure 4.6). The mixture of rutile and anatase phases enhance photocatalytic activity, leading to improve electron-hole separation (Ohtani et al., 2010). Also, clay TiO<sub>2</sub> pellets showed a larger surface area than the PE-TiO<sub>2</sub> pellets.



The large surface area relates to the greater number of active sites for reactive oxygen species (ROS) production to degrade glyphosate (Dârjan et al., 2013; Hurum, Agrios, Gray, Rajh, & Thurnauer, 2003; Kumar & Pandey, 2017).

Apart from the photocatalytic degradation of glyphosate, glyphosate can be adsorbed by PE-TiO<sub>2</sub> and CT30 pellets. The results showed that 5.66% of glyphosate was adsorbed by PE-TiO<sub>2</sub> pellets, while about 42.06% of glyphosate was adsorbed by using CT30 pellets within 240 mins (Figure 4.24b). Obviously, CT30 pellets showed the higher performance with convenient separation from the water than PE- TiO<sub>2</sub> pellets for photocatalytic degradation of glyphosate. Considering the removal efficiency of glyphosate, thereby, CT30 pellets were used to investigate mechanisms of the photocatalytic degradation of glyphosate.

#### 4.5 Mechanisms of the photocatalytic degradation of glyphosate

A possible photocatalytic degradation pathway of glyphosate was supposed to occur due to the strongly ROS. It is presumed that decomposition of glyphosate released AMPA, glycolic acid, sarcosine, phosphoric acid (H<sub>3</sub>PO<sub>4</sub>), carbon dioxide (CO<sub>2</sub>) and, inorganic anions i.e. phosphate (PO<sub>4</sub><sup>3-</sup>) and nitrate (NO<sub>3</sub><sup>-</sup>) (J. Q. Chen et al., 2012; Echavia et al., 2009; Muneer & Boxall, 2008). Among these byproducts, AMPA is initially produced and frequently occurs within glyphosate decomposition, while PO<sub>4</sub><sup>3-</sup> is stable major byproduct. In relation to glyphosate decomposition pathway, this study investigated AMPA and PO<sub>4</sub><sup>3-</sup> formation. The concentrations of AMPA and PO<sub>4</sub><sup>3-</sup> during photocatalytic degradation of glyphosate by TiO<sub>2</sub> powder and CT30 pellets are shown in Table 4.19 and Figure 4.25.

**Table 4.19** Concentration of glyphosate and its byproducts during photocatalytic degradation by using TiO<sub>2</sub> powder and CT30 pellets

Time	TiO <sub>2</sub> powder			CT30 pellet		
	Glyphosate	AMPA	PO <sub>4</sub> <sup>3-</sup>	Glyphosate	AMPA	PO <sub>4</sub> <sup>3-</sup>
	Conc. (mgL <sup>-1</sup> )	Conc. (mgL <sup>-1</sup> )	Conc. (mgL <sup>-1</sup> )	Conc. (mgL <sup>-1</sup> )	Conc. (mgL <sup>-1</sup> )	Conc. (mgL <sup>-1</sup> )
0	1.06±0.00	0.00±0.00	0.00±0.00	1.19±0.12	0.00±0.00	0.00±0.00
30	0.55±0.01	0.00±0.01	0.00±0.00	0.87±0.07	0.01±0.00	0.05±0.01
60	0.00±0.01	0.00±0.02	0.40±0.00	0.49±0.11	0.02±0.00	0.22±0.01
90	0.00±0.01	0.00±0.03	0.40±0.01	0.40±0.05	0.02±0.00	0.24±0.03
120	0.00±0.00	0.00±0.04	0.42±0.00	0.22±0.09	0.02±0.22	0.22±0.02
180	0.00±0.00	0.00±0.05	0.42±0.01	0.04±0.05	0.01±0.00	0.22±0.02
240	0.00±0.00	0.00±0.06	0.42±0.00	0.01±0.01	0.01±0.00	0.22±0.01

Note: Each value represents the mean ± S.D. (n = 3)

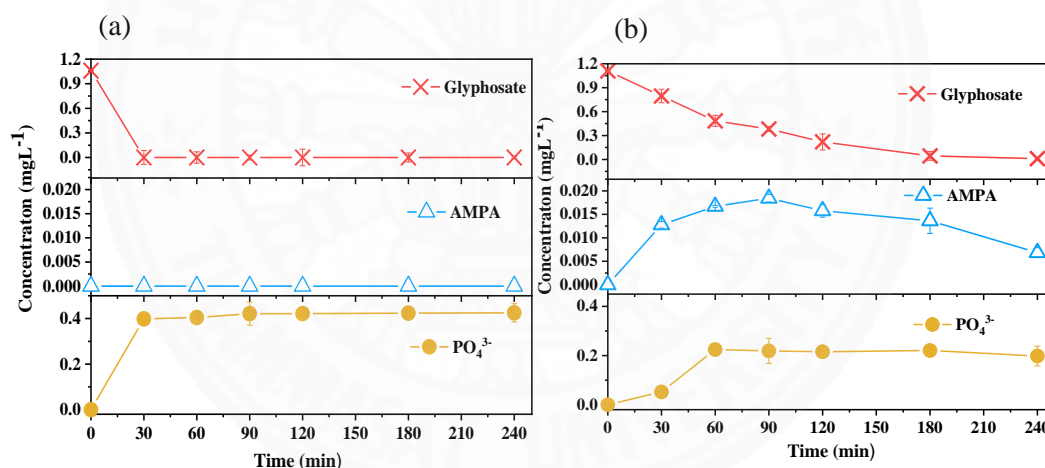


**Figure 4.25** Concentration of glyphosate and its byproducts during photocatalytic degradation: (a) TiO<sub>2</sub> powder and (b) CT30 pellets

The concentrations of AMPA and PO<sub>4</sub><sup>3-</sup> during photocatalytic degradation of glyphosate by using TiO<sub>2</sub> powder are shown in Figure 4.25a. The complete removal of glyphosate at concentration of 1 mgL<sup>-1</sup> was achieved, and 0.4 mgL<sup>-1</sup> of PO<sub>4</sub><sup>3-</sup> formation was observed at 30 mins and stable until 240 mins. It can be seen that the formation of PO<sub>4</sub><sup>3-</sup> was related to the disappearance of glyphosate. Compare to CT30 pellets, the photocatalytic degradation of glyphosate by using CT30 pellets showed a different result in the formation of PO<sub>4</sub><sup>3-</sup> (Figure 4.25b). The concentration of glyphosate was gradually decreased, PO<sub>4</sub><sup>3-</sup> concentration increased gradually. About 0.22 mgL<sup>-1</sup> of

$\text{PO}_4^{3-}$  formation was observed at 60 mins and quite stable until 240 mins (Figure 4.25b).

Also, the formation of AMPA is related to the decrease of glyphosate (Table 4.19 and Figure 4.25b). When the concentration of glyphosate was gradually decreased, AMPA concentration increased gradually, reaching its highest level, with  $0.02 \text{ mgL}^{-1}$  at 90 mins. Thereafter, AMPA decreased to  $0.008 \text{ mgL}^{-1}$  at 240 mins. From previous studies, glyphosate can be directly oxidized to AMPA. The generated AMPA can be also directly changed into  $\text{PO}_4^{3-}$  (J. Q. Chen et al., 2012; Echavia et al., 2009; Muneer & Boxall, 2008). Thereby, it is presumed that the gradual decrease of AMPA is resulted from the decrease of glyphosate and increase of  $\text{PO}_4^{3-}$  in water. Additionally, the fact that  $\text{PO}_4^{3-}$  reached its highest level at 60 mins before AMPA started to decrease at 90 mins indicates that apart from AMPA formation, there may be other glyphosate breakdown pathways such as the sarcosine (Figure 2.5). The sarcosine can produced  $\text{PO}_4^{3-}$  directly (Echavia et al., 2009). This highest concentration of  $\text{PO}_4^{3-}$  is possibly due to sarcosine decomposition. Interestingly, AMPA was not observed in the photocatalytic degradation of glyphosate by using  $\text{TiO}_2$  powder. This is possibly due to high photocatalytic performance of  $\text{TiO}_2$  powder for degradation of the AMPA and glyphosate.

Overall, formation of by products during the photocatalytic degradation of glyphosate by using  $\text{TiO}_2$  powder showed different result from CT30 pellets. Photocatalytic degradation of glyphosate by using  $\text{TiO}_2$  powder found only  $\text{PO}_4^{3-}$ , while photocatalytic degradation of the glyphosate by using CT30 pellets found both AMPA and  $\text{PO}_4^{3-}$ . This difference is might be due to the lower photocatalytic activity of CT30 pellets than  $\text{TiO}_2$  powder, resulting in AMPA is not rapidly decomposed. However, there was a trend in decreasing of AMPA after 90 mins (Figure 4.25b). Due to AMPA are more toxic and longer half-life than glyphosate (Grandcoin et al., 2017), complete degradation of AMPA is essential. Therefore, increase photocatalytic activity of CT30, e.g. increasing reaction time, light intensity and amount of clay  $\text{TiO}_2$  pellets, can lead to complete degradation of AMPA as well as degradation of glyphosate. In Figure 4.26, AMPA can be completely disappeared with increasing the reaction time into 300 mins

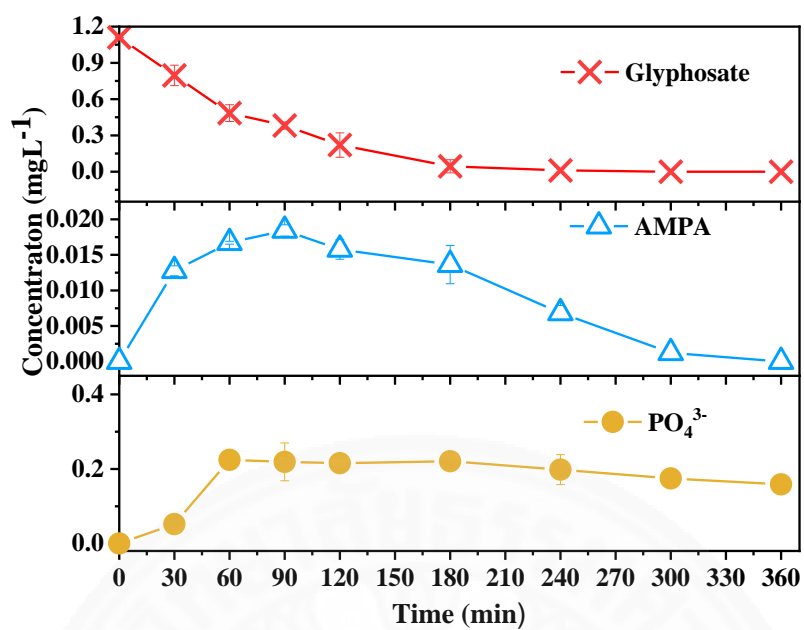


**Figure 4.26** Effects of illumination time on the photocatalytic degradation of glyphosate and its byproducts by using CT30 pellets

## CHAPTER 5

### CONCLUSION

To decontaminate glyphosate in water,  $\text{TiO}_2$  photocatalysis has been an effective process to remove glyphosate in water. Also, CT30 pellets which consisted of 30wt% of  $\text{TiO}_2$  powder and 70wt% of clay powder were prepared through the calcination temperature at 600 °C for 2 h to solve the separation problem of  $\text{TiO}_2$  powder (Degussa -P25). As shown in this work, CT30 pellets can be immersed in water, easily removed from water and resulted in highly photocatalytic. CT30 pellets showed the high performance for removal in both MB (cationic molecule) and glyphosate (anionic molecule). When the CT30 pellets were employed under UVA light, the removal efficiency of MB solution was reached 79.19% after illumination for 120 mins. For removal glyphosate in water, the removal efficiency of glyphosate was also reached 99.15% after UVA illumination for 240 mins. The formation of by products during the photocatalytic degradation of glyphosate by using  $\text{TiO}_2$  powder showed different result from CT30 pellets. Photocatalytic degradation of glyphosate by using  $\text{TiO}_2$  powder found only  $\text{PO}_4^{3-}$  while photocatalytic degradation of the glyphosate by using CT30 pellets found both AMPA and  $\text{PO}_4^{3-}$ . It was also found that since CT30 pellets was employed under UVA light with 240 mins illumination time. The complete degradation of toxic intermediate including AMPA was not achieved. With extending the reaction time into 300 mins, therefore, the complete degradation of AMPA was achieved.

## REFERENCES

- Al-Rajab, A. J., & Hakami, O. M. (2014). Behavior of the non-selective herbicide glyphosate in agricultural soil. *American Journal of Environmental Sciences*, 10(2), 94.
- Al-Rajab, A. J., & Schiavon, M. (2010). Degradation of <sup>14</sup>C-glyphosate and aminomethylphosphonic acid (AMPA) in three agricultural soils. *J. Environ. Sci*, 22(9), 1374-1380.
- Barrett, K., & McBride, M. (2005). Oxidative degradation of glyphosate and aminomethylphosphonate by manganese oxide. *Environmental science & technology*, 39(23), 9223-9228.
- Bayan, E. M., Lupeiko, T. G., Kolupaeva, E. V., Pustovaya, L. E., & Fedorenko, A. G. (2017). Fluorine-Doped Titanium Dioxide: Synthesis, Structure, Morphology, Size and Photocatalytic Activity *Advanced Materials* (pp. 17-24): Springer.
- Baylis, A. D. (2000). Why glyphosate is a global herbicide: strengths, weaknesses and prospects. *Pest management science*, 56(4), 299-308.
- Bergaya, F., & Lagaly, G. (2006). Chapter 1 General Introduction: Clays, Clay Minerals, and Clay Science. In F. Bergaya, B. K. G. Theng, & G. Lagaly (Eds.), *Developments in clay science* (Vol. 1, pp. 1-18): Elsevier.
- Bouna, L., Rhouta, B., Amjoud, M., Maury, F., Lafont, M.-C., Jada, A., . . . Daoudi, L. (2011). Synthesis, characterization and photocatalytic activity of TiO<sub>2</sub> supported natural palygorskite microfibers. *Applied Clay Science*, 52(3), 301-311.
- Bourikas, K., Kordulis, C., & Lycourghiotis, A. (2014). Titanium dioxide (anatase and rutile): surface chemistry, liquid–solid interface chemistry, and scientific synthesis of supported catalysts. *Chemical reviews*, 114(19), 9754-9823.
- Bowering, N., Croston, D., Harrison, P. G., & Walker, G. S. (2007). Silver modified Degussa P25 for the photocatalytic removal of nitric oxide. *International Journal of Photoenergy*, 2007.
- Breuer, S. (2012). The chemistry of pottery. *chemistry*.

- Carp, O., Huisman, C. L., & Reller, A. (2004). Photoinduced reactivity of titanium dioxide. *Progress in solid state chemistry*, 32(1-2), 33-177.
- Chatterjee, D., & Mahata, A. (2001). Demineralization of organic pollutants on the dye modified TiO<sub>2</sub> semiconductor particulate system using visible light. *Applied Catalysis B: Environmental*, 33(2), 119-125.
- Chen, J. Q., Hu, Z. J., & Wang, N. X. (2012). Photocatalytic mineralization of glyphosate in a small-scale plug flow simulation reactor by UV/TiO<sub>2</sub>. *Journal of Environmental Science and Health, Part B*, 47(6), 579-588.
- Chen, S., & Liu, Y. (2007). Study on the photocatalytic degradation of glyphosate by TiO<sub>2</sub> photocatalyst. *Chemosphere*, 67(5), 1010-1017.
- Chen, Y., Wu, F., Lin, Y., Deng, N., Bazhin, N., & Glebov, E. (2007). Photodegradation of glyphosate in the ferrioxalate system. *Journal of hazardous materials*, 148(1-2), 360-365.
- Chong, M. N., Vimonses, V., Lei, S., Jin, B., Chow, C., & Saint, C. (2009). Synthesis and characterisation of novel titania impregnated kaolinite nano-photocatalyst. *Microporous and Mesoporous Materials*, 117(1-2), 233-242.
- Cortés, J., Alarcón-Herrera, M., Villicaña-Méndez, M., González-Hernández, J., & Pérez-Robles, J. (2011). Impact of the kind of ultraviolet light on the photocatalytic degradation kinetics of the TiO<sub>2</sub>/UV process. *Environmental Progress & Sustainable Energy*, 30(3), 318-325.
- Coutinho, C. F., Coutinho, L. F., Mazo, L. H., Nixdorf, S. L., & Camara, C. A. (2008). Rapid and direct determination of glyphosate and aminomethylphosphonic acid in water using anion-exchange chromatography with coulometric detection. *Journal of Chromatography A*, 1208(1-2), 246-249.
- Dârjan, A., Drăghici, C., Perniu, D., & Duță, A. (2013). Degradation of Pesticides by TiO<sub>2</sub> Photocatalysis *Environmental Security Assessment and Management of Obsolete Pesticides in Southeast Europe* (pp. 155-163): Springer.
- Department of Agriculture, O. o. A. E. (2019). Value of Agricultural Chemicals Imports in Thailand from 2011 to 2018. Retrieved December 4, 2018, from Office of Agriculture Economics <http://oldweb.oae.go.th/economicdata/pesticides.html>
- Devipriya, S., & Yesodharan, S. (2005). Photocatalytic degradation of pesticide contaminants in water. *Solar energy materials and solar cells*, 86(3), 309-348.



- Duke, S. O. (2010). Glyphosate degradation in glyphosate-resistant and-susceptible crops and weeds. *Journal of Agricultural and Food Chemistry*, 59(11), 5835-5841.
- Echavia, G. R. M., Matzusawa, F., & Negishi, N. (2009). Photocatalytic degradation of organophosphate and phosphonoglycine pesticides using TiO<sub>2</sub> immobilized on silica gel. *Chemosphere*, 76(5), 595-600.
- Economics, O. o. A. (2013). *Agricultural Statics of Thailand 2013*. Retrieved from Food and Agriculture Organization, T. U. N. (2017). Top Pesticide Using Countries. Retrieved December 4, 2018, from Worldatlas [www.worldatlas.com/articles/top-pesticide-consuming-countries-of-the-world.html](http://www.worldatlas.com/articles/top-pesticide-consuming-countries-of-the-world.html)
- Gaya, U. I., & Abdullah, A. H. (2008). Heterogeneous photocatalytic degradation of organic contaminants over titanium dioxide: a review of fundamentals, progress and problems. *Journal of Photochemistry and Photobiology C: Photochemistry Reviews*, 9(1), 1-12.
- Grandcoin, A., Piel, S., & Baures, E. (2017). AminoMethylPhosphonic acid (AMPA) in natural waters: Its sources, behavior and environmental fate. *Water research*, 117, 187-197.
- Hao, Y., & Jiaqiang, X. (2010). Preparation, characterization and photocatalytic activity of nanometer SnO<sub>2</sub>. *International Journal of Chemical Engineering and Applications*, 1(3), 241.
- Henderson, A. M. G., J. A.; Luukinen, B.; Buhl, K.; Stone, D. (2010). Glyphosate Technical Fact Sheet. from National Pesticide Information Center, Oregon State University Extension Services <http://npic.orst.edu/factsheets/archive/glyphotech.html>.
- Hurum, D. C., Agrios, A. G., Gray, K. A., Rajh, T., & Thurnauer, M. C. (2003). Explaining the enhanced photocatalytic activity of Degussa P25 mixed-phase TiO<sub>2</sub> using EPR. *The Journal of Physical Chemistry B*, 107(19), 4545-4549.
- Ibrahim, Y. A. (2015). A regulatory perspective on the potential carcinogenicity of glyphosate. *Journal of Toxicology and Health*, 2(1), 1.

- Kertesz, M., Elgorriaga, A., & Amrhein, N. (1991). Evidence for two distinct phosphonate-degrading enzymes (CP lyases) in *Arthrobacter* sp. GLP-1. *Biodegradation*, 2(1), 53-59.
- Khrolenko, M. V., & Wieczorek, P. P. (2005). Determination of glyphosate and its metabolite aminomethylphosphonic acid in fruit juices using supported-liquid membrane preconcentration method with high-performance liquid chromatography and UV detection after derivatization with p-toluenesulphonyl chloride. *Journal of Chromatography A*, 1093(1-2), 111-117.
- Kosmulski, M. (2006). pH-dependent surface charging and points of zero charge: III. Update. *Journal of Colloid and Interface Science*, 298(2), 730-741.
- Kumar, A., & Pandey, G. (2017). A review on the factors affecting the photocatalytic degradation of hazardous materials. *Material Sci & Eng Int J*, 1(3), 106-114.
- Kutláková, K. M., Tokarský, J., Kovář, P., Vojtěšková, S., Kovářová, A., Smetana, B., . . . Matějka, V. (2011). Preparation and characterization of photoactive composite kaolinite/TiO<sub>2</sub>. *Journal of hazardous materials*, 188(1-3), 212-220.
- Li, H., Wallace, A. F., Sun, M., Reardon, P., & Jaisi, D. P. (2018). Degradation of Glyphosate by Mn-Oxide May Bypass Sarcosine and Form Glycine Directly after C–N Bond Cleavage. *Environmental science & technology*, 52(3), 1109-1117.
- Li Puma, G., & Yue, P. L. (2002). Effect of the radiation wavelength on the rate of photocatalytic oxidation of organic pollutants. *Industrial & engineering chemistry research*, 41(23), 5594-5600.
- Liu, J., & Zhang, G. (2014). Recent advances in synthesis and applications of clay-based photocatalysts: a review. *Physical Chemistry Chemical Physics*, 16(18), 8178-8192.
- Mamy, L., Barriuso, E., & Gabrielle, B. (2016). Glyphosate fate in soils when arriving in plant residues. *Chemosphere*, 154, 425-433.
- Manassero, A., Passalia, C., Negro, A. C., Cassano, A. E., & Zalazar, C. S. (2010). Glyphosate degradation in water employing the H<sub>2</sub>O<sub>2</sub>/UVC process. *Water research*, 44(13), 3875-3882.

- Marques, M., Passos, E., Da Silva, M., Correia, F., Santos, A., Gomes, S., & Alves, J. (2009). Determination of glyphosate in water samples by IC. *Journal of chromatographic science*, 47(9), 822-824.
- Miles, C., Wallace, L., & Moye, H. A. (1986). Determination of glyphosate herbicide and(aminomethyl) phosphonic acid in natural waters by liquid chromatography using pre-column fluorogenic labeling with 9-fluorenylmethyl chloroformate. *Journal of the Association of Official Analytical Chemists*, 69(3), 458-461.
- Ministry of Digital Economy and Society, N. S. O. (2019). *Summary of the labor force survey in Thailand : MAY 2018*. Retrieved from
- Motojyuku, M., Saito, T., Akieda, K., Otsuka, H., Yamamoto, I., & Inokuchi, S. (2008). Determination of glyphosate, glyphosate metabolites, and glufosinate in human serum by gas chromatography–mass spectrometry. *Journal of Chromatography B*, 875(2), 509-514.
- Muneer, M., & Boxall, C. (2008). Photocatalyzed degradation of a pesticide derivative glyphosate in aqueous suspensions of titanium dioxide. *International Journal of Photoenergy*, 2008.
- National Center for Biotechnology Information, N. I. o. H. (2018). Glyphosate. Retrieved Dec 10, 2018, from PubChem Compound Database
- Office of Agricultural Regulation, D. o. A. (2019). *Summary Report on the Import of Chemical Products - Thailand 2018*. Retrieved from
- Ohno, T., Sarukawa, K., Tokieda, K., & Matsumura, M. (2001). Morphology of a TiO<sub>2</sub> photocatalyst (Degussa, P-25) consisting of anatase and rutile crystalline phases. *Journal of Catalysis*, 203(1), 82-86.
- Ohtani, B., Prieto-Mahaney, O., Li, D., & Abe, R. (2010). What is Degussa (Evonik) P25? Crystalline composition analysis, reconstruction from isolated pure particles and photocatalytic activity test. *Journal of Photochemistry and Photobiology A: Chemistry*, 216(2-3), 179-182.
- Patsiriwong, W. P., A; Yeiyai, W; Jittham, C; Kerdnoi, T; Hongsibsong, S. (2015). *Research on Organophosphate Pesticide Risk Management in the Upper Northern Part of Thailand: Nan and Chaingrai Provinces*. Retrieved from Infinity Media Co., Ltd.:

- Pattarasiriwong, W. W., P; Sittisorn, T; Yindee, T; Kerdnoi, T; Hongsisong, S. (2016). *Research on Organophosphate Pesticide Risk Management in the Upper Northern Part of Thailand phayamengrai, Chaingrai Provinces*. Retrieved from Infinity Media Co., Ltd.:
- Piriapittaya, M., Jayanta, S., Mitra, S., & Leepipatpiboon, N. (2008). Micro-scale membrane extraction of glyphosate and aminomethylphosphonic acid in water followed by high-performance liquid chromatography and post-column derivatization with fluorescence detector. *Journal of Chromatography A*, 1189(1-2), 483-492.
- Rabindranathan, S., Devipriya, S., & Yesodharan, S. (2003). Photocatalytic degradation of phosphamidon on semiconductor oxides. *Journal of hazardous materials*, 102(2-3), 217-229.
- Raj, K., & Viswanathan, B. (2009). Effect of surface area, pore volume and particle size of P25 titania on the phase transformation of anatase to rutile.
- Razzaque, M. S. (2011). Phosphate toxicity: new insights into an old problem. *Clinical science*, 120(3), 91-97.
- Roy, D. N., & Konar, S. K. (1989). Development of an analytical method for the determination of glyphosate and (aminomethyl) phosphonic acid residues in soils by nitrogen-selective gas chromatography. *Journal of Agricultural and Food Chemistry*, 37(2), 441-443.
- Rueppel, M. L., Brightwell, B. B., Schaefer, J., & Marvel, J. T. (1977). Metabolism and degradation of glyphosate in soil and water. *Journal of Agricultural and Food Chemistry*, 25(3), 517-528.
- Sanchez-Soto, P., & Perez-Rodriguez, J. (1989). Thermal analysis of pyrophyllite transformations. *Thermochimica Acta*, 138(2), 267-276.
- Sheng, J., Xie, Y., & Zhou, Y. (2009). Adsorption of methylene blue from aqueous solution on pyrophyllite. *Applied Clay Science*, 46(4), 422-424.
- Sirotiak, M. B., A; Lipovský, M. (2015). SPECTROMETRIC DETERMINATIONS OF SELECTED HERBICIDES IN MODELLED AQUEOUS SOLUTIONS. *Journal of Environmental Protection, Safety, Education and Management*, 3.

- Sviridov, A., Shushkova, T., Ermakova, I., Ivanova, E., Epiktetov, D., & Leontievsky, A. (2015). Microbial degradation of glyphosate herbicides. *Applied Biochemistry and Microbiology*, 51(2), 188-195.
- Tagun, R. (2014). *The Effects of mixtures of pesticides, in use in Thailand, on the aquatic macrophyte Lemna minor*. University of York.
- Tawatsin, A. (2015). Pesticides used in Thailand and toxic effects to human health. *Medical Research Archives*(3).
- Torretta, V., Katsoyiannis, I., Viotti, P., & Rada, E. (2018). Critical Review of the Effects of Glyphosate Exposure to the Environment and Humans through the Food Supply Chain. *Sustainability*, 10(4), 950.
- Tsuji, M., Akiyama, Y., & YANO, M. (1997). Simultaneous determination of glufosinate and its metabolite, and glyphosate in crops. *Analytical sciences*, 13(2), 283-285.
- Umar, M., & Aziz, H. A. (2013). Photocatalytic degradation of organic pollutants in water *Organic Pollutants-Monitoring, Risk and Treatment*: InTech.
- Waiman, C. V., Avena, M. J., Garrido, M., Band, B. F., & Zanini, G. P. (2012). A simple and rapid spectrophotometric method to quantify the herbicide glyphosate in aqueous media. Application to adsorption isotherms on soils and goethite. *Geoderma*, 170, 154-158.
- Wang, B., Ding, H., & Deng, Y. (2010). Characterization of calcined kaolin/TiO<sub>2</sub> composite particle material prepared by mechano-chemical method. *Journal of Wuhan University of Technology-Mater. Sci. Ed.*, 25(5), 765-769.
- Wang, C., Shi, H., Zhang, P., & Li, Y. (2011). Synthesis and characterization of kaolinite/TiO<sub>2</sub> nano-photocatalysts. *Applied Clay Science*, 53(4), 646-649.
- Wang, G., Xu, L., Zhang, J., Yin, T., & Han, D. (2012). *Enhanced Photocatalytic Activity of TiO<sub>2</sub> Powders (P25) via Calcination Treatment* (Vol. 2012).
- Wang, S., Seiwert, B., Kästner, M., Miltner, A., Schäffer, A., Reemtsma, T., . . . Nowak, K. M. (2016). (Bio) degradation of glyphosate in water-sediment microcosms—A stable isotope co-labeling approach. *Water research*, 99, 91-100.
- Xue, W., Zhang, G., Xu, X., Yang, X., Liu, C., & Xu, Y. (2011). Preparation of titania nanotubes doped with cerium and their photocatalytic activity for glyphosate. *Chemical Engineering Journal*, 167(1), 397-402.

- Zhang, J., Zhou, Y., Jiang, M., Li, J., & Sheng, J. (2015). Removal of methylene blue from aqueous solution by adsorption on pyrophyllite. *Journal of Molecular Liquids*, 209, 267-271.
- Zhang, L. H., Xu, C. B., Chen, Z. L., & Li, X. M. (2011). *Effect of UV Intensity and Wavelength on Photocatalytic Degradation of Polycyclic Aromatic Hydrocarbons*. Paper presented at the Advanced Materials Research.
- Zhang, Q., Shan, A., Wang, D., Jian, L., Cheng, L., Ma, H., & Li, J. (2013). A new acidic Ti sol impregnated kaolin photocatalyst: synthesis, characterization and visible light photocatalytic performance. *Journal of sol-gel science and technology*, 65(2), 204-211.
- Zheng, R., Ren, Z., Gao, H., Zhang, A., & Bian, Z. (2018). Effects of calcination on silica phase transition in diatomite. *Journal of Alloys and Compounds*, 757, 364-371.
- Zhu, Y., Zhang, F., Tong, C., & Liu, W. (1999). Determination of glyphosate by ion chromatography. *Journal of Chromatography A*, 850(1-2), 297-301.

## BIOGRAPHY

Name	Ms. Kanokwan Yamsomphong
Date of Birth	August 29, 1994
Education	2015: Bachelor of Science (Environmental Science) Science and technology Thammasat University

### Publications

Yamsomphong, K., Pokhum, C., G Mariqui, E., Hirofumi, H., Sreearunothai, P., and Chawengkijwanich, C. (2019). Photocatalytic Degradation and Mechanism of Glyphosate Herbicide Contaminated in Water by TiO<sub>2</sub> Pellet Photocatalyst. *Proceedings of the 5<sup>th</sup> environment Asia international conference: transboundary environment nexus: from local to regional perspectives* (pp. 147-164).